MAGNETO-MINERALOGICAL STUDIES IN RELATION TO THE TECTONIC EVOLUTION OF THE ANORTHOSITE COMPLEXES IN AND AROUND CHILKA LAKE, EASTERN GHATS BELT OF INDIA

THESIS SUBMITTED FOR THE DEGREE OF DOCTOR OF PHILOSOPHY (SCIENCE) OF JADAVPUR UNIVERSITY

By:

SOLANKY DAS

Index No.: 16/21/Geol. Sc./27

GEOPHYSICAL LABORATORY
DEPARTMENT OF GEOLOGICAL SCIENCES
JADAVPUR UNIVERSITY

2025

যাদবপুর বিশ্ববিদ্যালয়
কলকাতা - ৭০০০৩২, ভারত

JADAVPUR UNIVERSITY
KOLKATA-700 032, INDIA

FACULTY OF SCIENCE : DEPARTMENT OF GEOLOGICAL SCIENCES

CERTIFICATE FROM THE SUPERVISOR

This is to certify that the thesis entitled **"Magneto-mineralogical Studies in relation to the Tectonic Evolution of the Anorthosite Complexes in and around Chilka Lake, Eastern Ghats Belt of India"** submitted by **Ms. Solanky Das,** who got her name registered on **18.03.2021** for the award of **Ph. D. (Science) degree** of **Jadavpur University**, is absolutely based upon her own work under the supervision of **Prof. Supriya Mondal** and that neither this thesis nor any part of it has been submitted for either any degree / diploma or any other academic award anywhere before.

Supriya Mondal.

Dr. Supriya Mondal 24.07.2025

DR.SUPRIYA MONDAL
Professor
Department of Geological Sciences
JADAVPUR UNIVERSITY
Kolkata-700032, W.B.(India)

Professor
Department of Geological Sciences
Jadavpur University
Kolkata-700032
India.

Dedicated to My Grandfather

CONTENTS

ACKNOWLEDGEMENTS

The author is profoundly grateful to her supervisor, Prof. Supriya Mondal, of the Dept. of Geological Sciences, Jadavpur University, Kolkata, for his guidance and support throughout her work. His constant supervision helped in completing the field and laboratory works. His vast expertise has enriched this work substantially. I consider myself fortunate in having Prof. Supriya Mondal as my supervisor and guide.

I would like to acknowledge my Research Advisory Committee (RAC) members, Dr. Susanta Chaudhuri and the Head of the Dept. of Geological Sciences of Jadavpur University for their invaluable suggestions.

I would like to thank SVMCM Non-Net Fellowship for Ph.D Student and UGC (Savitribai Jyotirao Phule Fellowship Single Girl Child) JRF and SRF, Govt. of India for the financial support during the research work and also Dept. of Geological Sciences, Jadavpur University for the necessary laboratory facilities provided for this research. I would also like to thanks CSIR-NGRI, Hyderabad for giving the permission to use their laboratory. Special thanks to Dr. M. Venkateshwarlu, for his guidance during rockmagnetic and palaeomagnetic sample analysis.

Writing the thesis was onerous and miserable task not only for me but all those who were beside me all along those days. At times I was very harsh with my family, especially my father (Prof. Sukhen Das) and grandmother (Mrs. Kamana Das). My father always has my back, without his constant support it was impossible to complete this chapter of life and my thamma was always ready with food on time and other requirements without any question. I will be always grateful to them.

I am extremely thankful to my aunties, uncle, mother and cousins for always making me believe that I can do and finish this work properly. I am also lucky for the blessings from my heavenly grandfather (Late Suresh Chandra Das) whom I use to call Chotu, I am sure he is smiling and blessing me today. Also, a kind regards to Dr. Ruma Basu for always checking on me. Last, but not the least I would like to express my deepest appreciation to my husband Shyanki for staying beside me from the very first day and continuously inspiring and supporting my work.

Date: 28.07.2025

Place: Kolkata

Solanky Das 28.07.2025

Solanky Das

Title: **MAGNETO-MINERALOGICAL STUDIES IN RELATION TO THE TECTONIC EVOLUTION OF THE ANORTHOSITE COMPLEXES IN AND AROUND CHILKA LAKE, EASTERN GHATS BELT OF INDIA**

Index No.: 16/21/Geol.Sc./27

Abstract

The present research work examines the magnetic history in relation to tectonic evolution of Balugaon and Rambha Anorthosite Massif Complexes along with the surrounding high-grade metamorphic rocks of the Chilka Lake area, Eastern Ghats Mobile Belts (EGMB), Odisha, India using a combined approach that includes Petrography, Magneto-mineralogy, Rockmagnetic Study, Anisotropy of Magnetic Susceptibility (AMS) Study and Palaeomagnetic Study. This study aims to ascertain the petrography, generations of Fe-Ti oxides, magnetic remanence carrier minerals, magnetic fabrics and stable magnetic vectors (by Thermal Demagnetization) present within the analysed rocks and the find respective pole position.

The magneto-mineralogical analysis indicates that the primary magnetic remanence carrier mineral is magnetite. Three generations of Fe-Ti oxides have been identified from the studied rocks. They are primary homogeneous titanomagnetite, primary in-homogeneous titanomagnetite (both high and low temperature phases) and ultrafine grained secondary magnetite. Multiple generations of magnetite within studied rocks corresponds to various temperature existed throughout their oxidation. These finding have tectonic implications that depict the upliftment of the crust. The rockmagnetic characteristics along with magnetic fabrics derived from AMS studies are utilized to figure out their tectonic significance. Rockmagnetic studies are carried out to identify the magnetic minerals residing within the studied samples including Isothermal Remanent Magnetization (IRM), Backfield IRM, Thermomagnetic Study and Hysteresis Study. The magnetic domains are identified using a modified Day Plot, using the magnetic hysteresis parameters (coercivity and remanence). All the magnetic domains fall under the Single Domain (SD), which also have great potential of recording the ancient Earth's Magnetic Field. The magnetic fabrics of the region are unravelled by the help of AMS studies. The magnetic susceptibility ellipsoids are dominantly oblate as revealed from the P_j-T_j shape plot. Highly variable magnetic

lineation states the multiple phased tectono-metamorphic conditions experienced by the region. The AMS study shows that, in addition to ferromagnetic and paramagnetic minerals, silicates also play a significant role in controlling the development of the magnetic fabrics. The magnetic fabric has tectonic implications related to metamorphism followed by felsic magmatism. One component of magnetization has been established by a thorough thermal demagnetization and Principal Component Analysis (PCA). This component does not include any significant record of the present day Earth's Magnetic Field (EMF) and is analogous to regional structure.

The mean value of declination and inclination (D_m / I_m) has been obtained from the Thermal Demagnetization analysis of the studied rocks. The primary high temperature phases of titanomagnetites are responsible for the carried vectors obtained during geologic event. This mean D_m / I_m value helps in defining the pole position obtained by this study. The identified pole position, C is (1.15˚ S and 16.15˚ E). The pole is dated (aligning with the established pole locations documented in the literature) in the age group of 850-900 Ma. It falls on the Apparent Polar Wandering Path (APWP) of the Proterozoic India.

List of Figure and Table Captions:

List of Figure Captions:

List of Table Captions:

LIST OF ABBREVIATIONS

AF: Alternating Field
AMS: Anisotropy of Magnetic Susceptibility
APW: Apparent Polar Wander
APWP: Apparent Polar Wandering Path
ChRM: Characteristic Remanent Magnetization
CRM: Chemical Remanent Magnetization
D: Declination
DRM: Detrital Remanent Magnetization
EGB: Eastern Ghats Belt
EMF: Earth's Magnetic Field
I: Inclination
IRM: Isothermal Remanent Magnetization
MD: Multi Domain
NRM: Natural Remanent Magnetization
pDRM: Post Depositional Remanent Magnetization
PPL: Plane Polarised Light
PSD: Pseudo Single Domain
SD: Single Domain
SIRM: Saturating Isothermal Remanent Magnetization
SSD: Stable Single Domain
TRM: Thermal Remanent Magnetization
UHT: Ultra High Temperature
VRM: Viscous Remanent Magnetization
WCZ: Western Charnockite Zone
WKZ: Western Khondalite Zone
XPL: Cross Polarised Light
AVFTB: Advanced Variable Field Translation Balance
CHL: Chilka Lake, Eastern Ghats Belt
CMZ: Central Migmatite Zone
DC: Direct Current
EGMB: Eastern Ghats Mobile Belts
EKZ: Eastern Khondalite Zone
F: Magnetic Foliation
H_c: Coercivity
H_{cr}: Coercivity of Remanence
K: Magnetic Susceptibility
K_m: Mean Susceptibility
L: Magnetic Lineation
MA: Magnetic Anisotropy
M_{rs}: Saturation Remanent Magnetization
M_s: Saturation Magnetization

mT: Milli Tesla
P: Anisotropy Degree
P': Corrected Anisotropy Degree
PCA: Principal Component Analysis
pDRM: Post Depositional Remanent Magnetization
PSM: Portable Spinner Magnetometer
T_{Mag}: Thermal Demagnetization Temperature
T: Shape Parameter
TBSZ: Terrain Boundary Shear Zone
T_c: Curie Temperature
TD: Thermal Demagnetizer
UHT: Ultra-High Temperature
VpTRM: Partial Thermo-Chemical Remanent Magnetization
WCZ: Western Charnockite Zone
WKZ: Western Khondalite Zone
λ_p: Pole Latitude
Φ_p: Pole Longitude

Chapter: 1

INTRODUCTION

1. Introduction:

The Precambrian orogenic belts of India which are mostly around the periphery of the crustal area preserve many answers to the questions regarding crustal evolutions of Indian sub-continent. The Eastern Ghats Mobile Belts (EGMB) of India, consists of multiply deformed, high-grade metamorphic rocks which belong to granulite facies of Grenvillian age (1.1-0.9 Ga). Reassembly of East Gondwana has juxtaposed the EGMB along the parts of East Antarctica. Understanding the spatial and temporal variations and chronological variation of the Precambrian orogenic processes relies on the recognition of the metamorphic events and the magneto-stratigraphy in the EGMB and their evolutionary history of the East Antarctica granulites and provide significant and distinct limitations on East Gondwana's structure prior to ~500 Ma. In general, deep strata of the continental crust have been exposed by multiphase deformation in the anorthosite massif complexes of the Precambrian shield. Additionally, metamorphic gradations near the edge of these terrains suggest that extended profiles into the continental crusts are visible. The EGMB thus give considerable opportunities for examining and analysing the geophysical features of the deep crust as a function of depth across a long geological time span. This direct method offers significant advantages. The study of anorthosites and accompanying intrusive can be analysed to discover about the evolutionary history of the crust. The anorthosite and the alkaline rock complexes of the Eastern Ghats serve as the geochemical probes for their mantle origins. Information about the anorthosite complexes, its emplacement mechanisms, magma sources and evolutionary processes are extremely significant.

The anorthosites and alkaline rock complexes of Eastern Ghats Belt are potentially useful geochemical probes of their mantle sources. Information on magma sources and formation processes and on emplacement mechanisms of the complexes are of utmost significance. The main problem that needs to be addressed about the anorthosites and associated rocks in Eastern Ghats may be stated as: Are these rocks dismembered oceanic crust or subducted oceanic lithosphere, or accumulated material of an underplated basaltic magma, or cumulates from precursors of tonalitic gneisses or cumulates complementary to greenstone belt basaltic volcanics? The research studies on the Anorthosite Complexes of Eastern Ghats Mobile Belts can provide the critical data to test the applicability of plate tectonics model, because these belts are

"fossil" plate margins. Magnetic anisotropy study on these orogenic belts may provide a means to reconstruct the large structural changes in the crust that occurred over a long period of geologic time. The remanent magnetizations preserved within Precambrian rocks are the only available record of geodynamic behavior during early Earth's history. Careful studies of the Fe-Ti Oxide mineralogy that hold these recordings are required, in order to address questions about the strength of the Precambrian Earth's Magnetic Field, the convective behavior of the liquid core, and potentially, the formation of the solid inner core.

A large-scale variation of rock types is revealed throughout the EGMB. The geological age of these rock units varies greatly from one another. Several anorthosite massifs intrude within the granulites. The most distinctive anorthosite massifs and the main concern of this study are Balugaon and Rambha Anorthosite Massifs. In this regard the current research work conducts geological and geophysical investigations to examine the geologically significant metamorphic rocks of the EGMB. Palaeomagnetic investigations can only link these rocks based on the tectonic history of the inter-cratonic blocks.

This Ph. D. Research work is divided into three stages:

First, is the extensive Geological Field Investigation (several in numbers).

Second, is Laboratory Investigation, which is consisting of the different Rockmagnetic and Palaeomagnetic Experiments and the Petrographic and Magneto-mineralogical Studies.

Third, is the Data Interpretation, where we interpret the obtained data from the different magnetic experiments and microscopic studies.

During the field investigations, mainly the natural in-situ oriented block of rock samples and the structural data are collected for detailed study. From these oriented block samples, the cores are drilled out for further experiments (elaborately explained in Chapter-3). For different rockmagnetic measurements a part of the samples are powdered. Further, the laboratory experiments are divided as follows:

1) Petrographic and Magneto-mineralogical Study
2) Magnetic Measurements
    - Rockmagnetic Study,

- Anisotropy of Magnetic Susceptibility (AMS) Study,
- Palaeomagnetic Study.

The primary topic of this thesis study is to determine the Rockmagnetic properties, Magnetic Fabrics from Anisotropy of Magnetic Susceptibility (AMS) analysis and Palaeomagnetic characteristics of Anorthosites and associated high-grade metamorphic rocks from the Chilka Lake area, Eastern Ghats Mobile Belts, India.

On the basis of petrographic study, the rocks, associated with the study are identified depending upon its rock forming minerals. Under the reflected light microscope study, the determination of the different oxidation phases of magnetic minerals at different temperature can aid in predicting the tectonic events that led to their formation. Rocks become magnetized in the geomagnetic field direction when they are uplifted and then cooled through Curie temperature during tectonic and metamorphic process. Later, when these minerals experience further metamorphic and tectonic events, they produce a secondary remanence component. Rockmagnetic studies help in identifying the magnetic remanence carrier minerals and the domain state within them (SSD, MD or PSD). These minerals when treated to different rockmagnetic experiments, the identification of the minerals can be done observing the Curie temperature and the nature of the obtained Curie curves. The nature and domain state of the magnetic minerals can be detected with the support of the rockmagnetic investigations. In order to correlate these rocks with the regional tectonics, AMS studies are crucial. AMS is a helpful tool for understanding deformation and tectonics which can be derived from the many AMS related statistical variables and orientational characteristics. It also helps in identifying the magnetic fabrics based on the shape and orientation i.e., the microstructures. The demagnetization process reveals the magnetization history of the rocks. The high-grade metamorphic rocks present have a complex deformational history which can be analysed using the AMS fabrics since the post tectonic recrystallization usually destroys textures created at high temperatures, making it challenging to identify the lineation and /or foliation under microscope or in field. Then these records are attempted to correlate with the geologic age. Further, a relationship between the magnetic properties and the petrographic features will be explored.

The significant contributions to the geophysical research onto the continental crust may be made by Magnetic Anisotropy (MA) and palaeomagnetic investigations of the Anorthosite complexes of the Eastern Ghats Belt:

i) First, the ancient magnetic field that was acquired at various points during the early tectonic history of this terrain is always present in the Proterozoic crustal rocks in a strong and consistent record. The magnetism has documented the palaeomagnetism throughout long periods of the geologic time and is usually resident in one or more phases of magnetite/ magnetic mineral development. The sole confirmation of the Eastern Ghats Belt's past tectonic history will come from this palaeomagnetic record, which is also crucial for establishing a correlation between the crustal rocks in the region ad those found elsewhere.

ii) Second, two factors primarily control the orientational anisotropy of the minerals, which can be measured in the form of magnetic anisotropy fabrics in crustal rocks: a) the impact of metamorphism induced pressure and b) the influence of the geomagnetic field over the early formed magnetic particles during metamorphism and post metamorphic episodes. These lead to two MA components within the rocks; a planar component whose easy plane is equivalent to the rocks shear plane and an orientational component, which is not as significant as the major strong planar anisotropy. This helps in identifying the geomagnetic field direction, because the geomagnetic field is responsible for the anisotropy after the post metamorphic span; i.e., determining palaeomagnetism.

Natural Remanent Magnetization (NRM) is the term used to define the permanent magnetism that is present within the rock prior to nay thermal treatment. The majority of the crustal rocks possess NRM, acquired by various physical processes depending on their formation mode. They are as follows:

- Thermo-remanent Magnetization (TRM),
- Detrital Remanent Magnetization (DRM),
- Post Depositional Remanent Magnetization (pDRM),
- Chemical Remanent Magnetization (CRM),
- Viscous Remanent Magnetization (VRM),

- Isothermal Remanent Magnetization (IRM).

The rocks forming the continental crust those are exposed in the Precambrian shields and mobile belts are metamorphic rocks covering the igneous or sedimentary rocks. The primary thermo-remanent magnetization (TRM) are replaced by these secondary magnetization components as partial thermo-remanent magnetization (pTRM), Chemical or thermo-chemical remanent magnetization (CRM or TCRM) or viscous partial thermo-chemical remanent magnetization (VRM or VpTRM). Two coexisting magnetic minerals or coexisting Multi-Domain (MD), Single Domain (SD) and Stable Single Domain (SSD) states of same mineral carry superimposed primary and secondary remanences. The rocks of the study area of EGB are mainly metasedimentary and metaigneous rocks, hence the TRM and CRM are taken under concern.

The NRM is the summation of the total magnetic component within the rock, the primary along with the secondary magnetization, which is acquired during the later phase of geologic time. The major role of the palaeomagnetic investigations is identifying and separating the Characteristics Remanent Magnetization (ChRM) from all magnetic components within the rock. The thermal demagnetization and alternating field demagnetization are two different demagnetization techniques for separation of magnetic components. While demagnetization the secondary magnetization is removed leaving behind the partially demagnetized sample termed as ChRM. It is a vector quantity which has both direction (declination and inclination) and magnitude (intensity). Using these remanent magnetization directions, the sampling sites' palaeolatitude can be determined from the relation:

$$2 \tan \lambda = \tan I \qquad \text{(Keary et al., 2009)}$$

Where, λ is the palaeolatitude, I is the inclination of magnetic vector.

The palaeopole position can be obtained by many mathematical equations (Butler, 1992). These help in identifying the past movements of the tectonic plates through geologic time. The palaeopole position of Anorthosite complexes of the Chilka Lake area, EGMB, Odisha, India is not examined yet. Hence, the different magnetic data is a good initiative to determine or locate the position of EGMB on the Apparent Polar Wandering (APW) path of the Proterozoic times.

The principle aims of this study is to examine the capability of storing ancient Earth's Magnetic Field (EMF) in the Proterozoic high-grade rocks of the EGMB and to reveal the orientation anisotropy of the minerals, the magnetic fabrics of the minerals by using AMS and cause of the magnetic fabrics. The palaeopole position to identify the Proterozoic magnetization events experienced by the area.

The main objectives of the present study are:

- ❖ To identify the magnetic remanence carrier and its nature of residence within the rocks.
- ❖ To determine of magnetic fabrics of the rocks by AMS analysis and correlate then with the mesoscopic fabrics and microstructures to implicate their tectonic significances.
- ❖ To unravel the magnetization history of the rocks along with its tectonic implications.
- ❖ To determine the palaeopole from the studied rocks.

Since, these techniques rely on magnetic examinations of the rock's cores; it makes sense to combine them in determination of both magnetization of the massif-type anorthosite complexes and their ancient recoverable tectonic history.

The palaeomagnetism of the Precambrian rocks is way different from that of the Phanerozoic ones. The Phanerozoic palaeomagnetic data can be assigned to a certain geological age on the basis of stratigraphic evidence, fossil contain or radiometric dating. From a single continental block the accumulating findings across several eras, help in computing time and subdivision. For a certain block, there may be significant internal dispersion of 10˚-15˚ within the results from same period, the period span may be established with precision and few mistakes. Then the resulting path of all the poles can be in most of the cases be explained most prominently (McElhinny, 1973 and 1979). In case of Precambrian studies, this concept is not possible since only radiometric dating are used, in 10^9years range, age uncertainties are generally larger than that of Phanerozoic geologic periods. Hence it is not possible to get the best possible apparent polar wandering path by plotting the average data from period to period for the general trend (Spall, 1971). Inaccuracies in individual

palaeomagnetic data are amplified by the lack of sequentially averaged results. The Proterozoic rocks have less complication in palaeomagnetism than that of Proterozoic rocks. Older the rocks, more exposed to thermal or chemical deformation overprinting the primary magnetization and tectonic reorientation. Hence, several experiments regarding magnetization are conducted for detailed vector analysis of the multi-components present within the rock acquired in due time after formation (Roy and Park, 1974; Buchan and Dunlop, 1976). In all the studies regarding metamorphic rocks it is important to know the age of formation of the rock as well as time of magnetization.

The new Precambrian paths offer insights into the nature of Precambrian tectonics, similar to how the Phanerozoic APW paths provide essential proof to tectonics throughout the previous 600 Ma. Palaeomagnetic studies on Precambrian rocks of North America and other continents have shown a relation to the origin of the orogenic belts of that country (Piper et al., 1973), using the poles of different time span on the APW path, proposed tectonic model and intercratonic orogenesis. Not much elaborated palaeomagnetic study regarding the Precambrian rocks of India are done, some are done, Charnockite from Southern Granulite Terrain (Mondal et al., 2008), Dalma Volcanics of Singhbhum Mobile Belt (Chatterjee et al., 2018a, b), Kondapalle–Pangidi Layered Complex (Gain et al., 2022). On the basis of complete demagnetization, which defined the ancient remanence. Until now, no palaeo-intensity results meeting modern reliability criteria have been reported from the Massif Anorthosite Complexes and surrounding high-grade granulite terrain of Eastern Ghats Belts, Odisha. Only petrology, geochemistry such study is done but no palaeomagnetic and rockmagnetic study as well as AMS are demonstrated till date. Hence, this study aims to study regarding the magneto-mineralogic study and palaeomagnetic study on the anorthosites and high-grade granulitic rocks of Chilka Lake area, Eastern Ghats Belt, Odisha, India.

Chapter: 2

BACKGROUND GEOLOGY

2. Background Geology:

The Eastern Ghats Mobile Belt (EGMB) covers an area of about 50,000 sq. km, with an overall general trend of NE-SW, extending from Brahmani River in Odisha to Ongole in Andra Pradesh for a distance of about 900 km. This belt is wider in Odisha (~300 km), and gradually tappers downward to tens of Km in Andra Pradesh towards south, along the Eastern coast of India.

The Eastern Ghat province consists of both igneous and high-grade metamorphic rocks. The fold belt is surrounded by three cratonic blocks, Singbhum Craton in the north (Odisha), the Bastar Craton in west and the Dharwar Craton in the south and southwest (Fig. 2.1). The contact between the cratons and EGMB is known as Transition Zone, having characteristics in common (Bhattacharya and Kar, 2002). The boundary between Bastar Craton and EGMB is gradational. Ramakrishnan and Vaidyanadhan, 2008 explained that along the marginal zone basic granulites, dykes

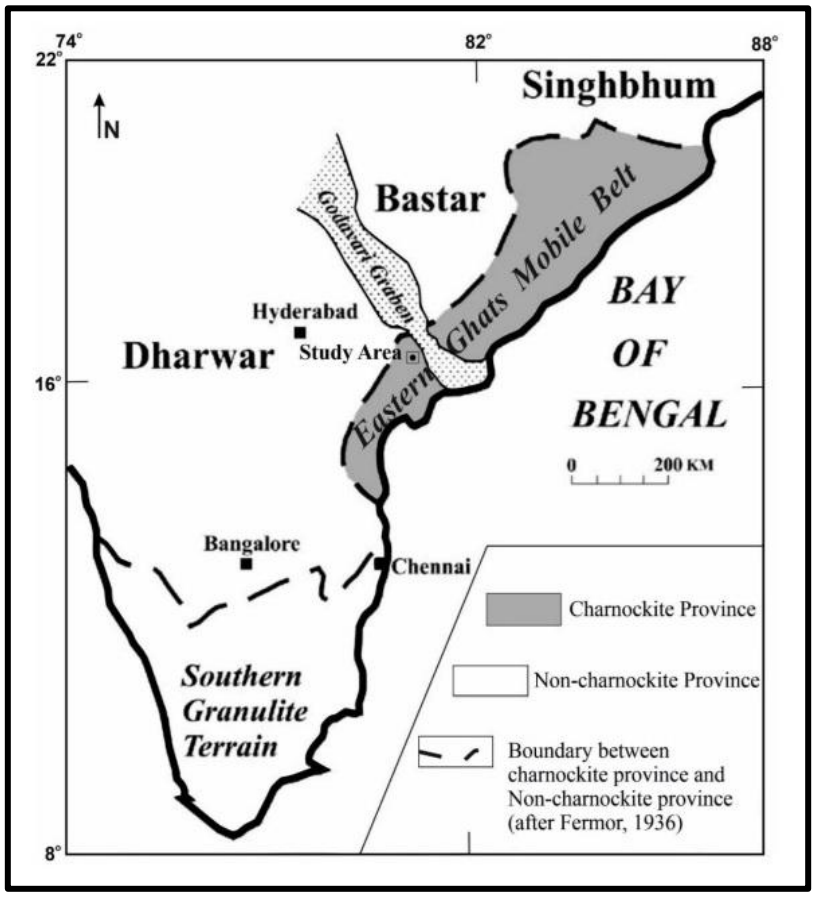

Fig. 2.1: Geological Map of Peninsular India, locating the EGB with respect to Bastar, Dharwar and Singhbhum Cratons (after Gupta et al., 2020).

with chilled margins with charnockite patches arrested in the marginal zone. Around, Deobhog the contact is marked by a Terrain Boundary Shear Zone (TBSZ) (Biswal et al., 2001). On the map of Ramakrishnan et al., (1998), this contact is named as Eastern Ghats Boundary Shear Zone. The EGMB and Shingbhum Craton is noticeably marked by shear zones, mainly Sukinda Thrust. The high-grade gneiss-granulite of the EGMB is surrounded all around. The oldest event that the Eastern Ghats Granulite Belt that has been dated is ~2600 Ma, which corresponds to the regional granulite facies metamorphism. The metamorphism is mostly dated around mid-Proterozoic time.

The Eastern Ghats Belt of the Indian Peninsula is combined of several crustal units with deformational histories (Mezger and Cosca, 1999; Rickers et al., 2001; Dobmeier and Raith, 2003 and Simmat and Raith, 2006). There is a diverse rock types exposed all throughout the mobile belt which experienced a high-grade granulite facies metamorphism. Longitudinally this terrain is divided in four zones (Fig. 2.2) based on their lithology (Ramakrishnan et al., 1998). They are:

- Western Charnockite Zone (WCZ)
- Western Khondalite Zone (WKZ)
- Central Migmatite Zone (CMZ)
- Eastern Khondalite Zone (EKZ)

The WCZ is separated from the Dharwar and Bastar craton by a granulite facies transition zone consisting of small amount of charnockite, basic granulite dykes and within orthogneisses enclaves of high-grade schists of cratons are available. This transitional zone is marked a by a zone of thrusting and a zone witnessing positive Bouguer gravity anomaly with a steep gradient from craton to the mobile belt.

The deeper metamorphosed parts of the adjacent Dharwar and Bastar cratons are probably represented by WCZ. The WCZ consists charnockite and enderbite, basic granulite and BIF. Even the layered anorthosite with chromite layers of the igneous complex of Kondapalle and Chimalpahad is also a part of WCZ. A prominent ductile shear zone known as Sileru-Machkund Shear Zone separates WCZ from main supra-crustals of EGMB (WKZ, CMZ and EKZ).

The WKZ is about 30-50 Km wide and at some places 80 km wide. The WKZ is comprised of khondalite suite of rocks, such as garnet-sillimanite-k-feldspar-

graphite schists and gneiss, calc-silicate rocks, rare sillimanite garnetiferous quartzite. The suite is interleaved with bands of charnockite. Concordant sheets of pyroxene granulite are common, some may be basaltic flows and others may be basic sills and dykes.

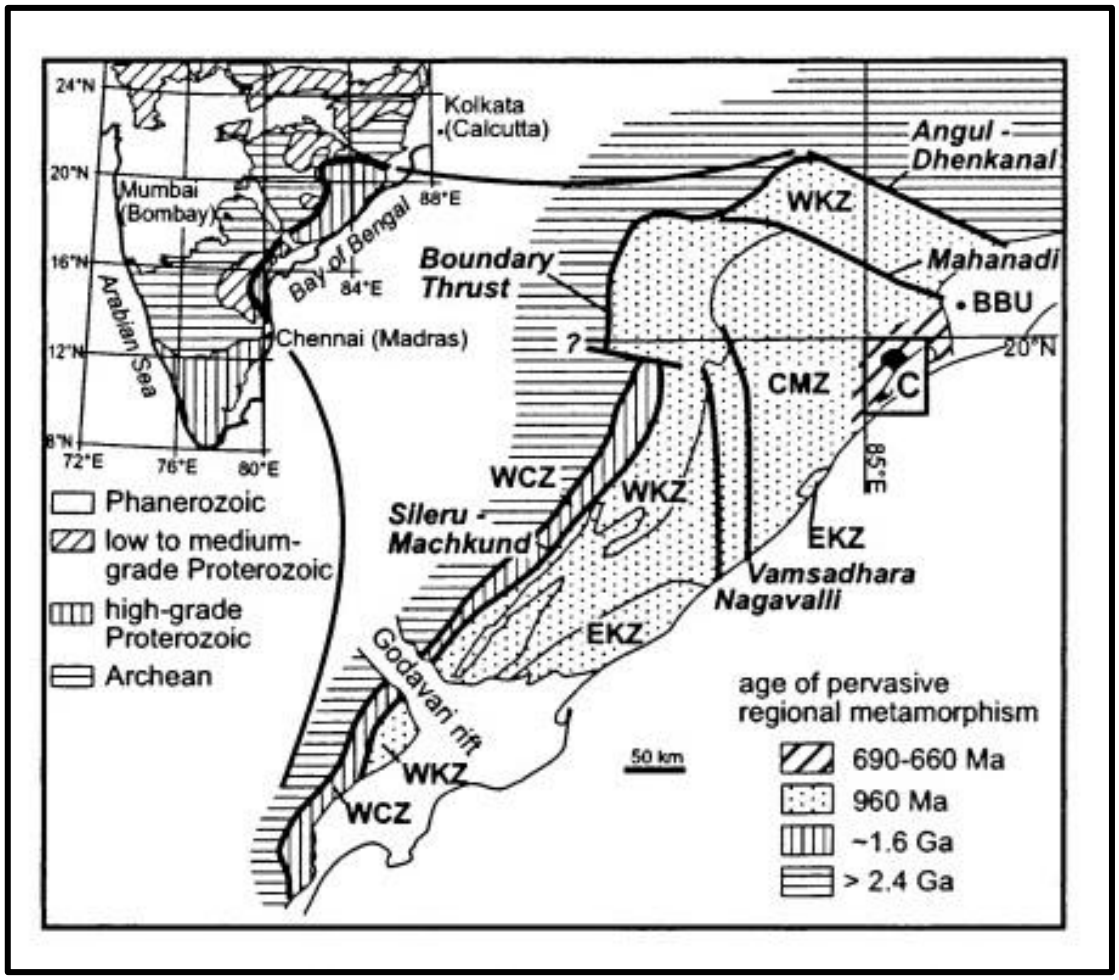

Fig. 2.2: The Eastern Ghats Belt of peninsular India. Location (external boundaries after Ramakrishnan et al., 1998) and different zones of the terrain.

A transitional contact is in between CMZ and WKZ and the width varies from 40-100Km. The CMZ dominantly contain migmatitic gneiss having two major components-

1. Hornblende-biotite gneiss bearing garnet and hypersthene.
2. Garnetiferousquartzo-feldspathic gneiss (leptynitic para gneiss)

The CMZ also comprise of different degree of migmatization of the khondalititic enclaves, charnockite with granulite enclaves and garnetiferous granitoid.

The EKZ is now considered as a separate unit from the CMZ after Ramakrishnan (1988). Earlier EKZ is mainly comprised of khondalite, quartzite, calc-silicate ricks. The interveining migmatite zone, a high-grade metamorphic and wide spread particle melting zone, leading towards granitization and migmatization. All these three zones together constitute the only the major supracrustal succession of EGMB. A huge amount of the massif anorthosites from mid-Proterozoic time and some alkaline rocks are widely present in the EGMB, mainly within the supracrustal belt sequence.

The complete anorthositic rocks of the belt of Eastern Ghats are intruded into three separate locations – Balugaon (Perraju, 1960, 1973; De, 1969), Kallikota (De, 1969) and Rambha (Ray, 1952; De, 1969). The anorthosite of the EGMB belongs to the syntectonic composite plutonic complex, first said by Sarkar et al., 1980. The name Chilka Lake igneous complex was first proposed (Sarkar et al., 1976), because the complex is in a close proximity with Chilka Lake.

The presence of anorthositic rocks around Banpur-Balugaon was first reported by Perraju (1960), and then the initial petrological description of these rocks was provided (Perraju, 1973). The regions charnockitic gneisses and granulite precede the anorthositic rocks based on reliable field data.

This study deals with the Chilka Lake Domain at the North Eastern part of EGB (latitude range of 19º 27′ N to 19º 58′ N and longitude 85º 00′ E to 85º 25′ E) (Fig. 2.3), which is characterised by one of the massif types anorthosite body of the Eastern Ghats Belt (Ray, 1952; Perraju, 1960; Sarkar et al., 1981). The anorthosite complexes are exposed onshore in two separate parts, one around Banpur and Balugaon villages (~ 295 km^2). This exposed part is known as ‘Balugaon Massif’. At the north-east part this massif is surrounded by poly-deformed high-grade granulite. The other part is at the extreme south western tip of the Chilka Lagoon, known as the Rambha Massif (12 km^2). These two islands of anorthosite are connected by extending into the lagoon, whereas several meta sedimentary outcrops suggests that they are not connected with each other (Sarkar et al., 1981). The occurrence of Rambha within the complex was first identified by Ray (1952). After the petrographic description of this intrusion De (1969) came to a conclusion that it is a lensoid mass that was deposited at high temperatures, resulting in contact metamorphism of the

nearby calc-silicate rocks. De and his co-workers (De, 1969), first reported patchy occurrences of rocks of anorthositic connections to the north and northwest of Kallikota. These rocks were termed as granitized anorthosites (where quartz and k-feldspar were introduced by charnockite intrusion). Both the massifs have identical petrographical and geochemical characteristics of the orthopyroxene bearing meta-anorthosite and meta-leuco-norite. Both massifs have identical geochemical and petrological compositions for their orthopyroxene bearing meta-anorthosite and meta leuconorite. A variety of melanocratic rocks, consisting ferrodiorite lenses and norite dykes and two chemically different ortho-pyroxenite xenoliths (Sarkar et al., 1981), were found only in the Balugaon Anorthosite Massif. At the zone of contact with the adjacent country rock, an identifiable leucocratic orthopyroxene bearing quartzo-feldspathic gneiss with venticles bearing blue quartz is observed.

The Balugaon Anorthosite Massif has distinct difference from that of the Bolangir Anorthosite Massif (Fig. 2.1) (Bhattacharya et al., 1998). The Bolangir Anorthosite Complex reflects crustal melts created by advective heating and partial melting of the country rocks encompassing the anorthosite complex. The country rock assemblage consists mostly of migmatitic quartzo-feldspathic gneiss, khondalite (Walker, 1902) (assemblage of sillimanite and garnet bearing metapelites), leptynite (Sen, 1987). At the south of Balugaon Massif a porphyritic leptynite body which is approximately 5 Km wide and 14 Km long is partially visible. There is a leucosome network against the plutons border which is tightly folded isoclinally. The garnet grains present have diameters larger than that of the leucosome width, which indicates significant flattening of the leucosomes. The leptynite of the porphyritic facies of the leptynite-enderbite association has similar modal composition and porphyric texture that of porphyritic leptynite. Calc-silicate gneisses and pyroxene granulites are observed as inclusions within khondalites. Way larger (250m x 50m) lens of the calc silicate gneisses is embedded within the Rambha Anorthosite Massif.

2.1. Deformational History and Structures:

The host rock of this complex is severely deformed as well as metamorphosed suite of high-grade granulite. The high-grade granulitic rocks are exposed surrounding the anorthosite massif. The relation between the different episodes of igneous activity, folding and metamorphism of the Eastern Ghats Belt. Previous structural investigation

of the Chilka Lake Anorthosite revealed several deformational events. The general trend of the Eastern Ghats Mobile Belt (EGMB) is ENE -WSW, which is the result banding compositional layering and lithological contacts those are closely parallel.

The Chilka Lake granulites comprises of high-grade gneisses and ortho-gneisses surrounding massif anorthosite.

- Ortho-gneiss formed by metamorphism of igneous rocks,
- Para-gneiss results from metamorphism of sedimentary rocks.

The area preserves folding, foliation, lineation developed during multiple stage of deformation.

Sarkar et al., (1981), informed that the rocks of this belt deformed in three phases. The different deformation suggests different petrogenetic events, tectonic impression on the rocks and folding events.

- In the first deformation, basic dykes like sills were emplaced at the declining phase of F_1. There was regional metamorphism and granitization. Axial plane schistosity (S_2) of F_1 developed, which is also the dominant planar fabric of the belt. During D_1 isoclinal folds developed trending NE-SW. Folds overturned NW, With moderate plunging southerly.
- In the second deformation, regional metamorphism is high temperature granulite facies. Along the axial plane of F_1, large scale faulting and fracturing occurred, folding the S_2. S_1 is parallel to S_2. F_2 is also coaxial after refolding isoclinal F_1 to antiform and synform trending approximately NS.
- During the third deformation, syntectonic emplacement of the Chilka Lake Complex took place. Along with the metamorphism and peripheral migmatisation took place. Domes and basin structure developed by superposition of F_2 and F_3 folds. F_3 is cross folding with trend EW. The study explains that the F_3 cross folding along with F_2/F_3 interference have a strong hold on the form and structure of the massif.

Bhattacharya et al., (1993,1994) also verified three deformational events using structural mapping and limited remote sensing. Das et al., (2012) designated the four penetrative deformations as D_1, D_2, D_3 and D_4 and four folds metamorphic (M_1-M_4).

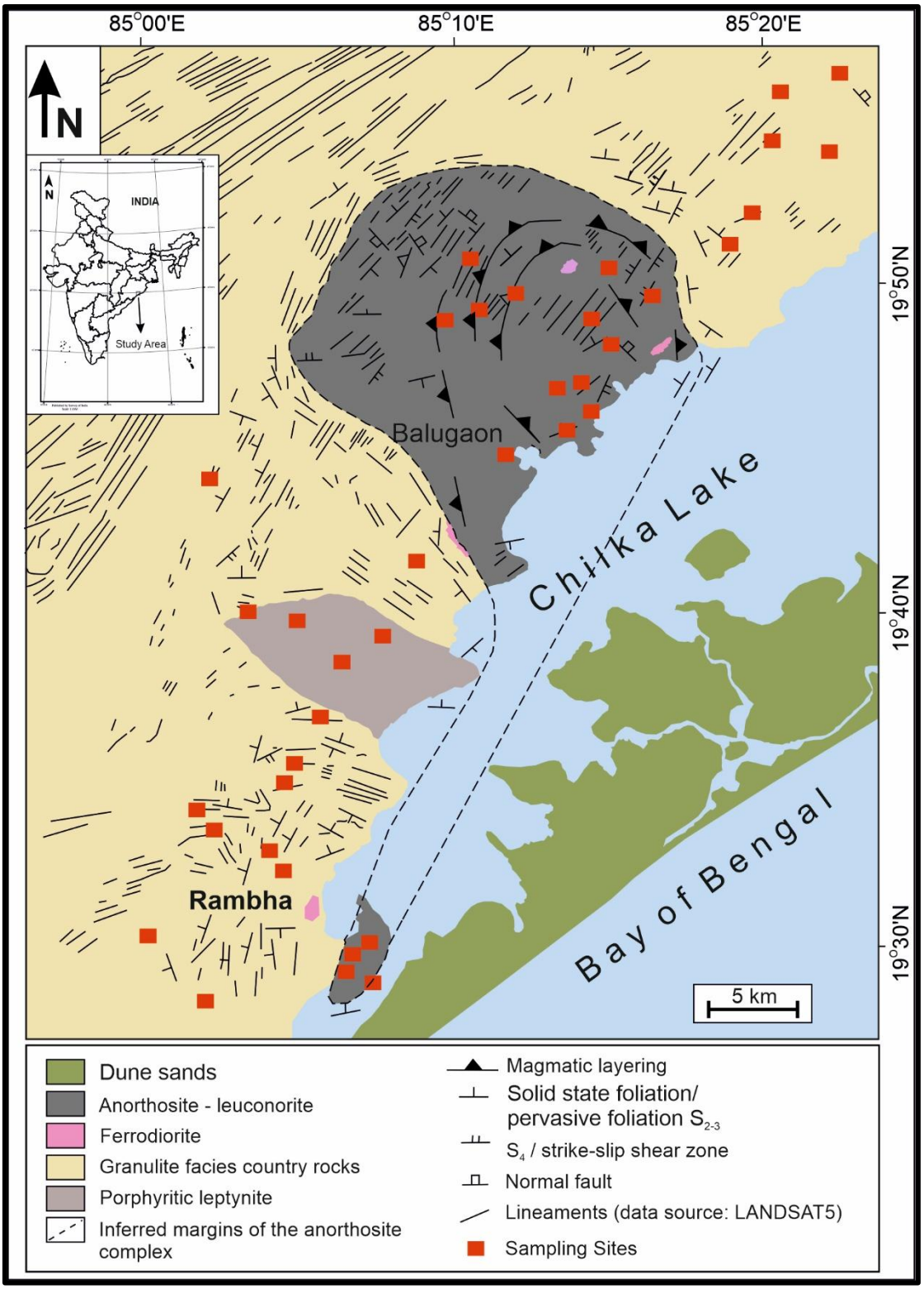

Fig. 2.3: General Geological Map of Balugaon-Rambha Anorthosite Massif Complexes, Chilka Lake, Eastern Ghats Mobile Belt, India (after Dobmeier and Simmat, 2002).

Mostly D_2 to D_4 are evident in both megascopic and mesoscopic scale, and a detailed description regarding the metamorphic assemblages that formed during various

phases of deformation allowing a detailed co-relation between these two processes are evident. These microstructural studies put strong evidence that the peak metamorphic stage is (M_2-D_2) assemblage and hence (M_3-D_3), (M_4-D_4) assemblages developed at post peak metamorphic stage, during the retrograde path.

2.1.1: Regional Scale Structures:

Observing the Balugaon Massif Anorthosite area, Chilka Lake, Odisha, EGB in regional scale, the markable lithotypes are anorthosite, khondalite, leptynite and a mix rock suite of granulites. Four stages of penetrating deformations are distinguished structurally. The primary S_0 is not preserved due to multiphase deformation and transposition of the S_0 with other related structural fabrics during the high-grade metamorphism. S_1 is also rarely preserved in regional scale. The S_2 which formed during the D_2 deformation is preserved in rock units and it is folded regionally as a result of D_3 deformational event. In regional scale the S_2 gneissic foliation varies from E-W to NE-SW at the northeastern part and N-S towards the southwestern part. F_2 is not observed in regional scale. The F_3 is close to tight fold, with regional trend NE-SW. The S_3 formed at the time of D_3 deformational event, signifies S_2 is almost parallel to S_3 at the limb of F_3 fold in regional scale. It is tight to isoclinal in nature. D_4, the last deformational activity, resulted in F_4 folds on S_2 or S_2 / S_3 foliation that truncated with F_3 in regional scale. The F_3 shows variable axial traces, this may have occurred due to the modifications during D_4 deformation. General trend of F_4 axes is N-S to NW-SE on regional scale. In the anorthosites the foliation has weak variation as a result of D_4 deformation.

2.1.2: Mesoscopic and Microscopic Structures:

$M_1 – D_1$ Assemblage: The imprint of the primary compositional band (S_0) has completely vanished and the initial planar fabric is the schistosity (S_1) only recognisable under microscope. Due to multiple deformation and high temperature metamorphism the earliest planar fabric S_1, is almost removed from macroscopic to megascopic scale. But microscopically S_1 is visible in the granulites. Folded foliation of sillimanite, biotite, ilmenite and quartz represent the planar fabric (S_1). Hence, these represent the early M_1 – D_1 assemblage, which developed in the pre-peak metamorphic condition.

$M_2 – D_2$ Assemblage: During the D_2 deformation, the mesoscopic penetrative foliation (S_2) formed which is well defined by gneissic fabric. Almost all the rocks of the area have imprints of this S_2. Because of the later deformational events the S_2 varies from the north-east to that at the south-western part. M_2 is the peak assemblage within all the litho-units.

$M_3 – D_3$ Assemblage: The folded S_2 is visible in all the litho-units as regional folding. The F_3 is the resultant fold formed during this stage. It is a type to isoclinal fold with a gentle inclination and plunge. Some indication regarding plunge reversalsis also stated. Newly formed S_3 fabric is defined differently in different litho-units. Within khondalite the S_3 is defined by the flattening of the quartz and feldspar present from beforehand, axial planar to the F_3 folds. In all F_3, S_2 and S_3 are at high angle at the hinge. Whereas at the limbs of the isoclinal F_3 the S_2 and S_3 are parallel to each other. Within the aluminous granulites, the S_2 foliations are refolded to form small F_3 folds. Within the leptynite, the F_3 folds are isoclinal recumbent to gently plunging to inclined sub horizontal folds. During the M_3 phase the minerals which stabilized during the peak metamorphic event showed partial to complete removal of the inter growths. In all the rocks the breakdown or refinement of the porphyroblastic grains are a result of M_3 events.

$M_4 – D_4$ Assemblage: The D_4 deformation affected the S_2 gneissic foliation along with the transposed $S_2|S_3$ fabric. The folds formed during the D_4, are open to upright to steeply inclined with a different plunge amount (12˚-53˚) towards NW. Mostly, the F_4 axial plane orient along NW-SE direction, with some exception. Only some spaced cleavage developed along the axial plane of the F_4 fold, because the strength of this deformation was not strong to develop penetrating features all over. The last deformational event altered F_3 folds based on the orientation of folded $S_2|S_3$ transposed fabric, interlimb angle of F_3 folding, orientation of local strain ellipsoid and relation with changing F_3 fold axes. There is an angular relationship between the axial planes of F_3 and F_4 folds. This deformation rotated the early formed F_3 fold axes but not in the whole area.

Four folds deformational event on the basis of satellite image studying with a rare field data was also stated by Dobmeier and Raith (2000) and Dobmeier and Simmat (2002). Workers related with three- and four-folds deformational system

suggests compositional layering (S_0), which is really difficult to understand after such an intense high-temperature metamorphism of the rock. Bhattacharya et al., (1994) stated that S_0 was folded isoclinally at the D_1 deformation stage. He also stated that F_2 is isoclinal fold, where S_1 is partially transformed to S_2. F_3 fold was open and upright, with S_3 visible along the axial plane of F_3 as fracture cleavage within metapelites and migmatite complex. Dobmeier and Simmat (2002) and Dobmeier and Raith (2003) stated that the compositional layering (S_0) during D_1 deformational event folded tightly forming a layer-parallel axial planar S_1 fabric. These workers believed that the fine grained leucosome layer within the 'migmatite complex' marks the S_2 and S_3 which transposed in nature.

2.2. Metamorphism:

The exposed rocks of the EGMB are high-grade gneisses experiencing regional granulite facies metamorphism. Three distinguishable metamorphic events can be explained by field and petrographic observations. The earliest identifiable units are supracrustal rocks, which were intruded by mafic magmas and ultramafic bodies. Thes bodies got deformed during the first granulite facies metamorphism (M_1), the ultra-high temperature (UHT) metamorphic condition reaching a temperature about 950˚C and a pressure 9kb (Sengupta et al., 1990, 1991; Dasgupta et al., 1991, 1992, 1993, 1994, 1995, 1996; Sen et al., 1995; Bhowmik et al., 1995 and Shaw and Arima, 1996a, b). In several locations, these rocks of EGB experienced partial melting. During the second-generation granulite facies condition (M_2) a huge amount of enderbite intruded and metamorphosed at a UHT condition, 6-8 kb and 800˚C-850˚C. Another generation of partial melting occurred. This granulite facies event (M_2) defines the main fabric defining (D_2). The mineral assemblages often reflect the physicochemical circumstances associated with the second regional metamorphism. Later, to this peak M_2 event, a tectono-thermal event occurred, when a voluminous granites intruded along with a huge anorthosite body at the Chilka Lake segment of the Eastern Ghats Belt (Bhattacharya et al., 1994). These activities show signatures of metamorphic (M_3) and deformation (D_3). Imprints of these three metamorphic and deformation events are evident from the area regionally.

2.3. Tectonic Evolution:

Age (Ma)	EVENTS	
550-650	Exhumation and stabilisation (= Pan African)	
800-850	Emplacement of anorthosite massifs, some alkaline rocks (?), younger granitoids and charnockites	
950-1100	Main Eastern Ghats orogeny (=Grenville)	
	Khondalite Group	Garnet-sillimanite-graphite gneiss (khondalite) with minor cordierite-sapphire-spinel gneiss (Mg-Al gneiss). Calc-silicate rocks and rare marbles Quartzites (garnet+sillimanite)
~1500	Emplacement of alkaline rocks along the rift margins.	
1800-1600	Evolution of platform ('Purana') basins like Cuddapah, Chattisgarh, Indravati etc. Evolution of Nellore-Khammam schist belt in Dharwar Craton.	
2600-2800	Charnockites and gneisses of basements (WCZ).	

Table 2.1: Event Stratigraphy of EGMB (Ramakrishnan and Vaidyanadhan, 2008).

Isotope study of the Chilka Lake Anorthosite Complex: The coeval and co-magmatic character of the ferrodiorites makes U-Pb zircon data acceptable for determining anorthosite emplacement time. The Chilka Lake ferrodiorites have prismatic zircon grains, with zoned igneous centers with uneven boundary probably of metamorphic origin. The data points acquired from abraded grain fractions are consistent, indicating an age 792±2 Ma. This is indicating the age of the magmatic crystallisation forming the ferrodiorite (Krause et al., 2001). Hence, the Chilka Lake Anorthosite Complex, emplaced at the same time that of ferrodiorite792±2 Ma. This also proves the formation of the Chilka Lake Anorthosite is post-date to that of Grenvillian deformation and high-grade metamorphism. So, the Chilka Lake Anorthosite experienced a ductile transgressive deformation and high-grade metamorphism during an individual orogenic event.

Chapter: 3

SAMPLING PROCESS AND SAMPLE PREPARATION

3. Sampling Process and Sample Preparation:

The oriented drilled-core samples with a specific dimension are very much essential for different types of magnetic experiments in laboratory. The drilled-core samples should be prepared from oriented block samples or the oriented core samples were collected using Portable Drill Machine and Sun Compass from in-situ rock exposures in field (Figs. 3.1a and 3.1b) for the Rockmagnetic, Palaeomagnetic and Anisotropy of Magnetic Susceptibility (AMS) measurements. The core samples of specific dimension (i.e., 2.54cm in diameter and 2.2cm in height) were drilled out from oriented block samples, which were collected from field. The oriented block samples were collected from different rock types in and around Balugaon and Rambha areas of Odisha for different types of the magnetic experiments and petrographic studies. More than 150 nos. of oriented drilled core samples were collected from 25 sites considering the variation of lithology of the studied area.

In field we used clinometer to mark and orient the in-situ outcrop before detaching the block sample. All the block samples were well-marked before collecting. Either of the two processes was used to orient before collecting the samples:

I. By marking the horizontal lines with the help of clinometer and marker on the adjacent side walls of the outcrop, the geographical north was also marked on the top surface of the exposed in-situ rock (Fig. 3.2a).
II. By marking the attitude of the top surface of the in-situ rock sample and marking the geographical north with the help of a clinometer and marker (Fig. 3.2b).

The second method of collecting the block samples is generally used where the adjacent walls are not available in the outcrop. For the present study, both the processes were used to collect the oriented block samples from Odisha. The oriented block samples were collected from different rock types, which were brought back to section preparation laboratory and individual core sample with specific dimension were prepared in this laboratory. For petrographic studies and the Fe-Ti oxide studies polished thin sections were prepared from the chip samples obtained from the block samples (Fig. 3.3).

Fig.: 3.1: a) Sample collection using portable drilling machine, b) Data collection using sun compass in the field, c) Drilling apparatus and associated accessories for sampling, d) Drilled core samples in the field, e) and f) Collecting data from the field.

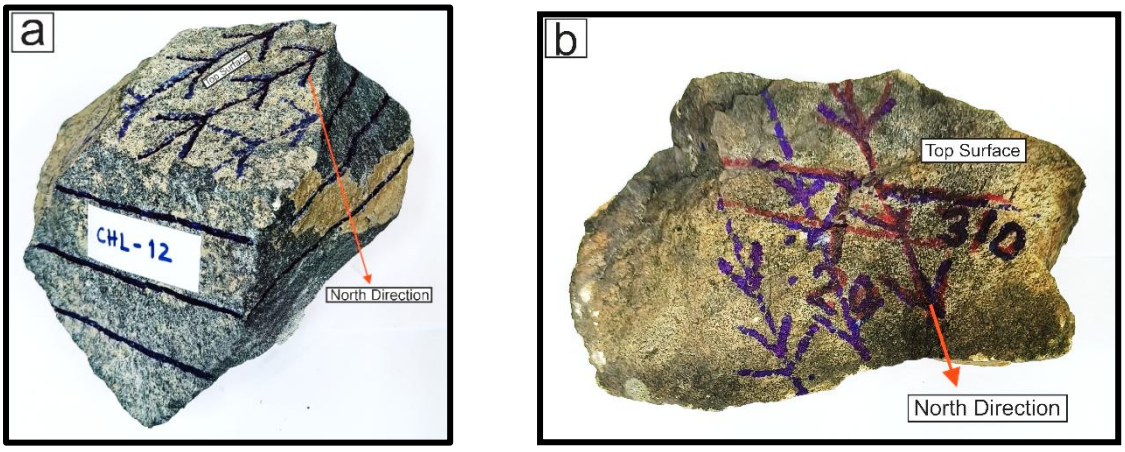

Fig.: 3.2: Processes of collecting oriented block samples.

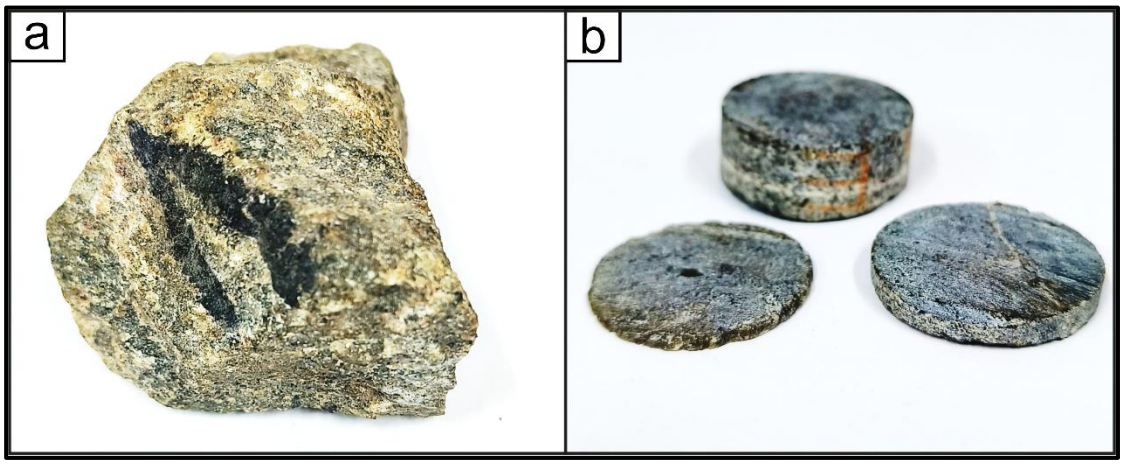

Fig.: 3.3: Chip samples.

Some of the samples were drilled at the sampling site itself where the access of water was easy. The portable drilling machine along with the sun compass was carried to some of the field sites. During the day time with proper sun visibility these samples were taken. For each core the north was marked on the top surface and the vertical line

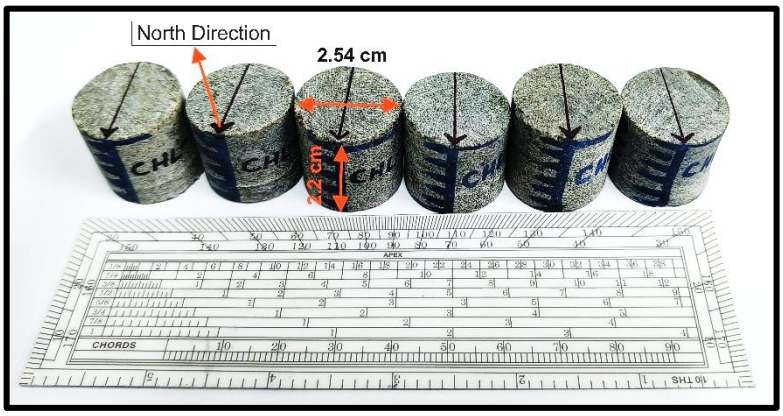

Fig.: 3.4: Oriented core samples of specific dimension.

is drawn along the slit of the sun compass. Some of the important data are noted like, the latitude and longitude along with the date and time (IST). While coring on the surface of the in-situ outcrop the dip angle, Y-site and the shadow angle are noted for the recalculation of the cores attitude after returning to the laboratory. From each site at least 6 cores were drilled out of definite size, 2.54cm in diameter and 2.2cm in height and all the data were noted for individual core sample.

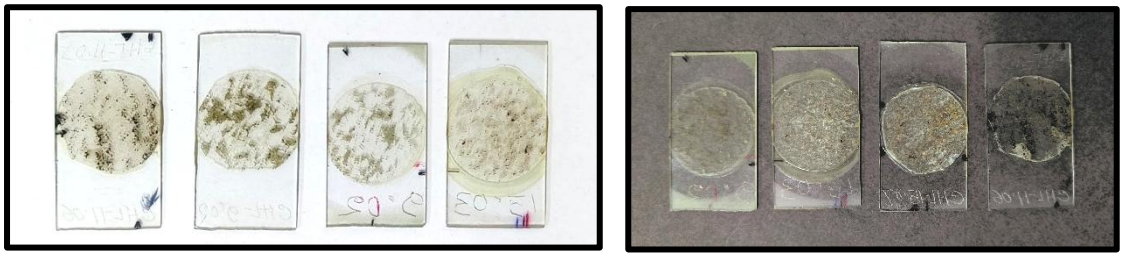

Fig. 3.5: Polished thin sections.

The AMS and the Palaeomagnetic studies required the core samples (2.54cm and 2.2 cm). On the top surface of each of the core samples the north was marked using heat proof marker (Fig 3.4). The marking was done so that the samples can be oriented during various magnetic measurements. At some time while drilling the top surface may wear out, hence a vertical line is drawn along the surface and towards the

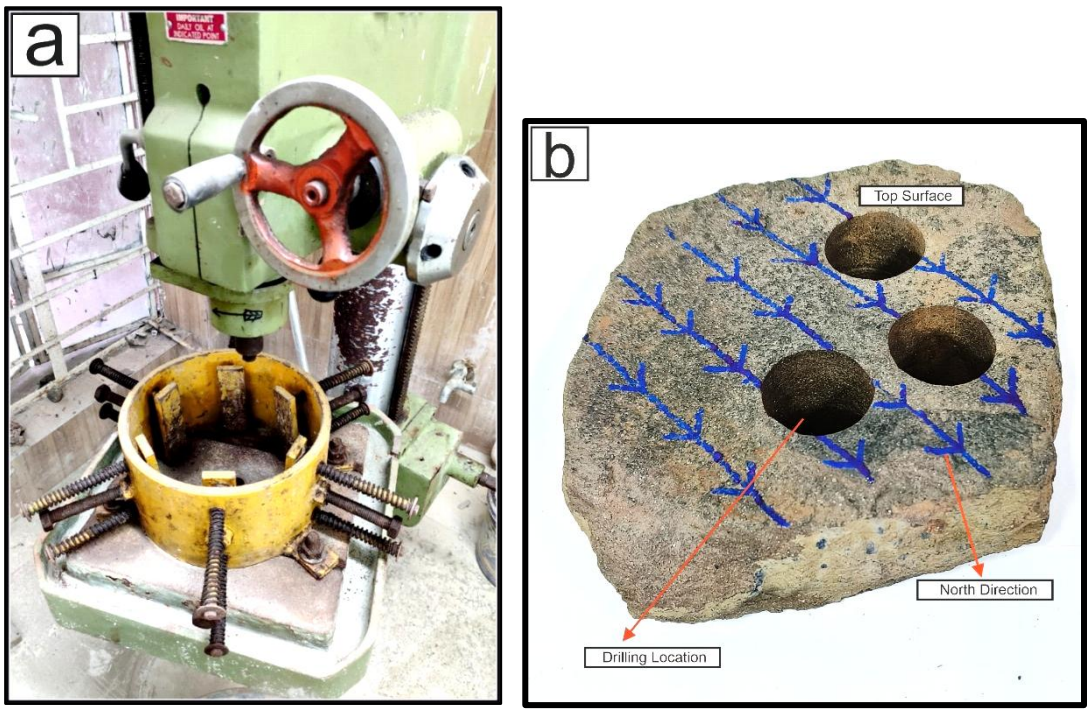

Fig.: 3.6: a) Drilling machine, b) Oriented block sample vertically drilled.

right of the arrow head the dash is marked (Fig 3.4). Polished thin sections are made for the microscopic study (Fig. 3.5). Using the drilling machine (Fig 3.6a), the vertical coring (Fig 3.6b) was done at the rock cutting laboratory of Jadavpur University with non-magnetic diamond drill bit.

For the Rockmagnetic measurements, a part of the sample was also mortared to powder, at the laboratory of the Department of Geological Sciences, Jadavpur University, Kolkata. All the rock-magnetic measurements were carried out in the Geomagnetism Laboratory at CSRI-NGRI, Hyderabad using Advanced Variable Field Translation Balance (AVFTB) (Fig. 3.7). The AVFTB is an ultra-sensitive instrument

Fig.: 3.7: Photograph of Advanced Variable Field Translation Balance (AVFTB).

with multifunctional capability. All the rockmagnetic measurements are done using this instrument. The Curie Temperatures (upto 800°C), the Isothermal remanent magnetisation acquisition curve as well as Backfield and Hysteresis loops all are acquired with the help of a sophisticated windows software connected with the instrument. For these studies samples required in very few quantities (450-500mg).

The main laboratory equipment for measuring the magnetic susceptibility is the Bartington Susceptibility Meter (MS-2) (Fig. 3.8) at Geophysical Laboratory, Jadavpur University. The MS2 Meter comprises portable measuring instruments, the MS2 meter and a variety of sensors. The measurements are obtained digitally using a time dependent method. This results in precise and repeatable measurements. The sensors are independently calibrated before every measurement.

Fig 3.8: Photograph of Bartington Susceptibility Meter (MS-2).

The demagnetization measurements were carried out in the Geomagnetism Laboratory at CSRI-NGRI, Hyderabad, using the Thermal Demagnetization Process. For this experiment a Portable Spinner Magnetometer (PSM) (Fig. 3.9) and the Thermal Demagnetizer (TD) (Fig. 3.10) machines were used. The PSM was calibrated before starting every batch of samples. Each core sample was measured in four

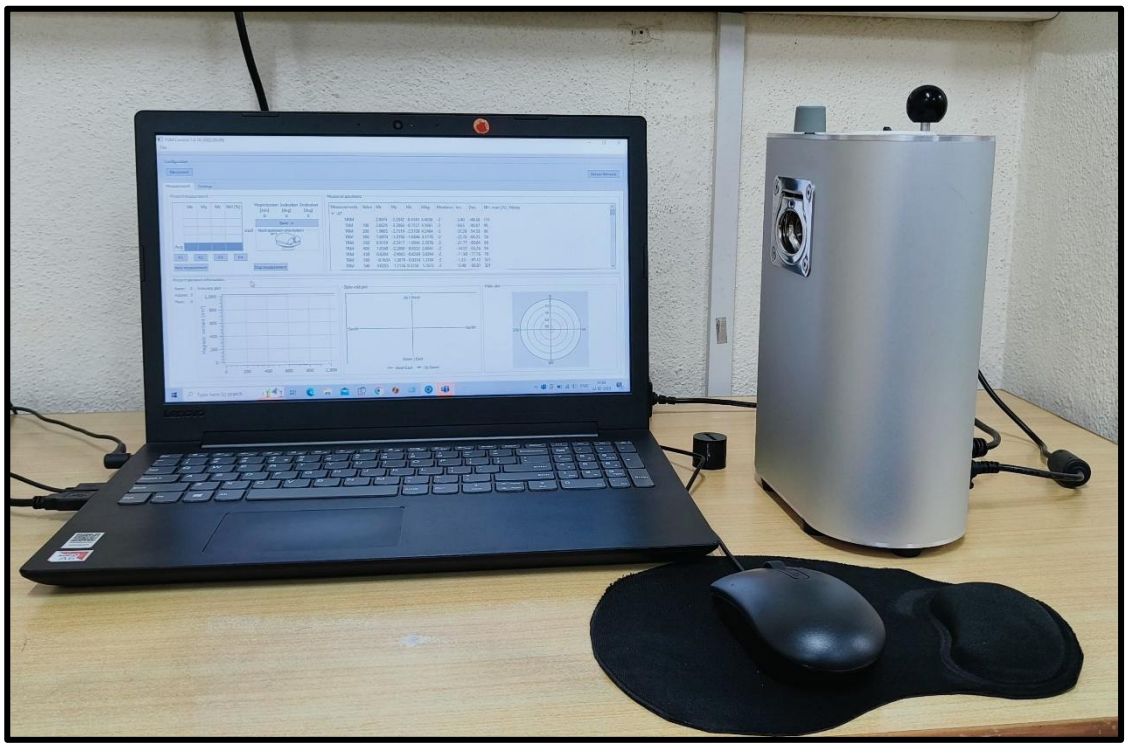

Fig. 3.9: Portable Spinner Magnetometer (PSM).

directions with respect to the North marking on the core for measuring the intensity of magnetization before the heating process (NRM) and also after each progressive step of heating for knowing the remaining magnetization intensity. The TD was used for demagnetizing the samples step by step upto 700°C.

Fig. 3.10: Thermal Demagnetizer.

Chapter: 4

PETROGRAPHY AND MINERALOGY

4. Petrography and Mineralogy:

4.1. Introduction:

The highly deformed and metamorphosed areas of the Indian Precambrian denotes the Eastern Ghats Orogenic Province of the Indian Sheild. Both the high-grade terrain of the Archean time (Windley and Bridgwater, 1971) and Precambrian Anorthosite massifs are present in the study area (Chatterjee, 1960; De 1969). The study area is characterised by multiple ultrahigh temperature metamorphism (UHT). The Eastern Ghats belt has the unique character among the Precambrian belts of Indian Peninsula due to the presence of charnockite, khondalite, leptynite, enderbite, quartzo-feldspathic granulite gneiss, calc-silicate granulite and anorthosite. The massif anorthosite intruded within the Archean high-grade granulite facies rocks in most of the Proterozoic mobile belts of the World (Ashwal, 1993). The granulite rocks of the Eastern Ghats granulitic terrain along with the Anorthosite massifs were further metamorphosed to UHT granulite facies metamorphism (Dobmeier and Simmat 2002).

The major rock type concern of the study area is the Balugaon Anorthosite, which was first introduced by Perraju (1960). These anorthosite massifs have been restudied by many other workers for last few decades – among them De (1969); Perraju (1973); Raith et al., (2007); Dobmeier and Simmat (2002) and Sengupta et al., (2008). The Rambha Anorthosite massif is also under consideration in this study, which was first introduced by Ray (1952). Later, De (1969) gave an elaborate petrographical account of these rocks. Hence, the study comprised the large Balugaon Massif in the north and the small isolated Rambha Massif towards the south (Fig. 2.3). The high-grade granulite facies, calc silicate rocks in and around these anorthosite massifs are also under consideration.

Surrounding the anorthosite massifs several major rock types have been identified in the Balugaon-Rambha, Chilka Lake area. These rock types are garnet sillimanite gneiss (khondalite), calc-silicate granulite, mafic granulite, leptynite, orthopyroxene granulite, enderbite and charnockite. In spite of all the petrographic study by several workers, no such importance or interest was ever showed to the textural relations between the silicate and the opaque minerals. The different textures of the Fe-Ti oxides can also help to reveal the metamorphic history of the studied

rocks. The grain size, shape and textural association of the silicate grains as well as oxide grains are studied under the transmitted and reflected light microscope.

4.2. Petrology and Mineral Assemblages:

Petrographical study reveals that, the major litho-units of the concerned studied area as follows:

1. Anorthosite,
2. Orthopyroxene Granulite,
3. Mafic Granulite,
4. Leptynite, and
5. Khondalite,

A brief mineralogical description of each rock type is as follows:

4.2.1: Anorthosite:

The anorthosite of the Balugaon-Rambha, Chilka area has the major cumulus phases, as plagioclase, clinopyroxene, amphibole and oxides. They show a granoblastic texture with plagioclase porphyroblasts as the main constituent (Figs. 4.1a and 4.1b).

Ample amount of plagioclase feldspar is present throughout the samples. The plagioclase is present in two modes; one is as porphyroblasts and the second is as recrystallized small plagioclase grain (Fig. 4.1c). The porphyroblasts of plagioclase show triple junction sharing prominent sharp grain boundary (Fig. 4.1d). They show tapered lamellar twinning along with bend lamellar twinning (Fig. 4.1f), which indicates deformation. The recrystallized small plagioclase along grain boundaries or within the groundmass indicates post-crystalline deformation. These small recrystallized plagioclases show no twinning and are associated with the porphyroblasts (Fig. 4.1e).

4.2.2: Orthopyroxene Granulite:

The orthopyroxene granulite of the Balugaon-Rambha, Chilka area, is coarse grained with adequate amount of orthopyroxene, followed by plagioclase, k-feldspar,

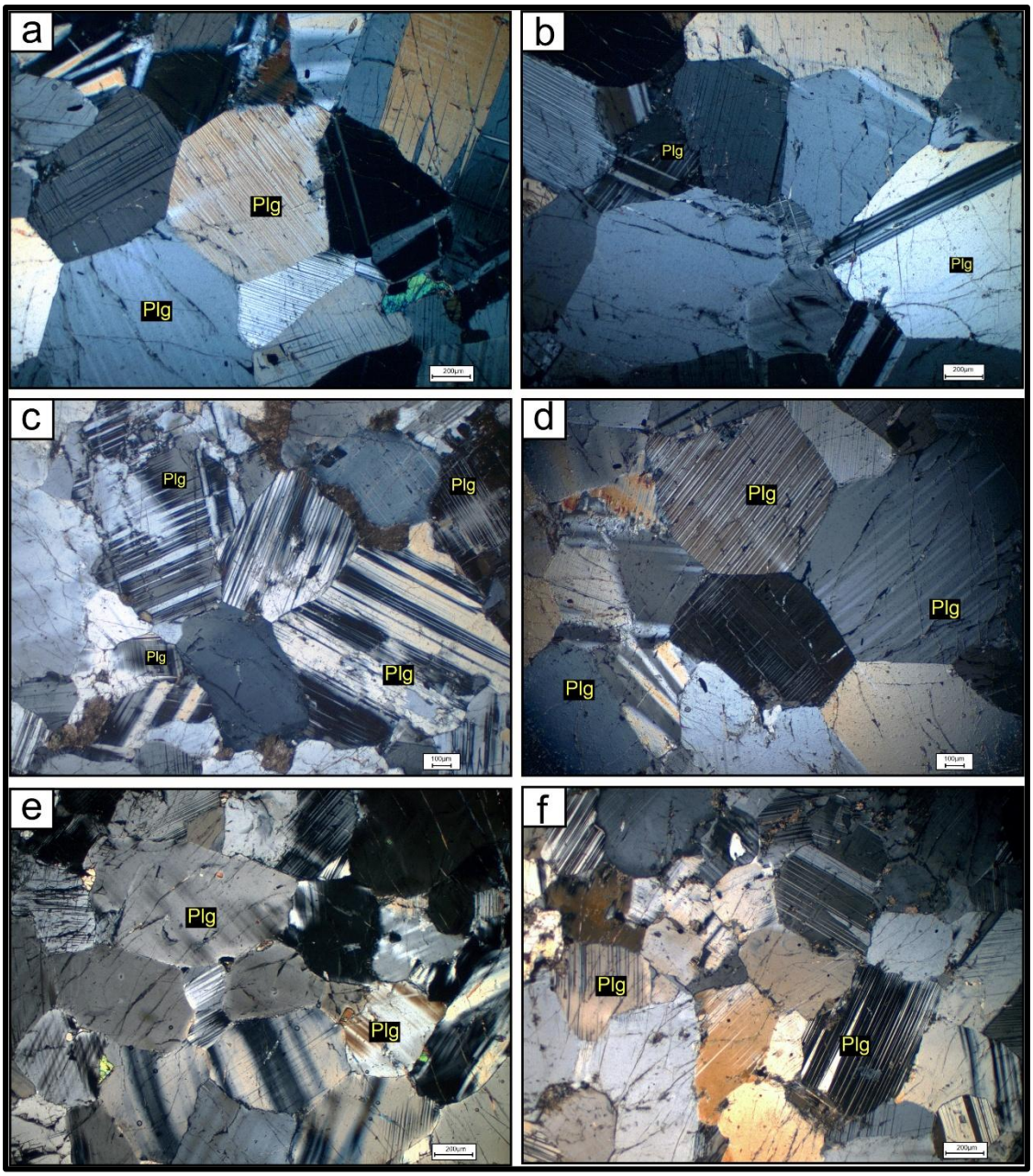

Fig. 4.1: a) and b) Anorthosite defined by ample amount of plagioclase feldspar (XPL), b) Tapered lamellae within plagioclase porphyroblasts (XPL), c) Recrystallised plagioclase associated with other porphyroblasts, d) Plagioclase porphyroblast showing triple junction (XPL), e) Highly deformed plagioclase feldspar as the phenocrysts within Anorthosite (XPL) and f) Bend lamellar twinning along with tapered lamellar twinning (XPL).

garnet and minor amount of quartz and biotite (Fig. 4.2a). Mesocratic rocks with ortho pyroxene and quartz porphyroblasts are scattered throughout. The plagioclase, k-feldspar are also present within the framework and the orthopyroxenes have sharp contact with each other.

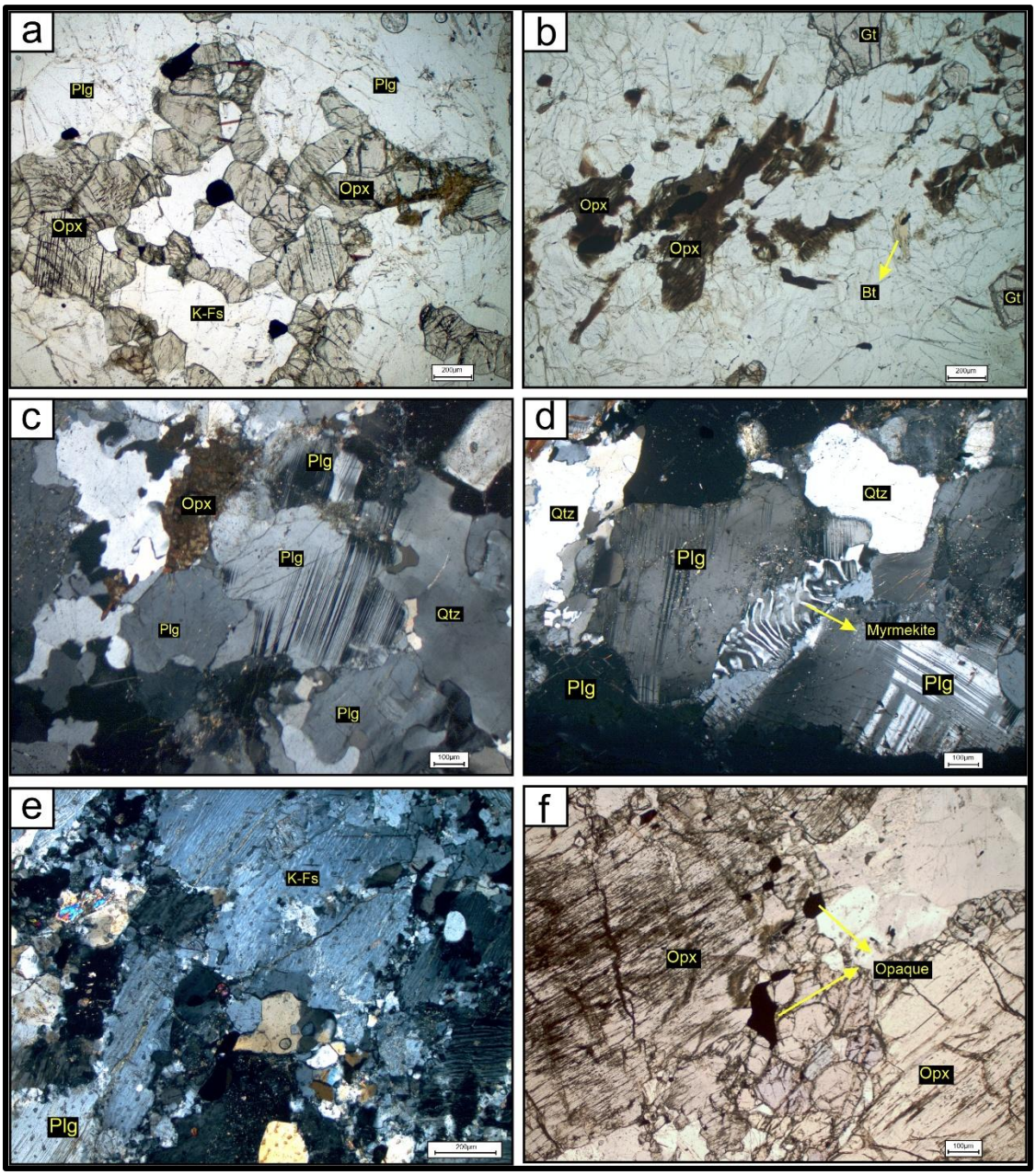

Fig. 4.2: a) Orthopyroxene granulite showing granoblastic texture defined by plagioclase, orthopyroxene, k-feldspar and minor opaque (PPL), b) Orthopyroxene granulite showing granoblastic texture defined by orthopyroxene, plagioclase, k-feldspar and minute garnet, biotite and opaque (PPL), c) Tapered lamella in plagioclase porphyroblasts (XPL), d) Wedge shaped twinning within plagioclase. Also, myrmekite replacing the periphery of Plagioclase (XPL), e) K-feldspar showing perthitic texture. Along the grain boundary recrystallized grains are present (XPL) and f) Opaque as inclusion with in orthopyroxene (PPL).

The orthopyroxene granulite defines a granoblastic texture by orthopyroxene, plagioclase, k-feldspar, opaque, garnet and minor biotite (Fig. 4.2b). Coronal garnet separates the orthopyroxene from the k-feldspar. The feldspar and orthopyroxenes

present within the studied sample are highly fractured. Lamellar twinnings of the plagioclase feldspars are not continuous, but tapered (Fig. 4.2c). Orthopyroxenes are not only present as coarse grains but also as smaller fine grains at some zones along some grain boundaries (Fig. 4.2e). Inclusions of opaque minerals are observed within the orthopyroxene as well (Fig. 4.2f). The opaques are present along the grain boundaries and also as large coarse grain within the framework (Fig. 4.2e).

The coronal garnet or the garnet-quartz symplectite separates the orthopyroxene and opaque minerals (Fig. 4.3b). Overall, the lamellar twinning was observed in different form. Some of the plagioclase has prominent shape and continuous lamellar twinning (Fig. 4.2d). At places where it has intense deformation, the lamellar twinnings are deformed, tapered and discontinuous throughout the grain. Smaller quartz, feldspar, orthopyroxene grains surround the larger porphyroblast grains defining recrystallization (Fig. 4.2e). These small grains are strain free recrystallized grains. Overall, these zones are high strain zones where orthopyroxene grains show recrystallization into smaller strain free grains which indicates varying degrees of deformation.

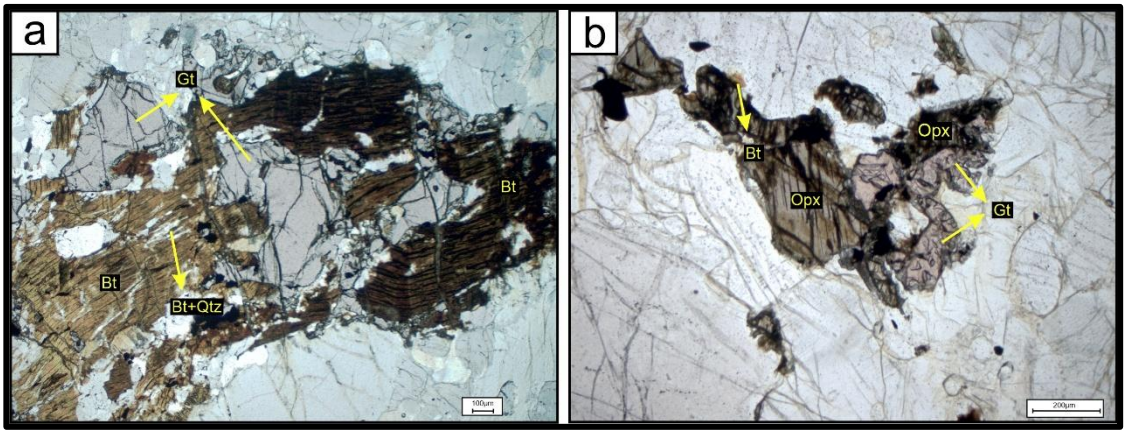

Fig 4.3: a) Highly foliated biotite and fractured garnet porphyroblast with opaque inclusions. Quartz-biotite symplectite (PPL) and b) Coronal garnet rimming opaque and orthopyroxene (PPL).

Acicular shaped biotite associated with orthopyroxene and garnet are present (Fig. 4.3 a). Highly foliated biotite and orthopyroxene associated with fractured garnet and opaque minerals where biotite inclusions are present within the fractured garnet (Fig. 4.3a). The opaque inclusions within the orthopyroxene are observed (Fig. 4.2f). Quartz intergrowths with plagioclase known as myrmekite are observed replacing the k-feldspar along the grain boundary (Fig. 4.2 d).

The k-feldspars present in the studied samples are of orthoclase and microcline variety. Adequate perthites are also present. Perthite shows k-feldspar as host with blebs like exsolution of plagioclase feldspar which resulted due to un-mixing of k-feldspar with some plagioclase at low temperature (Fig. 4.3e).

After studying all the orthopyroxene samples, it can be said that there are two types of garnet present. One is the porphyroblastic garnet (Fig. 4.3a) and the other one is the coronal garnet (Fig. 4.3b). The porphyroblastic garnets are of various shapes, some rhombic, some equant shape with fractures. Inclusions of oxides, biotite are seen. On the other hand, the coronal garnet rims the orthopyroxene along the periphery forming a boundary in between feldspar and orthopyroxene (Fig. 4.3b). Quartz and orthopyroxene also occur in two modes, one as the porphyroblast (Fig. 4.2a) and other as small recrystallised grains (Fig. 4.2e).

The biotite occurrences are also in two modes. One is as elongated foliated biotite associated with oxides, k-feldspar, orthopyroxene and garnet as the framework mineral (Fig. 4.2b). Biotite and quartz symplectite, probably indicates retrograde type (Fig. 4.3a). Inclusions of biotite within garnet (Fig. 4.3a) probably indicate prograde type.

4.2.3: Mafic Granulite:

The mafic granulites of the Balugaon-Rambha, Chilka area are coarse to medium to fine grained. The major minerals comprising the rock are orthopyroxene, clinopyroxene, plagioclase, k-feldspar, garnet, quartz, biotite and oxides (Fig. 4.4a). The rock samples studied are mesocratic in nature. The orthopyroxene porphyroblasts are anhedral to subhedral in shape and distributed almost all over the studied samples. The orthopyroxenes are embedded randomly within the quartzo-feldspathic matrix. The orthopyroxene does not show preferred orientation. The orthopyroxene has sharp contacts with the oxide minerals (Fig. 4.4b). Some of the orthopyroxenes have inclusions of quartz (Fig. 4.4c). The clinopyroxene also appears in more than one mode. Clinopyroxene porphyroblasts occur randomly within the studied rock with sharp contacts with surrounding grains (Fig. 4.4b). The clinopyroxenes are also subhedral. Another type of clinopyroxene is symplectic clinopyroxene associated with

coronal garnet, quartz, oxides rimming the porphyroblasts of orthopyroxene, clinopyroxene, plagioclase (Fig. 4.4d).

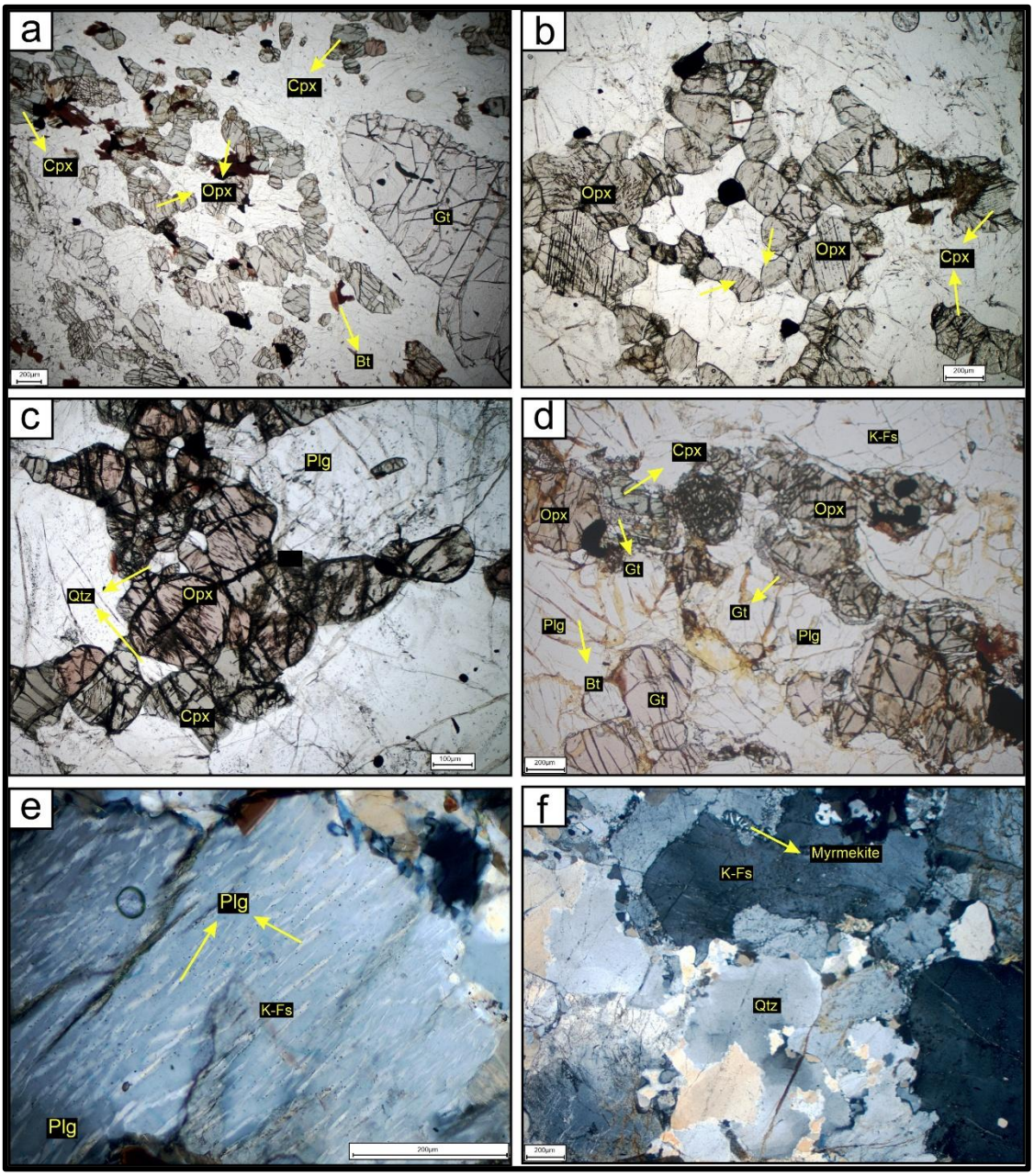

Fig. 4.4: a) Mafic granulite consisting orthopyroxene, clinopyroxene, plagioclase, quartz, garnet, biotite and opaque (PPL), b) Opaque minerals having sharp contact with orthopyroxene (PPL), c) Inclusion of quartz within orthopyroxene and clinopyroxene (PPL), d) Coronal garnet between quartz and orthopyroxene. Coronal garnet rimming orthopyroxene, clinopyroxene and opaque (PPL), e) K-feldspar showing perthitic texture with intergrowth of plagioclase within it (XPL) and f) Bimodal quartz grain with polycrystalline quartz. Myrmekite along the grain boundary of k-feldspar.

The plagioclase grains are also present in three different modes. Firstly, the plagioclase porphyroblasts, which associate with the orthopyroxene as well as clinopyroxene, quartz, garnet, biotite (Fig. 4.4b). At some places, it is separated by coronal garnet from the surrounding k-feldspar, orthopyroxene and clinopyroxene (Fig. 4.4d). Secondly, the occurrence is as exsolved plagioclase within host k-feldspar defining perthitic texture (Fig. 4.4e). Similarly, the K-feldspar is present as porphyroblasts, and as host for the perthite (Fig. 4.4e).

The quartz within the studied rock is present in different modes (Fig. 4.4f). The size of quartz is from coarse to fine. At some places, quartz is present as porphyroblasts. The polycrystalline quartz defines deformation. The occurrence of garnet within the mafic granulite is occurred as corona rim along the boundary of clinopyroxene and orthopyroxene (Fig. 4.4d).

4.2.4: Leptynite:

The Leptynite of the Balugaon-Rambha, Chilka area are medium to fine grained and leucocratic in nature. The leptynite has a crude alternate banding of light colour quartzo-feldspathic band with dark garnet-biotite band (Fig. 4.5a). The dominant minerals of the leptynite are k-feldspar, plagioclase, quartz, garnet, biotite and oxide minerals (Fig. 4.5b). The rock is bimodal in nature, coarse equant grains as well as finer grains in the groundmass and along grain boundaries (Fig. 4.5b). The coarse plagioclase grains are found as porphyroblasts throughout the rock section (Fig. 4.5b). Some occurs as inclusion within the garnet (Fig. 4.5c). The plagioclase is also showing myrmekitic intergrowth along the periphery (Fig. 4.5d). The lamellar twinnings are discontinuous and tapered defining deformation (Fig. 4.5d). Fine plagioclase grains are found along some grain boundaries indicating recrystallization (Fig. 4.5e). The quartz is present as porphyroblasts within the studied sample (Fig. 4.5b). The quartz is also observed as inclusion within the garnets (Figs. 4.5c and 4.5f). The undulose extinctions of the quartz indicate deformation (Fig. 4.5e).

The elongated biotite grains are observed within the studied sample, forming the gneissic nature along with garnet grain (Figs. 4.5a and 4.5d). The biotite occurs as inclusion, which is also present within garnet (Fig. 4.5c).

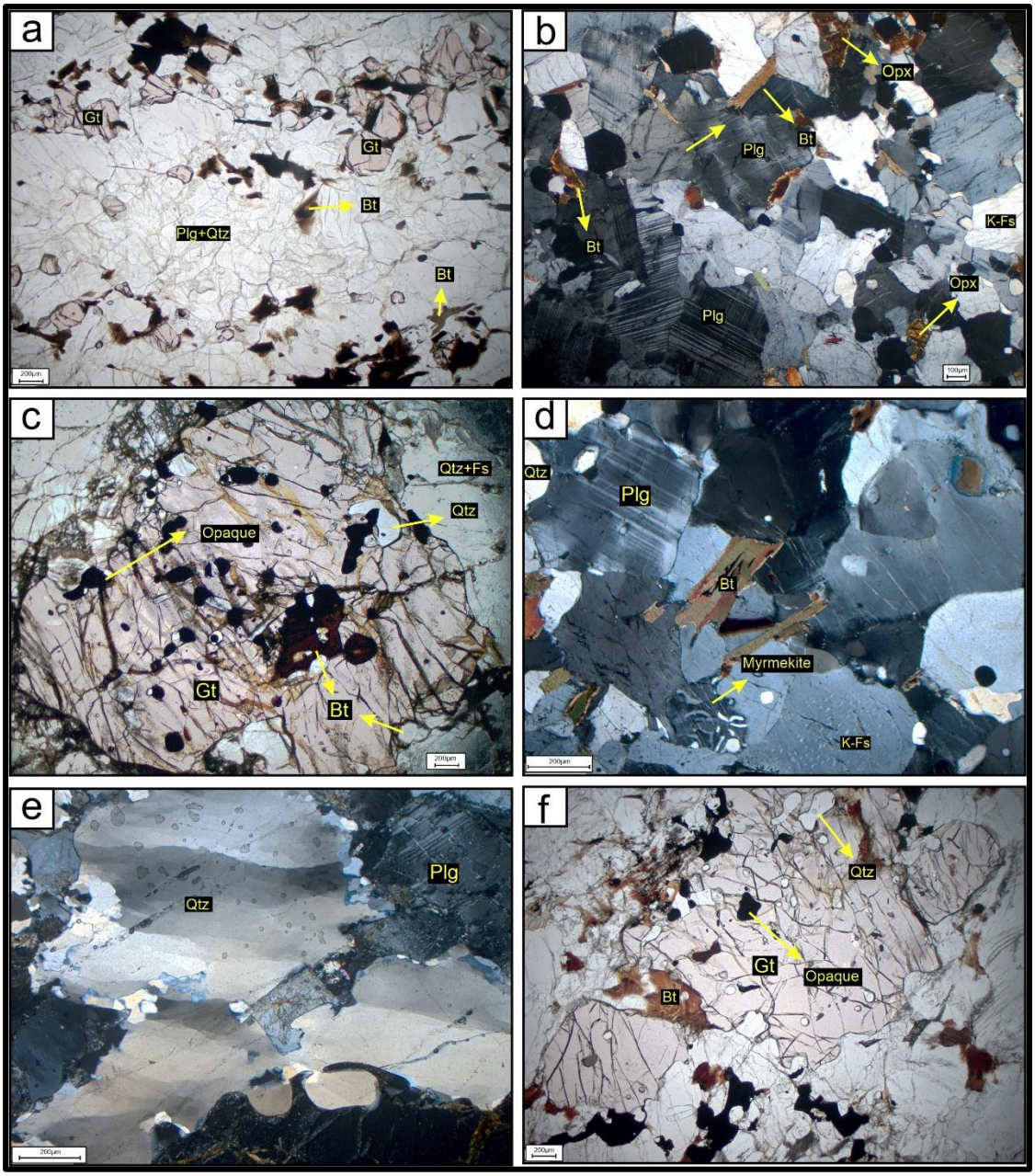

Fig. 4.5: a) Gneissic banding defined by alternate garnet-biotite rich layer and quartzo-feldspathic layer (PPL), b) Leptynite consisting of bimodal feldspar, quartz, biotite, garnet, pyroxene and opaque (XPL), c) Fractured pink garnet with inclusions of quartz, biotite and opaque (PPL), d) Myrmekite along the k-feldspar grain boundary. Discontinuous tapered lamellae in plagioclase (XPL) e) Quartz showing undulose extinction and recrystallised grain along the grain boundary (XPL) and f) Coarse grained garnet with numerous inclusions (PPL).

The garnets are very coarse grained with fractures (Fig. 4.5f). The garnets are pinkish in colour with numerous inclusions within it. The inclusion of quartz and opaque oxides are observed (Fig. 4.5f). The garnets are also associated with the biotite and opaque minerals, forming the darker band defining the gneissosity (Fig. 4.5a).

4.2.5: Khondalite:

The khondalite of the Balugaon-Rambha, Chilka area shows distinct gneissic bands within the samples (Fig. 4.6a). The bimodal grain present, medium to coarse sized grains observed throughout the slide (Fig. 4.6b). The minerals observed are quartz, feldspar, sillimanite, garnet, and oxides (Fig. 4.6a). The gneissosity is defined by sillimanite band with quartz and feldspar band. The elongated and highly fractured sillimanite grains are present within the studied sample (Fig. 4.6c). The sillimanites are colourless under plane polarised light but shows variegated colour under cross polarised light. The sillimanites are also present as inclusions within garnet grain.

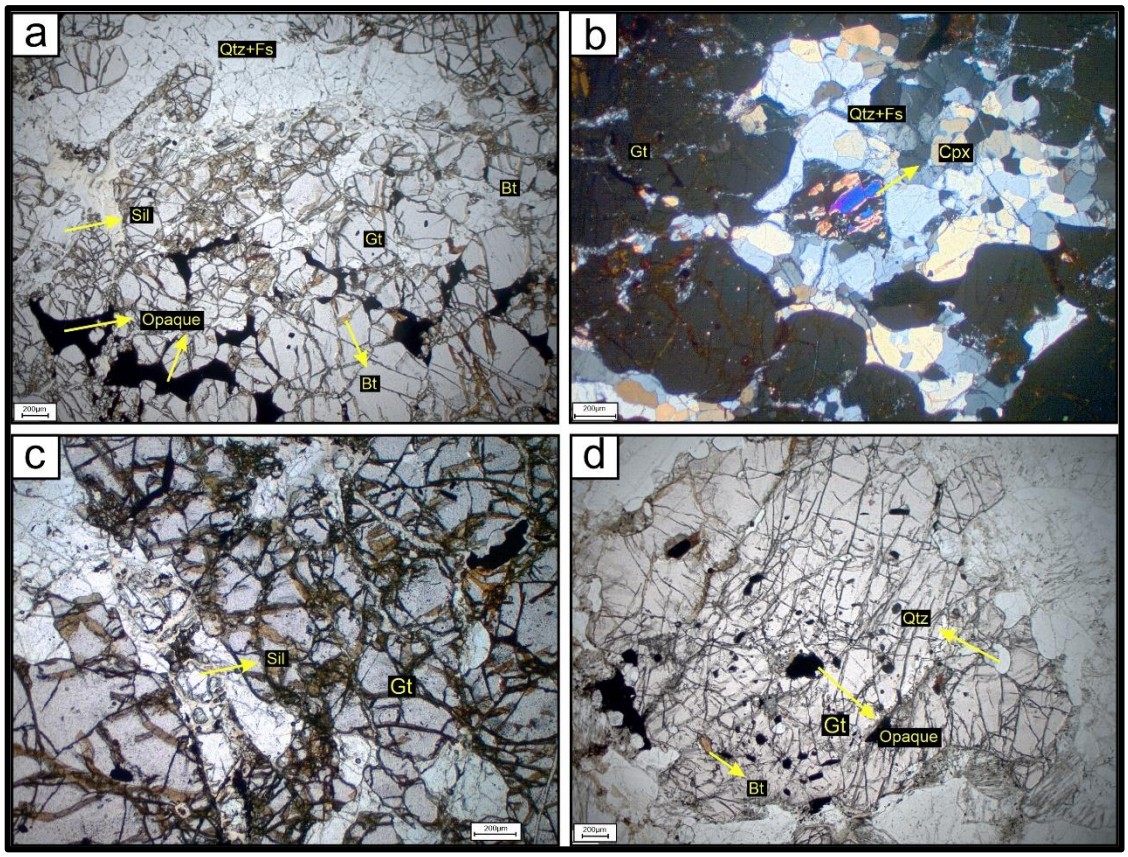

Fig. 4.6: a) Khondalite consisting quartz, plagioclase, garnet, sillimanite, biotite and opaque defining gneissosity (PPL), b) Bimodal grain size in khondalite (XPL), c) Fractured garnet and laths of sillimanite (PPL) and d) Garnet porphyroblast containing inclusion of quartz, opaque and biotite grain (PPL).

The equant garnet grain is present as porphyroblasts. Most of the garnets are highly fractured, broken apart into smaller fragments (Fig. 4.6d), which denotes deformation. The opaque inclusion, biotite and quartz inclusions form the sieve

texture within garnet (Fig. 4.6d). Throughout, the sillimanite and the garnets have a textural equilibrium with each other.

The k-feldspar and pyroxene both are present as the porphyroblasts. Both are medium to small grains in nature. The smaller grains occur along grain boundary or concentrate at a particular zone. The small grains of k-feldspar are also observed as inclusions within garnet. The quartz shows undulose extinction and the sillimanite present along the fracture (Fig. 4.6a).

Chapter: 5

MAGNETO-MINERALOGICAL STUDY

5. Magneto-mineralogical Study:

5.1. Theoretical Concepts:

The primary Fe-Ti oxide mineralogy plays an important role in the field of Rock-magnetism and Palaeomagnetism. These primary Fe-Ti oxides play a vital role in storing the natural magnetic phases i.e., the magnetic remanent carrier within the rocks. Further, these minerals help in interpreting the magnetization history of the country rocks. In the metamorphic rocks mainly the granulite facies, the oxide minerals are mostly Fe-Ti oxides and it records all the subsequent changes that effect during metamorphism. These chapter deals mainly with the different types of Fe-Ti oxides associated with the anorthosite and surrounding high-grade rocks of Balugaon-Rambha sector nearby Chilka Lake, Eastern Ghats Belt of India. The basic study regarding the magneto-mineralogy of the studied rocks has been carried out here. The different phases and generations of Fe-Ti-oxide minerals have and their change from primary crystal in igneous rocks or sub-solidus changes that the Fe-Ti oxides face in the igneous rocks or sedimentary and metasedimentary rocks can be explained.

5.1.1: Ternary diagram of Fe-Ti oxides:

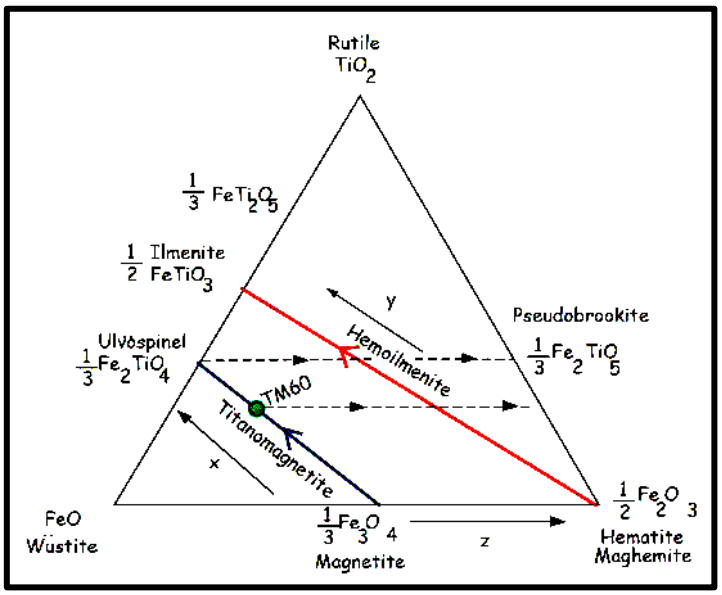

Fig. 5.1: Ternary diagram for Iron-oxides (modified from O'Reilly, 1984).

The different compositional Fe-Ti oxides are well classified in a ternary diargram. The TiO_2-FeO-Fe_2O_3 ternary diagram (Fig. 5.1) (Haggerty, 1976; Tauxe, 2010 and Piper, 1987) explains the magnetic oxides, on the basis of two solid solution

series. The extreme left enf at the bottom is Fe^{2+}, just the opposite end at the extreme right is Fe^{3+} and at the top is Ti^{4+} (Fig. 5.1). The three oxide minerals at these extreme ends of the triangle are Wustite (FeO), Haematite or Maghemite depending on the compositopnal structure (Fe_2O_3) and Rutile (TiO_2).

The study of the Fe-Ti oxides are the only concerned, those are on the two solid solutions. Titanomagnetite and titanohaematite (Fig. 5.1), because it is said that the igenous and the metamorphic rocks are constricted along these solid solution series (Grant and West, 1965). In (Fig. 5.1), the solid lines represent the solid solutions, and the solid arrows indicates the direction of increasing titanium incorporation within the crystal lattice structures of magnetite and haematite.

'x' denotes the amount of Ti within titanomagnetite

'y' denotes the amount of Ti within titanohaematite

The 'x' and 'y' value ranges from 0 (magnetite or haematite) to 1 (Ulvospinel or Ilmenite).

***Titanomagnetite*:** In igneous rocks Ti-magnetites accur as primary minerals. Detrital magnetites are often available within the sediments, which can also be as a result of bacterial product or during diagenesis by authigenesis. Magnetite in igneous rocks can be as a result of high temperature (Butler, 1992).

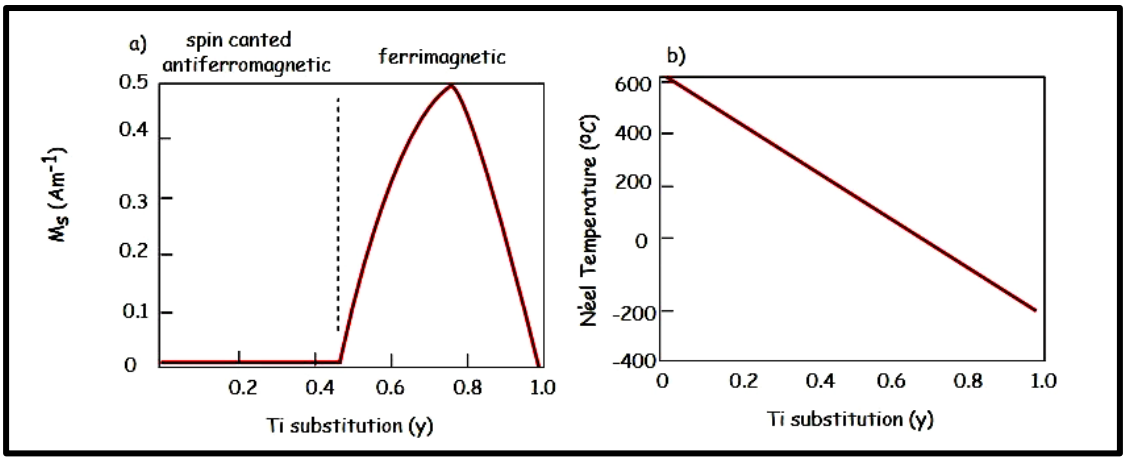

Fig.5.2: Variation of properties with Ti substitution in titanohaematite series. a) Saturation magnetization variation. b) Neel temperature varition. (Redrawn from Butler, 1992).

The general formula of titanomagnetite is $Fe_{3-x}Ti_xO_4$. The end members of titanomagnetite solid solution series are:

Magnetite $Fe^{3+}|Fe^{3+}\ Fe^{2+}|\ O_4$; x=0

Ulvospinel $Fe^{2+}|Fe^{2+}\ Ti^{4+}|O^4$; x=1

With the increase in 'x' the saturated magnetization decreases, and the temperature decreases due to increase in cell dimension (Butler, 1992 and Tauxe, 2010).

***Titanohaematite*:** In igneous rocks the haematite occurs as a very high temperature oxidation product (Tauxe, 2010 and Tarling Hrouda, 1993).The magnetic property of the red beds are dominated by haematite, even the oxidised sediments have huge amount of haematite which a good for palaeomagnetic study (Butler, 1992). The grain size among other properties has a huge role on the appearance of haematite, either black (specularite) or red (pigmentary) haematite. In most igneous rocks the Ti-magnetites are the major oxide minerals, where the titanohaematites and its associated oxidezed products have lesser contribution to the ferrimagnetic minerals, but Butler 1992, the highly oxidised igneous rocks have adequate amount of haematite. Substitution of Ti within the lattice structure of αFe_2O_3 also has a strong hold towards magnetic properties.

The substitution stages are as follows:

Where, y= 0; magnetization is spin-counted antiferromagnetic

y= 0.45; magnetization become ferrimagnetic (Fig. 5.2)

y> 0.45; resulting ferrimagnetic behaviour, Ti^{4+} ions have no net moment and the Ti cations occupy alternate layers.

5.2. Solid Solution Series:

The complete solid solution of both the marked line (Fig. 5.1), between magnetite and ulvospinel along with haematite and ilmenite takes place at a temperature above 600ºC. There are many metastable crystals in between with different x and y proportions, and thus the exsolution is hindered if the crystals cool rapidly. With decrease in temperature, the ilmenite and titanohaematite exolve outforming crystals with Ti-rich and Ti-poor lamallae (Fig. 5.3). Both the solid solutions have a very interesting property from the palaeomagnetic point of view.

Above the solid lines complete solid solution exists, but below the solid lines the exsolution starts as the temperature cools.

The initial composition of a certain liquid, the exsolution lamellae form alternating Ti-rich and Ti-poor bands. In the presence of demagnetization field of the

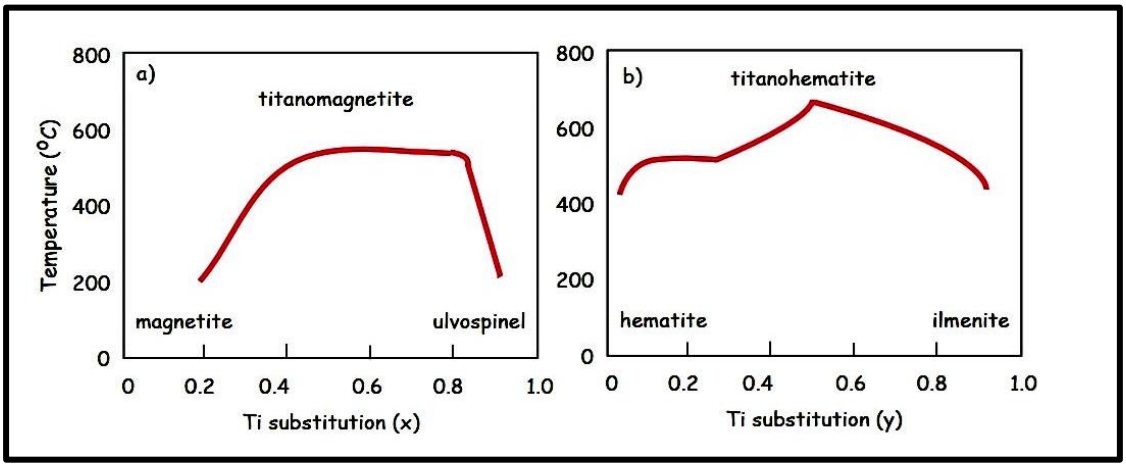

Fig. 5.3: Phase diagrams for Fe-Ti oxides. x and y indicates the composition. a) Titanomagnetite series. b) Titanohaematite series. (Redrawn from Dunlop and Ozdemir, 1997).

Ti-poor bands, the Ti-rich bands will get magnetized when their Curie temperature (T_c) is reached. Thus, aquire a remanence, which is antiparallel to the applied field. Finally, since these bands will have higher magnetization, the overall NRM will also show antiparallel to the applied field. This phenomenon will make the NRM antiparallel to the applied field and thus the rocks get self-reversed (Tauxe, 2010).

5.3. Oxidation of Fe-Ti Oxides:

Based on the history of evolution of the rock, the minerals which are crystallized under on eset of equilibrium condition and mostly the new phase are generally more oxidising than the initial phase when they were formed. Thus, the minerals follow the dashed line with increasing degree of oxidation (Fig. 5.1) (Tauxe, 2010).

The magnetic minerals of the Fe-Ti oxides on the basis of oxidation are classified as follows (Butler, 1992).

5.3.1. Primary Oxidation:

In the early stage of the crystallization of the igneous rocks, both the magnetites and the Ti-magnetites crystallize at a temperature ~1300ºC. The high-grade granulitic rocks and anorthosite, which are the major rock types of the study area, have both Ti-magnetite and magnetite present. The temperature attained by such rocks have major effects on the oxides present due to fluctuation of temperature. Both high and low temperature oxidation of primary oxides are present with their identifying features.

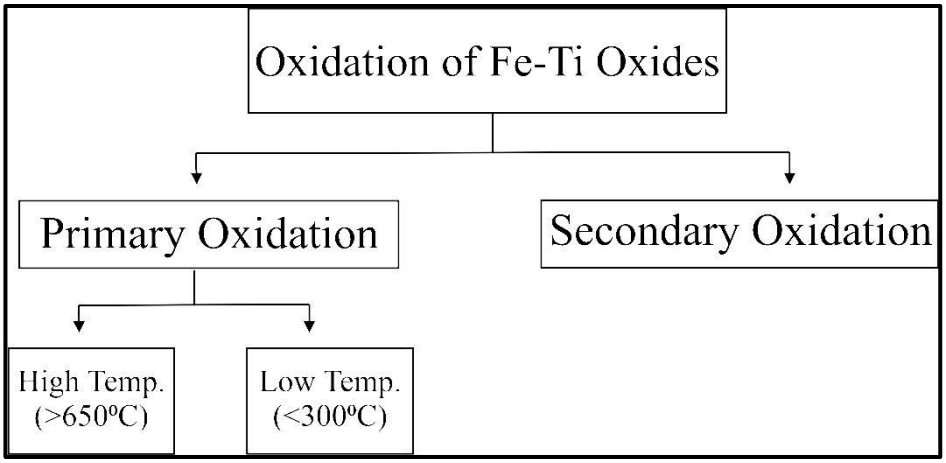

Fig. 5.4: Generations of Fe-Ti Oxides.

5.3.1.1 High Temperature Oxidation of Fe-Ti Oxides:

Two different textural assemblage of Fe-Ti oxides result by oxidation of Ti-magnetite; they are: Exsolution and Deuteric Oxidation.

***Exsolution*:**

Exsolution or oxidation exsolution is the process of formation of ilmenite lamellae along (111) parting planes in Ti-magnetite which is also called the trellis ilmenite (Buddington and Lindsley, 1964). Both the solid solutions, Ti-magnetite and Ti-haematite exists complete solid solution, at their crystallization temperature above ~1300ºC. At a temperature below this, at the intermediate compositions, the Ti-rich and Ti-poor zones get exsolved by solid state diffusion of Fe and Ti cations (Buddington and Lindsley, 1964). The primary homogeneous oxide grains change into alternate zones of Ti-rich (Fe-poor) and Ti-poor (Fe-rich), by the process of exsolution.

***Deuteric Oxidation*:**

Oxidation which takes place during the time of original cooling of an igneous rock is name as Deuteric Oxidation. This takes place post exsolution pseudomorphic oxidation resedue like rutile Ti-magnetite and pseudo-brookite. The ideal situation for the deuteric oxidation is 750ºC and fO_2 around 10^{-5}-10^{-6} atmospheres (Butler, 1992), generally above Curie temperature. This oxidation results in alteration of the primary Ti-magnetites and titanohaematite. By the alteration in Ti-magnetite, they are not any further homogeneous grain, they are grains with ilmenite laths along (111) plane of the host titanomagnetite. After the oxidation the host titanomagnetite become Fe enriched and proceed towards pure magnetite (Butler, 1992). Due to deuteric oxidation, in the titanomagnetites the characteristics of the magnetic property changes. The grain size changes drastically. The primary grain gets divided into several smaller grains seperated by paramagnetic ilmenite. Fe-rich titanomagnetite has both higher Curie temperature as well as higher saturation magnetization, hence the deuteric oxidation changes the magnetic properties. The rocks in the study area are entirely composed of Ti-magnetites. So, here in this study, I would like to concentrate only on the titanomagnetites.

The high temperature oxidation was classified into several stages by Haggerty (1976). The prefix 'C' is reffered to the oxidation stages those have resulted from Cubic phases.

C1 Stage: Optically homogeneous titanomagnetite solid solutions enriched with Ulvospinel.

C2 Stage: Titanomagnetite having the small number of "exsolved" ilmenite lamellae along (111) crystallographic plane.

C3 Stage: Titanomagnetite with densely crowded "exsolved" ilmenite lamellae along (111) crystallographic plane.

C4 Stage: Mottling of lamellar ilmenite – intra-lamellar titanomagnetite inter-growth and development of ferri-rutile in metailmenite lamellae.

C5 Stage: Rutile and titanohaematite extensively develop within the meta ilmenite lamellae and rutile-titanohaematite assemblages develop incipiently within the titanomagnetite.

C6 Stage: The incipient pseudo-brookite forms during this stage and three

phase assemblages, rutile, pseudo-brookite and exsolved spinel develop with or without unoxidized titanomagnetite.

C7 Stage: Pseudobrookite $_{(S\ S)}$ and haematite $_{(S\ S)}$ coexist with this stage of oxidation.

5.3.1.2 Low Temperature Oxidation of Fe-Ti Oxides:

The low temperature oxidation of Fe-Ti oxides differs in many respects from the high temperature oxidation. The low temperature oxidation generally takes place at a temperature below 300ºC. Either the weathering of the titanomagnetite at low temperature (ambient surface temperature) or the hydrothermal alteration which leads to the cation deficient spinel. This low temperature oxidation is a good example of 'Maghematization'. Maghematization is the process of yielding maghemite (γ-Fe_2O_3) from magnetite by low temperature oxidation. Maghemite retain the spinel structure but chemically similar to haematite. During maghematization the Fe^{2+} ions migrate creating a vacancy (Butler, 1992; Akimoto et al., 1984 and Johnson and Hall, 1978). Due to high mobility of Mn^{2+} and Mg^{2+} cations, they also migrate (Akimoto et al., 1984). Morphologically, this is identified by the cracks formed around the periphery of magnetite and silicates migrate through these cracks. The vacant spaces which are termed as the shrinkage cracks reduce the volume of magnetite (Johnson and Hall, 1978 and Akimoto et al., 1984). The overall Si^{4+} content within the titanomagnetites is too low, so even by the migration of the mobile cations, the Si^{4+} content is not increased remarkably. The migrating Si^{4+} is mainly supplied from the surrounding silicate minerals, and hydro circulation is the most expected carrier, which balance the chemical potential gradient within the lattice and the environment (Akimoto et al., 1984). Due to these hydro circulations, a weak plane forms where the internal stress accumulates, and when these stress releases the curvi-planar, irregular cracks form (Akimoto et al., 1984).

Based on the identifying microscopic features, of the low temperature oxidation of the Fe-Ti oxides, Johnson and Hall (1978), classified several stages, as follows:

Stage-1: Unoxidised titanomagnetite: Homogeneous titanomagnetite rich in high titanium, free of cracks (unoxidised).

Stage-2: Partial oxidation: The growth of very fine to submicroscopic cracks

along the grain boundaries of titanomagnetite is indicated by the change into bright color.

Stage-3: Formation of cracks: Cracks are curvilinear and prominent with the presence of some non-opaque minerals replacing original titanomagnetite towards their grain margins.

Stage-4: Formation of veins: Early formed cracks were filled with silicates and numerous new cracks developed from the earlier cracks as branches. Red pigmentary strain appears growing surrounding the silicates.

Stage-5: Relic grains: Isolated, bright, greyish white relic grains are left after almost complete replacement of titanomagnetite by non-opaque silicate minerals.

5.4. Generations of Fe-Ti Oxides in Studied Rocks:

5.4.1: High Temperature Oxidation:

Under the reflected light microscope, the high temperature oxidations of primary titanomagnetites are observed. Anorthosite samples and a few granulite samples exhibit the high temperature oxidation features. The high temperature oxidation features are mainly observed within the phenocrysts of the studied rock. High temperature oxidation features are observed within the phenocrysts in anorthosite and granulite samples. The phenocrysts are euhedral to subhedral in shape. C-1, C-2 and later stage of C-3 to C-4 are observed within the samples of this study area.

The titanomagnetites are whitish grey in color with moderate reflectivity. Titanium defuses from the host mineral while oxidation of titanomagnetite, which changes the appearance of the oxides. The grain becomes whiter with increase in reflectivity. In the host titanomagnetite (CHL 9, CHL 23) of the high-grade metamorphic rocks shows ilmenite along (111) parting planes. Optically homogeneous, having sharp contact with the surrounding silicate porphyroblasts is the typical identifying character of the C-1 Stage (Figs. 5.5a and 5.5b). The C-2 Stage of high temperature oxidation, single fine hair like exsolved ilmenite lamellae appear along the (111) crystallographic plane (Fig. 5.5c). The ilmenite and the host titanomagnetite can be identified by their colour variation. With increasing oxidation

stage, the ilmenite lamellae merge together to form thick ilmenite lamellae along (111) plane within the host titanomagnetite (Figs. 5.5d and 5.5f). The exsolved ilmenite lamellae are sandwiched within the titanomagnetite and are identified separately by colour, pleochroism and sharp contact with each other.

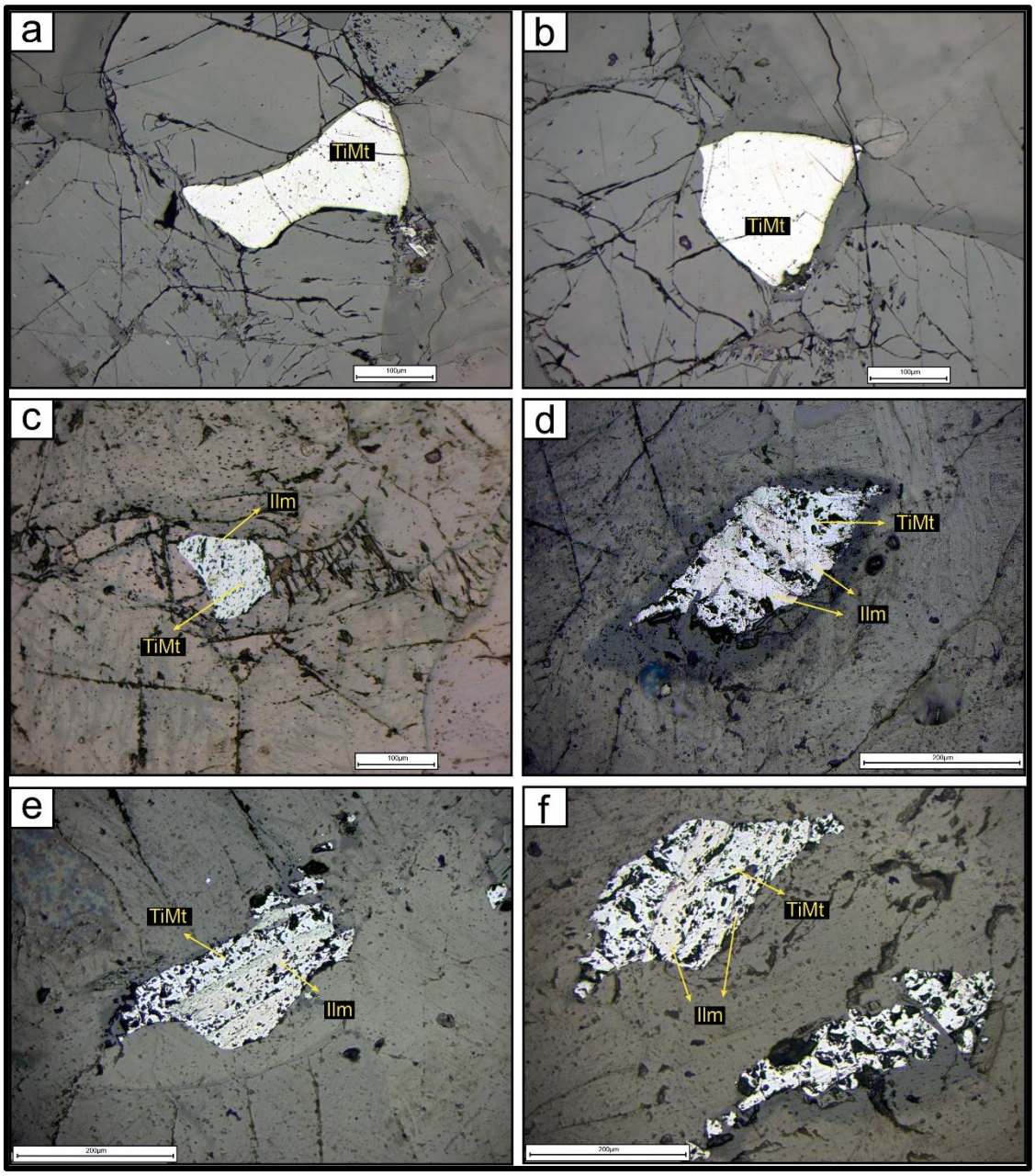

Fig. 5.5: a) and b) primary homogeneous titanomagnetite showing C1-Stage of high temperature oxidation (PPL), c) C2-Stage of high temperature oxidation of titanomagnetite showing one thin ilmenite lamellae (PPL), d) C3-Stage of high temperature oxidation of titanomagnetite showing thick exsolved lamellae of ilmenite, e) and f) crowded thick exsolved ilmenite lamellae within the titanomagnetites.

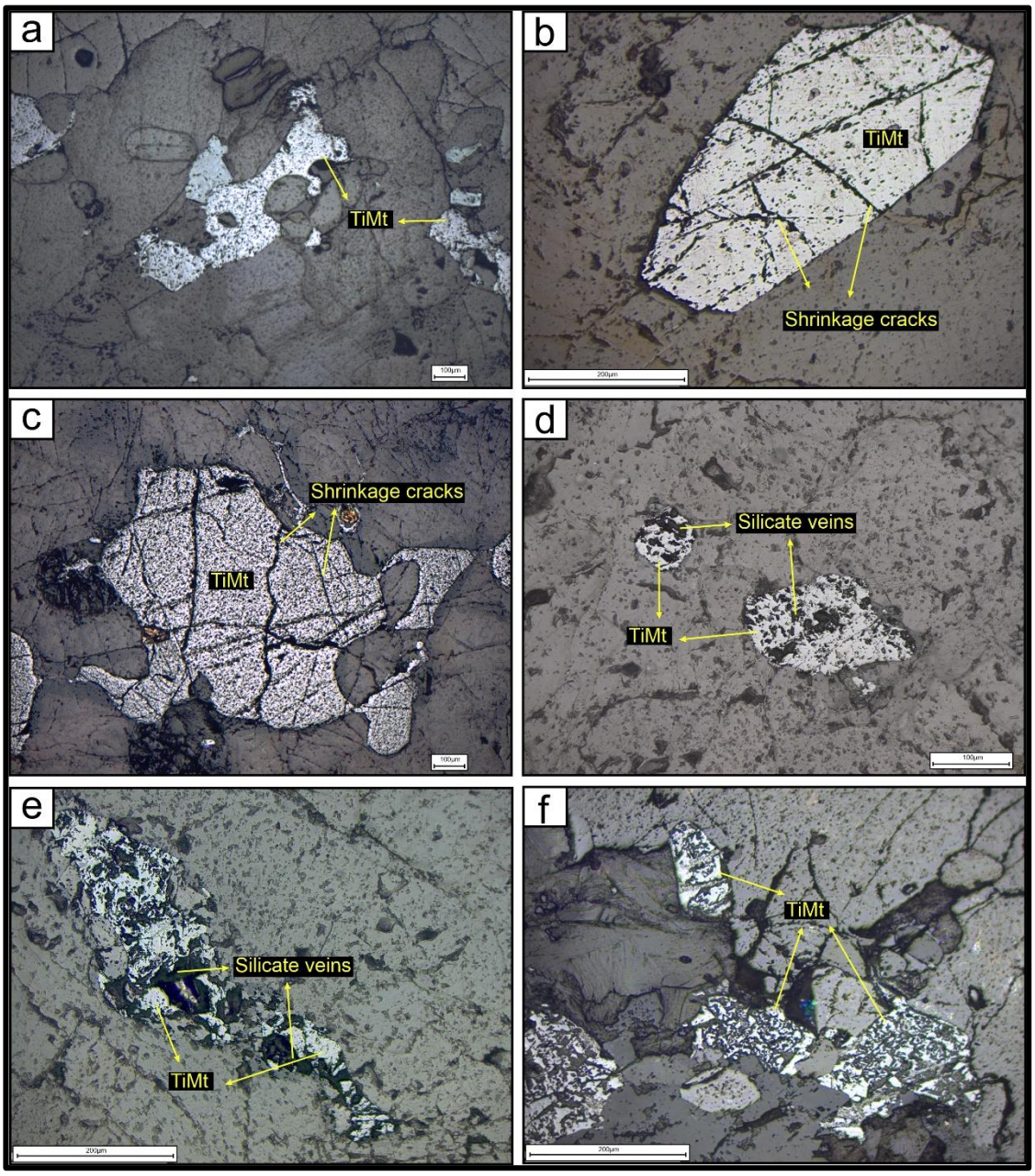

Fig. 5.6: a) Stage-1 of Low temperature oxidation in primary titanomagnetite (PPL), b) and c) Stage-2 of Low temperature oxidation in primary titanomagnetite (PPL), d) Stage-3 of Low temperature oxidation in primary titanomagnetite (PPL), e) Porphyroblast of primary titanomagnetite showing Stage-4 of Low temperature oxidation (PPL) and f) Porphyroblast of primary titanomagnetite showing Stage-5 of Low temperature oxidation (PPL).

In the granulites, the thick ilmenite laths, one – two laths are observed within the host titanomagnetite (Fig. 5.5e). These difference in texture, are the evidence of oxidation, which results in formation of the ilmenite laths from primary ulvospinel-magnetite solid solution.

The reaction that leads to C-2 and C-3 Stages of the high temperature oxidation are as follows (Haggerty, 1976b).

C-2: $6\ Fe_2TiO_4 + O_2 = 6\ FeTiO_3 + 2\ Fe_3O_4$ (Partial)

C-3: $4\ Fe_2TiO_4 + O_2 = 4\ FeTiO_3 + 2\ Fe_2O_3$ (Complete).

5.4.2: Low Temperature Oxidation:

Even low temperature oxidation of titano magnetite are observed in some of the samples of Balugaon-Rambha sector nearby Chilka Lake, Eastern Ghats Belt of India. The anorthosite, granulite, khondalite and leptynite show low temperature oxidation in the studied region. The most important identifying feature of low temperature oxidation of titanomagnetites are the curviplanar cracks of irregular shape along the periphery. The Stage-1, low teperature oxidation, the titanomagnetites are homogeneous and are free of cracks but a irregular grain boundary (Fig. 5.6 a). In Stage-2, minute thin cracks generate along the grain boundary of the homogeneous titanomagnetites (Figs. 5.6b and 5.6c). In Stage-3, these cracks further propagate inward forming secondary widened cracks (Fig. 5.6d). By further oxidation, these cracks get interconnected with each other which make the Ti-magnetite looks fragmented, which is the characteristic feature of Stage-4 (Fig. 5.6e). These cracks get widened and filled with silicates. In Stage-5, with increasing oxidation, only relicts of titanomagnetites are left within the grain boundary, which is almost replaced by silicates (Fig. 5.6f). Mostly, Stage-2 and Stage-3 titanomagnetites are found within the granulites and anorthosites. Very few Stage-4 to Stage-5 are observed. Small droplets of Ti-magnetite are left in few places indicating Stage-5 of low temperature oxidation (Fig. 5.6f). Hence, 'Maghematization' of Ti-magnetite is observed in the samples.

In the samples from Balugaon-Rambha sector nearby Chilka Lake, Eastern Ghats Belt of India, both high temperature oxidation and low temperature oxidation of titanomagnetite are observed. Within some sample both high and low Fe-Ti oxides are observed together. Besides the coarse grained primary Fe-Ti oxides, fine relatively smaller secondary Fe-Ti oxides are present in these studied samples. The association of secondary oxides are with the silicate minerals. The secondary Fe-Ti oxides are associated in different ways with the silicates. The secondary Fe-Ti oxides are present

along the grain boundary of garnet (Fig. 5.7a). Along the cleavage plane of pyroxene minute Fe-Ti oxides are present (Fig. 5.7c). The fine grain of Fe-Ti oxides are present along fracture plane (Figs. 5.7b and 5.7d) and cleavage plane (Fig. 5.7c) of silicates of the high-grade granulite samples. It is also present along along along the grain boundaries of silicate minerals (Fig. 5.7e).

5.5. Generations of Fe-Ti oxide and its Tectonic Implications:

The abundant amount of Fe-Ti oxides and their occurance within the high-grade metamorphic rocks of Balugaon-Rambha sector nearby Chilka Lake, Eastern Ghats Belt of India, are dependent on the composition of the rocks and the present mineral assemblage in stable phases and the temperature and pressure conditionduring metamorphism beacause all the rock forming minerals react with each other during metamorphism. The composition of the silicates, oxides and sulphides are interdependent and are controlled by oxygen fugacity and also the suphur fugacity of the fluid (Nesbitt, 1986a, b and Frost, 1988).

The major rock forming minerals under the transmitted light microscope are k-feldspar, plagioclase, orthopyroxene, clinopyroxene and quartz with or without minor garnet and biotite. Opaque minerals are present as porphyroblasts in different sizes. Ranging from coarse to fine all sizes oxides are observed. Coarse medium sized Fe-Ti oxides are seen in association with pyroxenes and within the matrix (Fig. 5.6d). These titanomagnetites are also seen as inclusions within garnet. Ultrafine, droplets of the Fe-Ti oxides are observed along fracture plane, cleavage plane and also along grain boundary of silicate minerals like biotite and pyroxenes (Fig. 5.7). Thermobaromatrical measurements of these similar mineral assembages of anorthosites and granulites of Balugaon-Rambha sector nearby Chilka Lake, Eastern Ghats Belt of India, are metamorphosed at an extreme temperature pressure condition, >1100ºC and ~10 kbar (Raith and Dobmeir, 2007) with a counter-clockwise P-T trajactory, at a lower crustal depth, by near-isobaric cooling (Sengupta et al., 2008).

Under the reflected light microscope, the studied rocks show the dominant Fe-Ti oxides, they are titanomagnetite and ilmenite. Homogeneous and inhomogeneous oxide phases, both are observed in the studied samples. The ilmenite is present as exsolved lamallae within the inhomogeneous titanomagnetite. These ilmenite lamallae

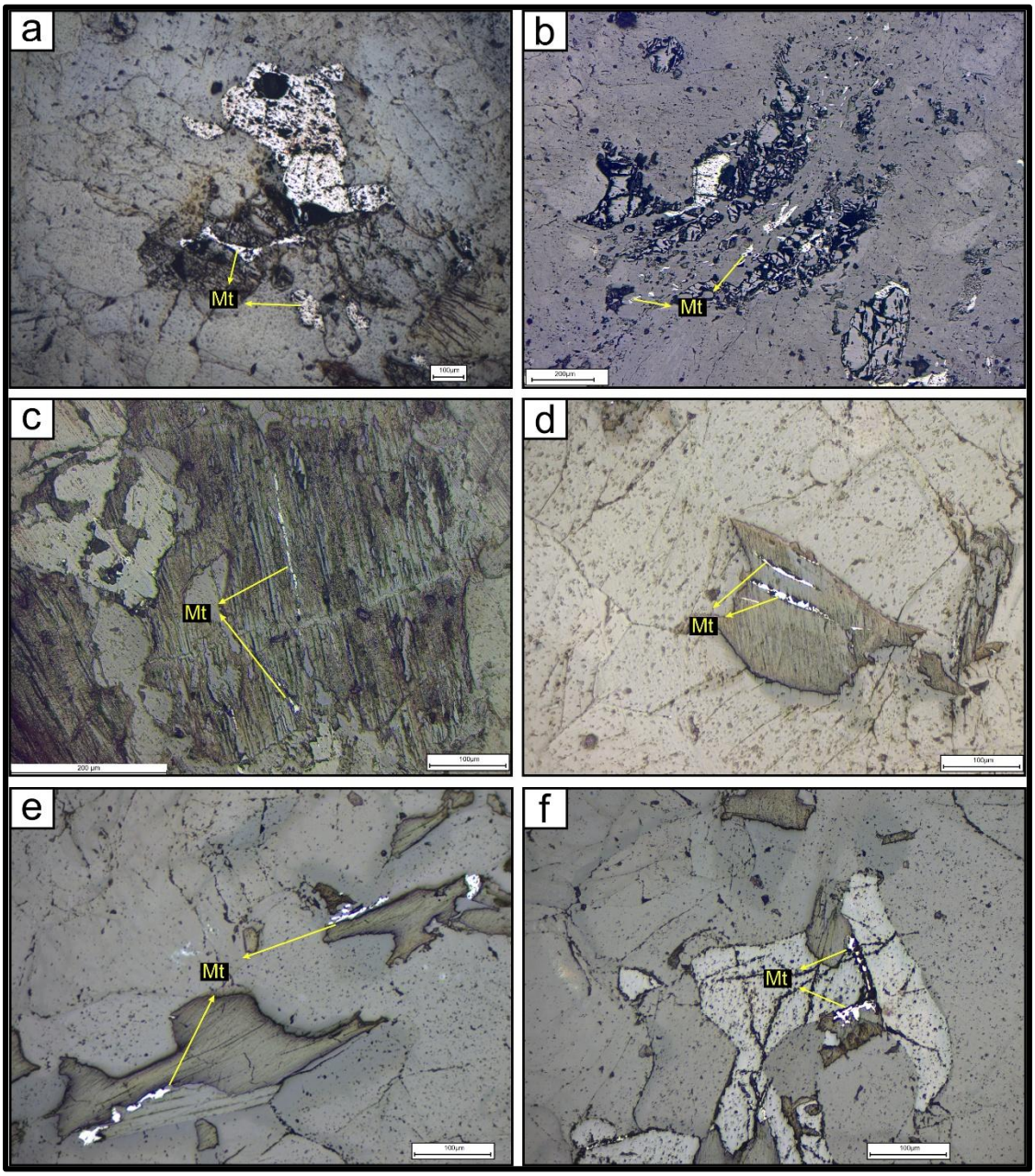

Fig. 5.7: a) Secondary Magnetite occurs along the grain boundary (PPL), b) Two different generations of Fe-Ti oxides. Coarser one is primary and finer one is the secondary magnetic minerals (PPL), c) Ultra fine grains of secondary magnetic minerals occur along the fractures within silicate (PPL), d) Ultra fine grains of secondary magnetic minerals occur along the cleavage planes of silicate (PPL), e) fine secondary magnetite occurs along the grain boundary of biotite (PPL), and f) fine secondary magnetic minerals occurs along the fractures (PPL).

within the inhomogeneous titanomagnetites are observed mainly in the anorthosite samples and very limited samples of granulite. Mostly, the low temperature oxidation effects in the titanomagnetites are observed in the granulites and very few high temperature titanomagnetite grains are observed within granulite. In the anorthosite only the high temperature oxidation of Fe-Ti oxides are observed prominantly. Having both high temperature oxidation and low temperature oxidation is good because these oxidation reduce the grain size which enhances the property of capturing the stable magnetic remanence within the titanomagnetite grain (Butler, 1992).

After studying the textural relationship under the reflected light microscope, at least, three generations of Fe-Ti oxides are identified:

a) The primary homogeneous titanomagnetite which range from coarse to medium grained and subhedral to anhedral in shape. Occurring individually in the groundmass or associated with pyroxene. The magnetite – ulvospinel complete solid solution takes place only at a temperature above ~600ºC. So, these homogeneous titanomagnetites occur at the peak P-T condition of the granulite facies metamorphism (Zhang and Piper, 1994). This is the first generation Fe-Ti oxides.

b) The host titanomagnetites, having exsolved ilmenite lamellae indicates a later stage thermos-tectonic event. This is the second generation titanomagnetite. The variation in this texture depends on the variable concentration of titanium, and this ferrimagnetic variation occurs at the cooling process from the peak metamorphic condition.

c) The fine grains of Fe-Ti oxides are the third generation. These grains occur along the fracture, cleavage or along the grain boundary of silicate minerals. These fine grains occurred during decompression of the terrain. During the cooling phase of high-grade metamorphic terrain and later stage of upliftment due to the release of pressure, solution cracks occur within the silicates and this secondary ferrimagnetic variety develops (Hay et al., 1988 and Bay et al., 2011).

The primary Fe-Ti oxides of the Balugaon-Rambha sector nearby Chilka Lake, Eastern Ghats Belt of India, are coarse to medium grained, indicating slow cooling and a prolonged period of metamorphism. The inhomogeneous primary titanomagnetite with the initial stage of high temperature oxidation, indicates that the

rocks have suffered prolonged period of high temperature metamorphism, followed by upliftment of the terrain with slow cooling.

On the basis of above textural features of Fe-Ti oxides, it is evident that, the studied rocks exhibit the presence of the multiple generations of magnetic minerals. These types of magnetic signatures indicate that, the studied rocks are very much suitable for the rock-magnetic and palaeomagnetic study. These magneto-mineralogical and palaeomagnetic studies will lead to the identification of pole position for the Indian subcontinent during the Neoproterozoic period.

Chapter: 6

ROCKMAGNETIC STUDY

6. Rockmagnetic Study:

6.1. Introduction:

The natural rocks consist of rock-forming minerals and iron-bearing oxides and sulphides. The rock-magnetic investigations are carried out to identify the magnetic carrier minerals residing in the natural rocks, resulting the magnetic remanences within the studied rocks. The principle aim of this chapter is to identify the magnetic minerals including their domain size. The rock-magnetic properties are investigated for Anorthosite, Granulite, Khondalite and Leptynite of the Precambrian / Proterozoic rocks of Balugaon-Rambha sector nearby Chilka Lake, Eastern Ghats Belt of India. Hence, the main aims for measuring the rocks of Balugaon-Rambha sector, Chilka Lake area in this chapter are:

a) To identify the magnetic minerals residing in the studied samples,
b) To determine the origin of the remanence carriers, and
c) To select the samples suitable for further palaeomagnetic study.

In natural rocks, the magnetic properties are depending on the magnetic susceptibility and magnetic remanence, which are highly sensitive to concentration of magnetic minerals along with the mineralogy, grain size and shape (Basavaiah, 2011 and Thompson and Oldfield, 1986). The different grain size of the magnetic minerals are classified as Super Paramagnetic (SP), Stable Single Domain (SSD), Pseudo Single Domain (PSD) and Multi Domain (MD) (Fig. 6.1). Amongst all, the most

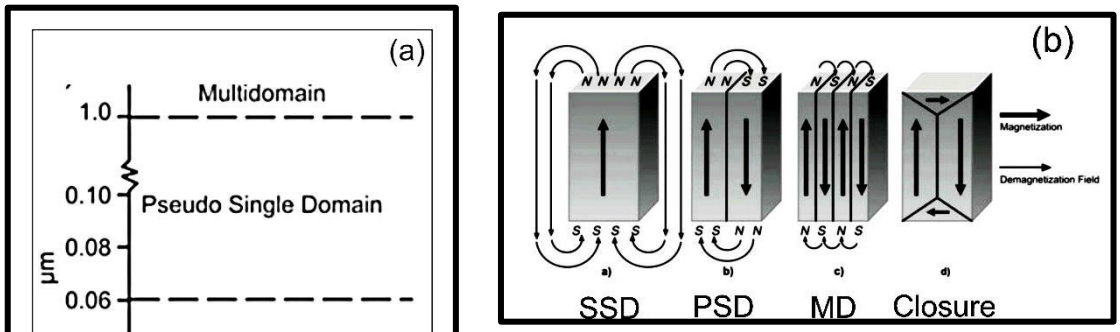

Fig.: 6.1: a) Magnetic Domains based on grain sizes (redrawn from Oldfield in Basavaiah, 2011) and b) Schematic illustration of Magnetic Domains (Basavaiah, 2011).

suitable for acquiring the ancient terrestrial magnetic field are the SSD grains. Under the reflected light microscopic study, the MD grains are easily observed but the SSD and the PSD grains are overviewed. For precise identification of the magnetic minerals further in depth, the different rock-magnetic experiments were carried out in laboratory. Magnetic grain size is very important for the magnetic studies, on the basis of different magnetic effect on the particular grain size (Basavaiah, 2011). The formation of the domain reduces the energy of the system. The demagnetization energy decreases with the increase in domain (Basavaiah, 2011). The boundary in between the two opposite charged domain is called the domain wall. More the number of domain wall, more the energy consumed for their formation. For every naturally formed substance the domains are variable, may be due to the crystal lattice defect, impurities and other internal properties (Basavaiah, 2011). From the rock-magnetic experiments, the magnetic minerals of the rock samples are revealed along with the grain size, composition and its concentration.

Thermo-magnetic Study: This study deals with the graphical representation of change in intensity of magnetization with temperature. Above the Curie Temperature (T_c) the remanent magnetization cannot be retained, the thermal energy is dominating the total system and behaves as a paramagnet. The behaviour of the magnetic minerals changes to ferromagnetic as the rocks cool passing the T_c (Tauxe, 2010). The Curie temperature was first introduced by Pierre Curie in 1895. Rock cooling below the T_c means the relaxation time increases resulting the magnetization to be blocked within the minerals residing in the rock. This range of temperature is known as the blocking temperature. This acquiring process of magnetization within the rock is known as Thermal Remanent Magnetization or TRM. The Curie temperature and the blocking temperature is different of every magnetic mineral.

Hysteresis Study: On the nature of hysteresis loop, the different types of magnetic mineral residing within the studied sample can be identified. When the magnetic field is induced with in a sample the magnetization increases and follows the path forming the hysteresis curve. On increasing the applied magnetic field, the magnetization also increased non-linearly up to a limit, and become non reversible. On removal of the induced field also the induced magnetization does not return to its origin, tends towards a level of remanent magnetization. For the removal of these remanent magnetization an opposite magnetic field is applied to tend the magnetization towards

zero, these applied field is known as the coercive force. Depending of this remanent magnetization and the coercive force, the nature of the curve changes and accordingly different magnetic minerals can be identified.

***Isothermal Remanent Magnetization (IRM) Study*:** The Isothermal Remanent Magnetization (IRM) is a naturally forming remanence, when the rock suddenly experiences a huge pulse of magnetic field in a short span. IRM is a remanent magnetization that occurs at a constant temperature. The remanence in IRM results due to the sudden pulse of direct current, DC field applied and withdrawn. By the application of the direct field, the magnetic material gets magnetized following a magnetization acquisition curve up to a point of saturation beyond the threshold value of χ (Fig. 6.2). Saturating IRM (SIRM) is the maximum IRM a sample can obtain. It is recorded by a sample when the magnetic field is applied progressively (Fig. 6.2). There is no further increase in IRM after reaching the SIRM, even on further application of magnetic field. Observing the saturation point and the associated value of applied field the magnetic mineral can be identified. Every magnetic mineral has different saturation point.

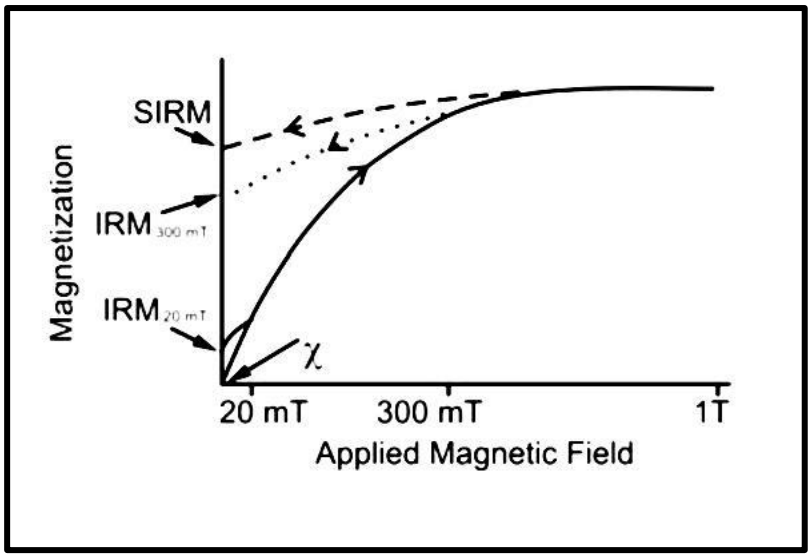

Fig.: 6.2: IRM Acquisition Curve (Oldfield, 1994).

This chapter deals with the data obtained from different rock-magnetic investigations of the rocks from Balugaon-Rambha sector nearby Chilka Lake, Eastern Ghats Belt of India (CHL). These measurements are rapid, inexpensive, non-destructive and sensitive to even low concentration of magnetic minerals. All the experiments are done using very little amount of powdered samples. Rock-magnetic

parameters include thermomagnetic curves (TRM), hysteresis curves and Isothermal Remanent magnetisation curves (IRM).

6.2. Thermo-magnetic Study:

The thermo-magnetic study is done to know the Curie point and change in the behaviour of the magnetic minerals within the sample during both heating and cooling cycle. High field thermomagnetic curves were generated by heating the powdered sample from room temperature to about 700°C in a saturated magnetic field and then cooling to ~100°C. Identification of the principal magnetic minerals present in the samples are possible by observing the nature of the thermomagnetic curves obtained

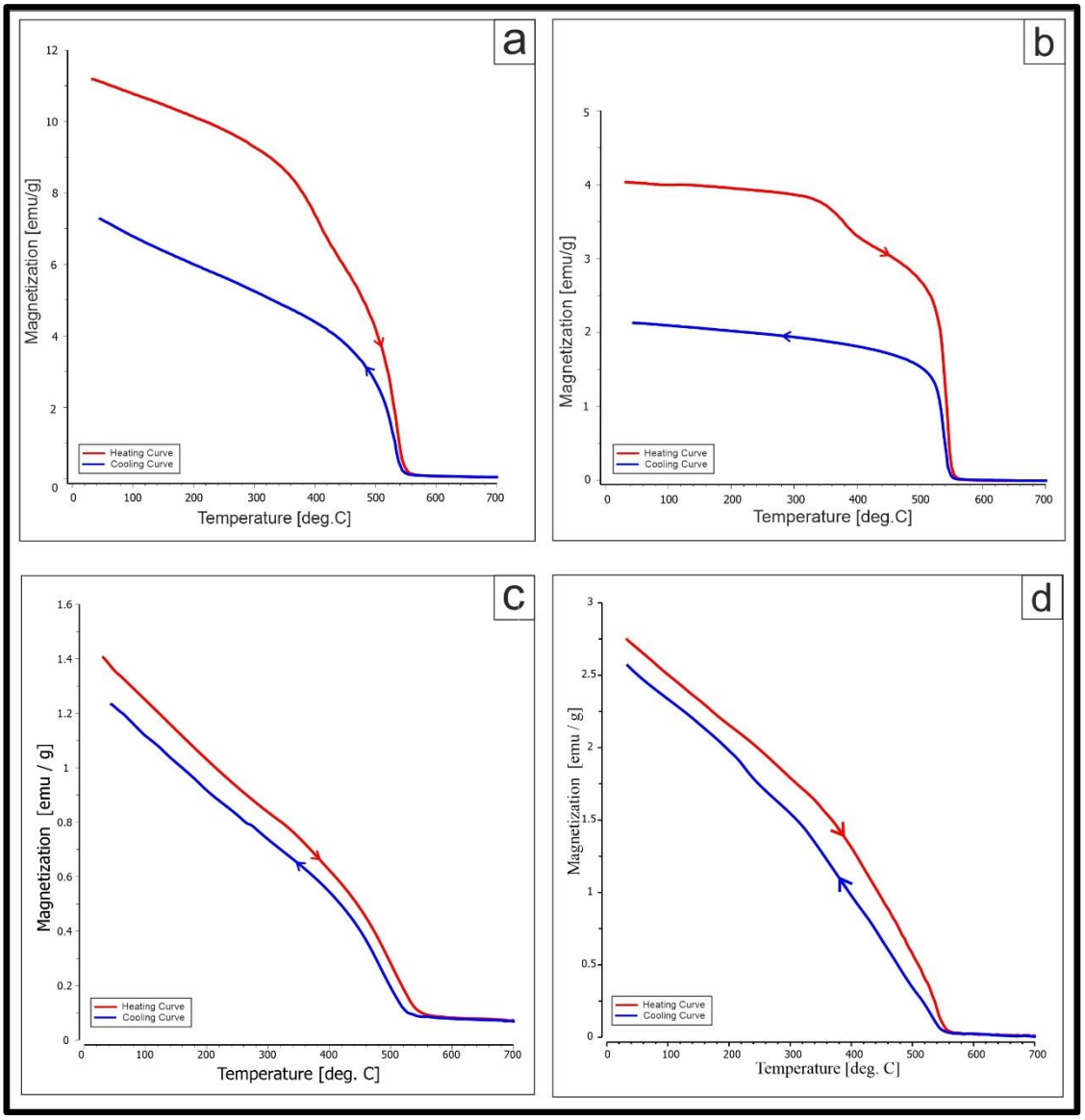

Fig 6.3: Reversible Thermomagnetic curves of representative samples showing ferromagnetic nature.

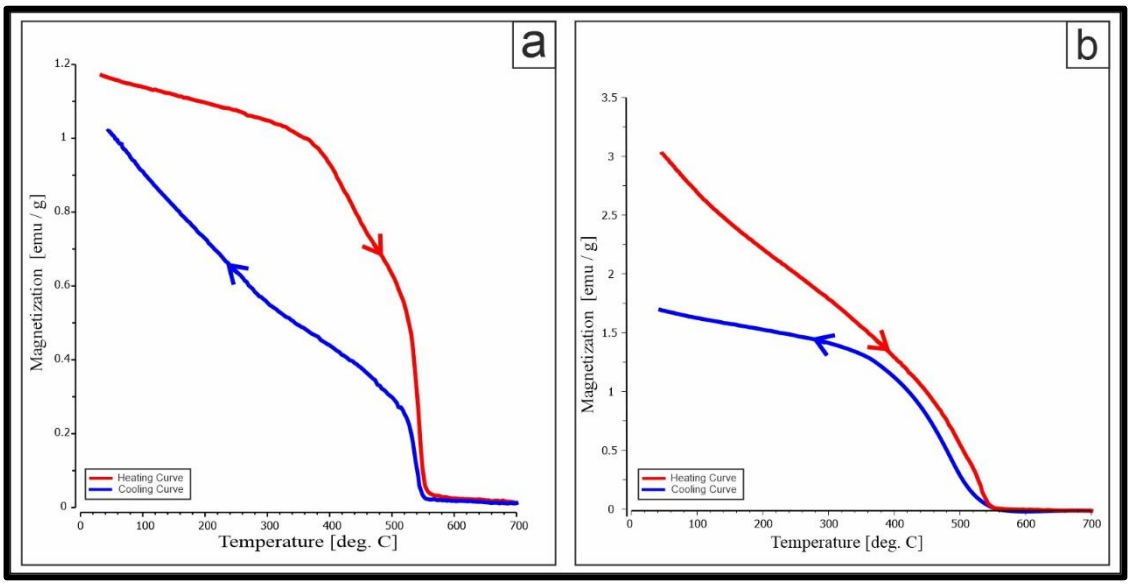

Fig 6.4: Irreversible Thermomagnetic curves of representative samples showing ferromagnetic nature.

and by observing the Curie temperature (T_c), where the saturation remanence falls to zero. Every magnetic mineral has its own characterizing T_c. From the thermomagnetic curves of the studied samples (CHL), it is observed that in most of the curves the magnetization shows a sharp drop in between ~560°C to 580°C during the heating cycle (red line). The heating curve (red) and cooling curve (blue) is reversible, do not have a crosscut between each other and have a curvature away from the origin (Fig. 6.3), CHL 5, CHL 11, CHL 3 and CHL 24 are some representative samples. The other curves in Fig. 6.4 shows a sharp drop in magnetization at ~580°, without any crosscut

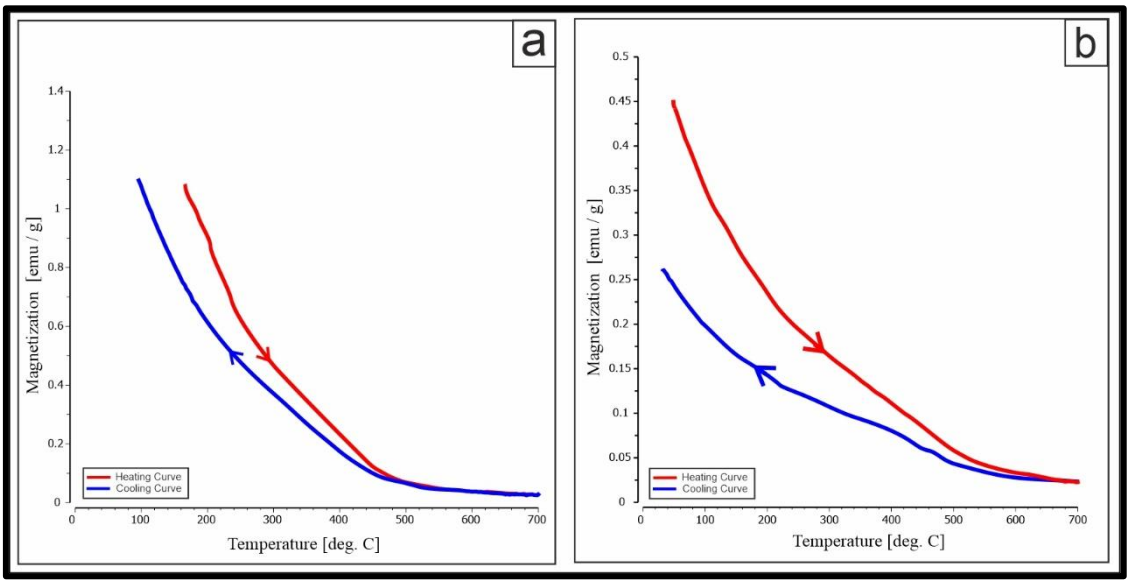

Fig. 6.5: Thermomagnetic curves of representative samples showing paramagnetic nature.

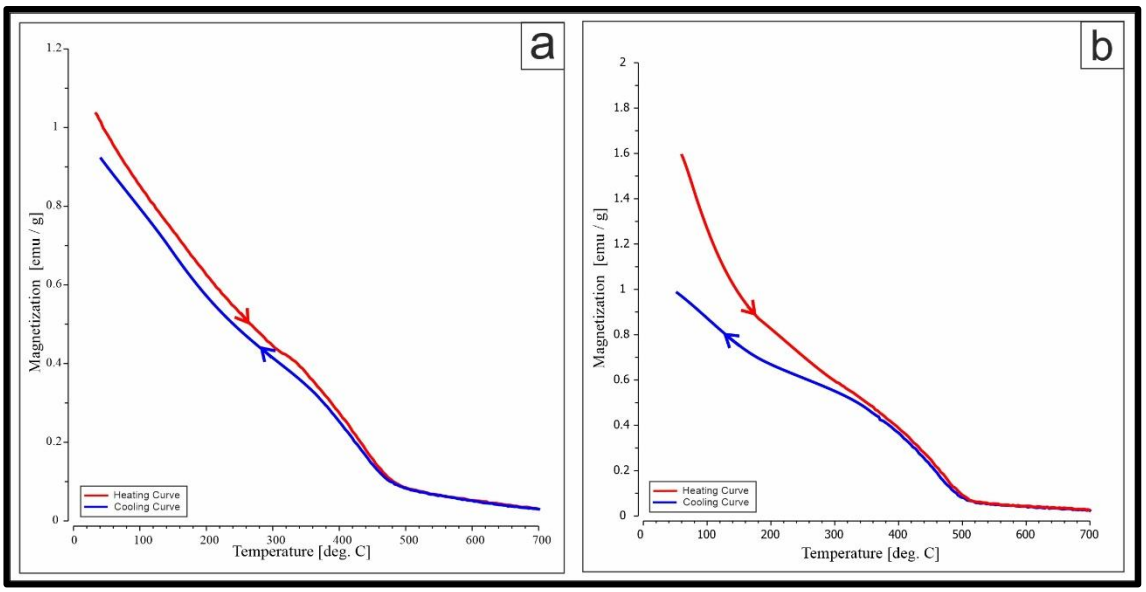

Fig. 6.6: Thermomagnetic curves of representative samples showing both paramagnetic and ferromagnetic nature.

between the curves but are irreversible in nature also indicates the presence of magnetite as ferromagnetic minerals. The nature of the curves from CHL 16 and CHL 23 (Fig. 6.4) depict the presence of ferromagnetic minerals. Some of the samples indicates the presence of paramagnetic mineral as the main magnetic carrier of CHL 4 and CHL 15 (Fig. 6.5).

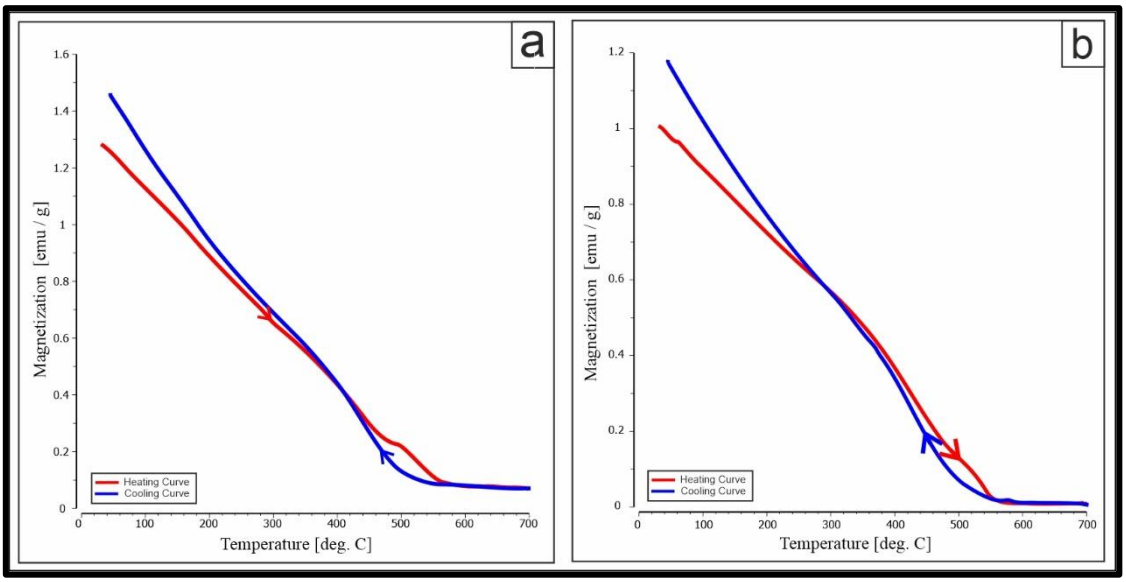

Fig. 6.7: Thermomagnetic curves of representative samples showing the crosscut nature.

Nature of few thermomagnetic curves of the CHL samples, CHL 13 and CHL 7 show the presence of both paramagnetic and ferromagnetic mineral within the same sample (Fig. 6.6). The paramagnetic nature extends to the T_c ~680° whereas the

ferromagnetic nature shows the drop at T_c ~580° (Das et al., 2024). Both the heating and cooling curves crosscut each other (Fig. 6.7), this cross-over attribute to the exsolution of the Ti-rich lamellae which is ilmenite (from petrographic studies) making the host Fe-rich in CHL 9 and CHL 8. Thus, the T_c increases and the curve becomes irreversible in nature (Lattard et al., 2006).

6.3. Hysteresis Study:

The hysteresis loops indicate the presence of whether ferromagnetic minerals or paramagnetic minerals in the samples in terms of saturation magnetization and coercivity. The hysteresis loops were obtained by applying alternative magnetic fields to the samples until saturation was attained. From individual hysteresis loop values of Saturation Magnetization (M_s), Residual Saturation Magnetization (M_{rs}) and Coercivity (H_c) were recorded and finally the domain state was identified.

Hysteresis loops obtained from the high-grade metamorphic rocks of Balugaon-Rambha sector nearby Chilka Lake, Eastern Ghats Belt of India, show the presence of both ferromagnetic as well as paramagnetic nature. Some of the samples exhibit saturated nature with moderately high remanence (Fig. 6.8), which strongly imply the presence of ferromagnetic minerals in CHL 17, CHL 18, CHL 20 and CHL 23. Few curves showing elongation with an unsaturation of magnetization and very low remanence indicating paramagnetic and ferromagnetic minerals present in the same sample, CHL 13 and CHL 7 (Fig. 6.9). Samples CHL 14 and CHL 15 indicate true paramagnetic behaviour which shows complete absence of any ferromagnetic component (Fig. 6.10).

The grain size of the magnetic minerals present within the rock can be estimated by plotting the ratio between magnetization (M_{rs}/M_s) and coercivity (H_{cr}/H_c,). The magnetic hysteresis parameters are plotted in a representative plot named as Day Plot (Day et al., 1977), with the variations in magnetic domain states. The plot is divided into SD, PSD and MD region. M_{rs}/M_s values are calculated which falls in between 0.03 and 0.41 with an average of 0.17. H_{cr}/H_c, the ratio of remanent coercivity and coercivity of remanence lies between 0.13 (for Leptynite) and 1.03 (for Anorthosite) and with an average of 0.88 (Fig. 6.11).

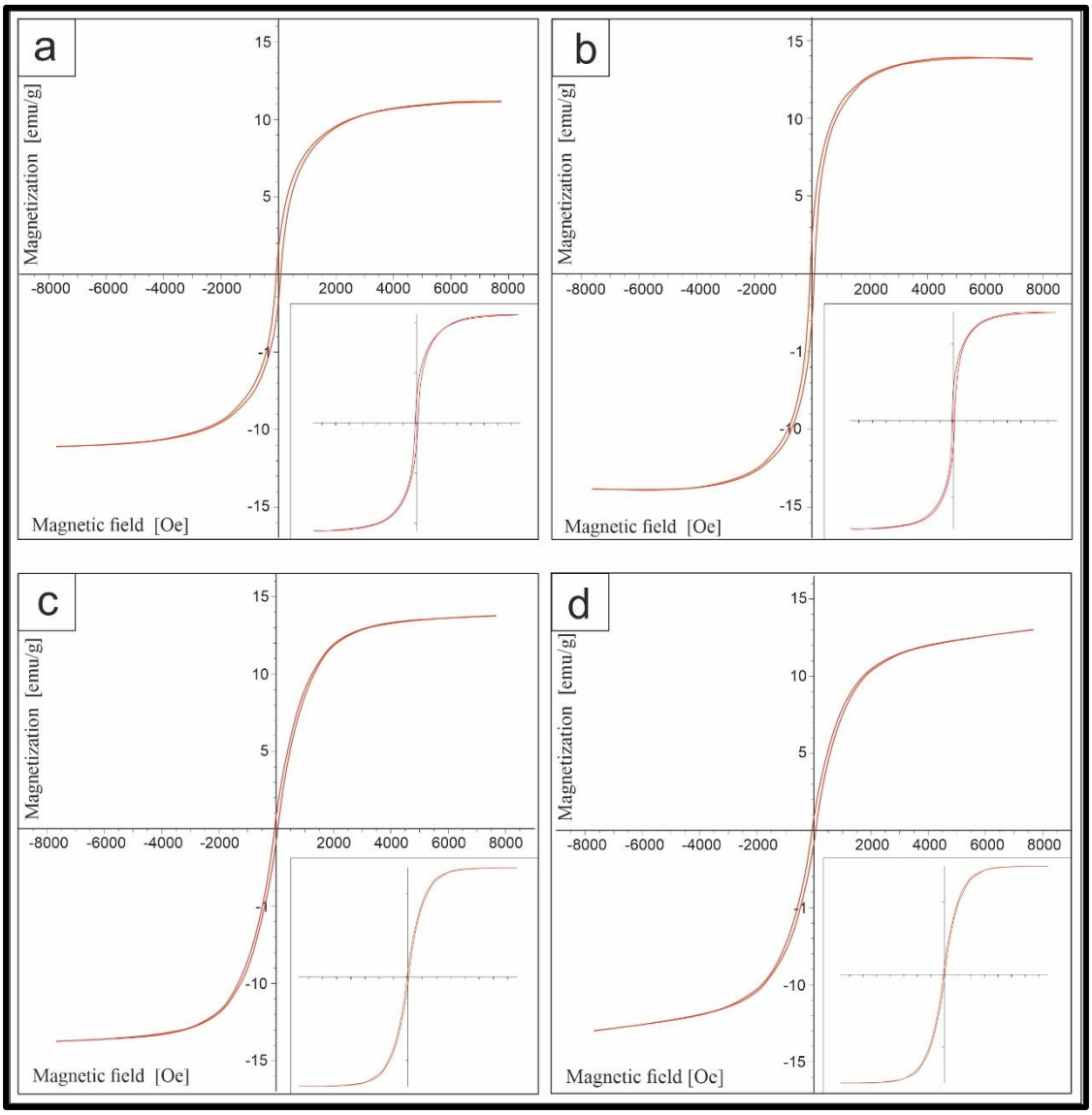

Fig. 6.8: Hysteresis loops of representative samples showing ferromagnetic nature.

6.4. Isothermal Remanent Magnetization (IRM) Study:

In the IRM acquisition curve study, the saturation curves were obtained by applying magnetic field to the samples with gradual increasing strength of magnetic field. After a sharp rise the curve starts to saturate below 3000 Oe and the saturation of magnetization were obtained for some samples. The isothermal remanent magnetization is plotted with magnetic field for CHL 6, CHL 8, CHL 11 and CHL 19 (Figs. 6.12). All the samples have a coercivity <10 mT. The nature of the obtained

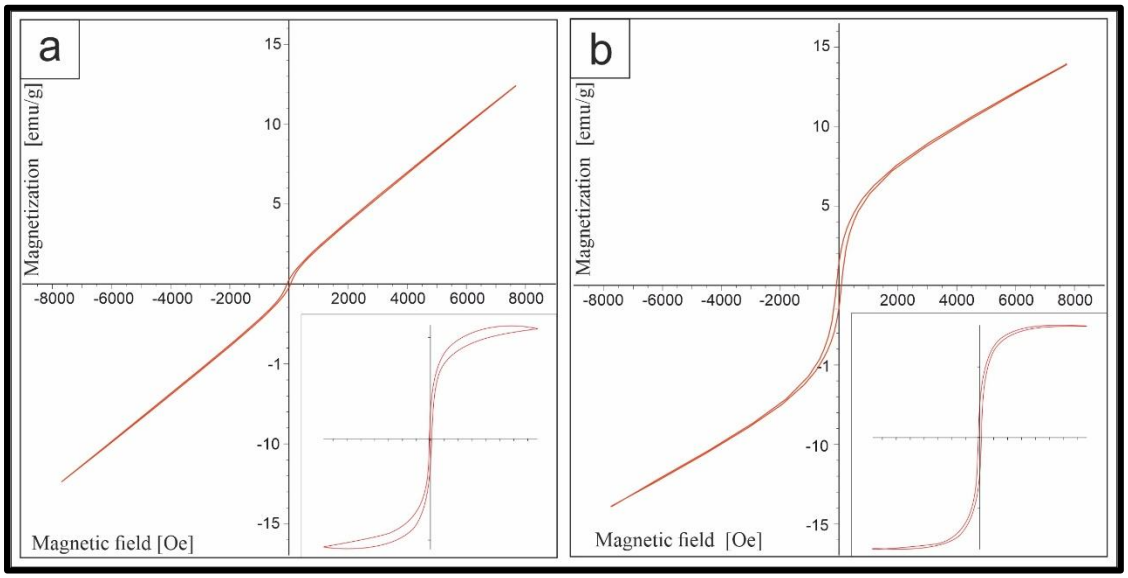

Fig. 6.9: Hysteresis loops of representative samples showing both paramagnetic and ferromagnetic nature.

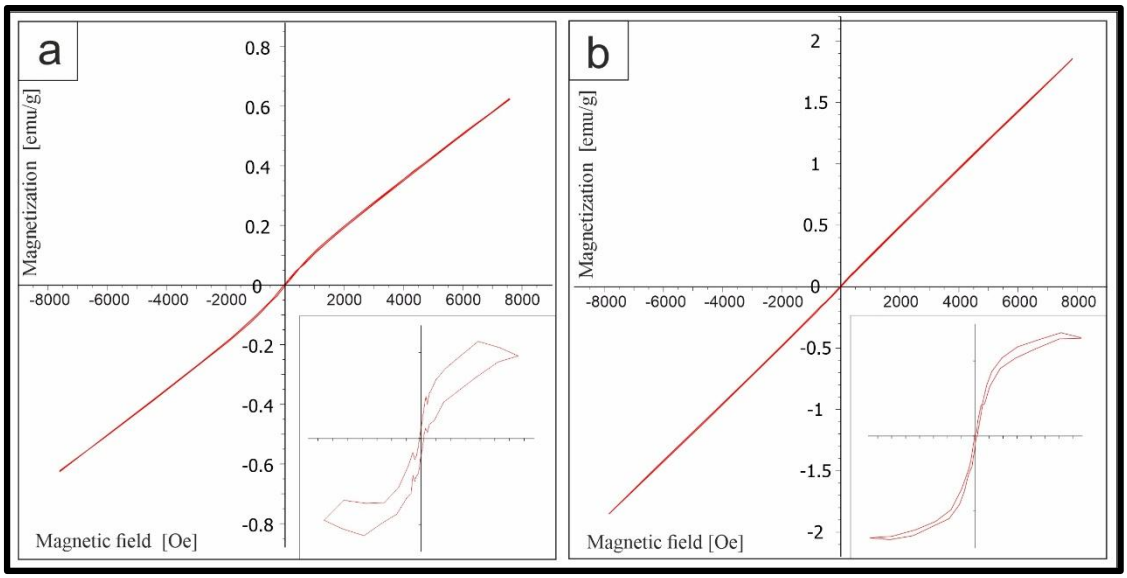

Fig. 6.10: Hysteresis loops of representative samples showing paramagnetic nature.

curves resembles that the presence of ferromagnetic minerals. Both the IRM and coercivity spectra point towards soft magnetic minerals (viz. magnetite or Titanomagnetite).

On the basis of the nature of curves obtained from different types of Rock-magnetic investigations, it is evident that the primary magnetite is present as ferromagnetic mineral in Anothosite and in case of high-grade granulites, khondalites and leptynites, two types of magnetic minerals are evident. 1st phase is primary magnetite as ferromagnetic and 2nd phase is haematite as paramagnetic mineral. So,

the source of the magnetic carriers in the studied rocks primary magnetite and haematite. On the basis of magnetic carrier minerals residing in the studied rock samples, I am able to select the final set of oriented core samples for further palaeomagnetic study.

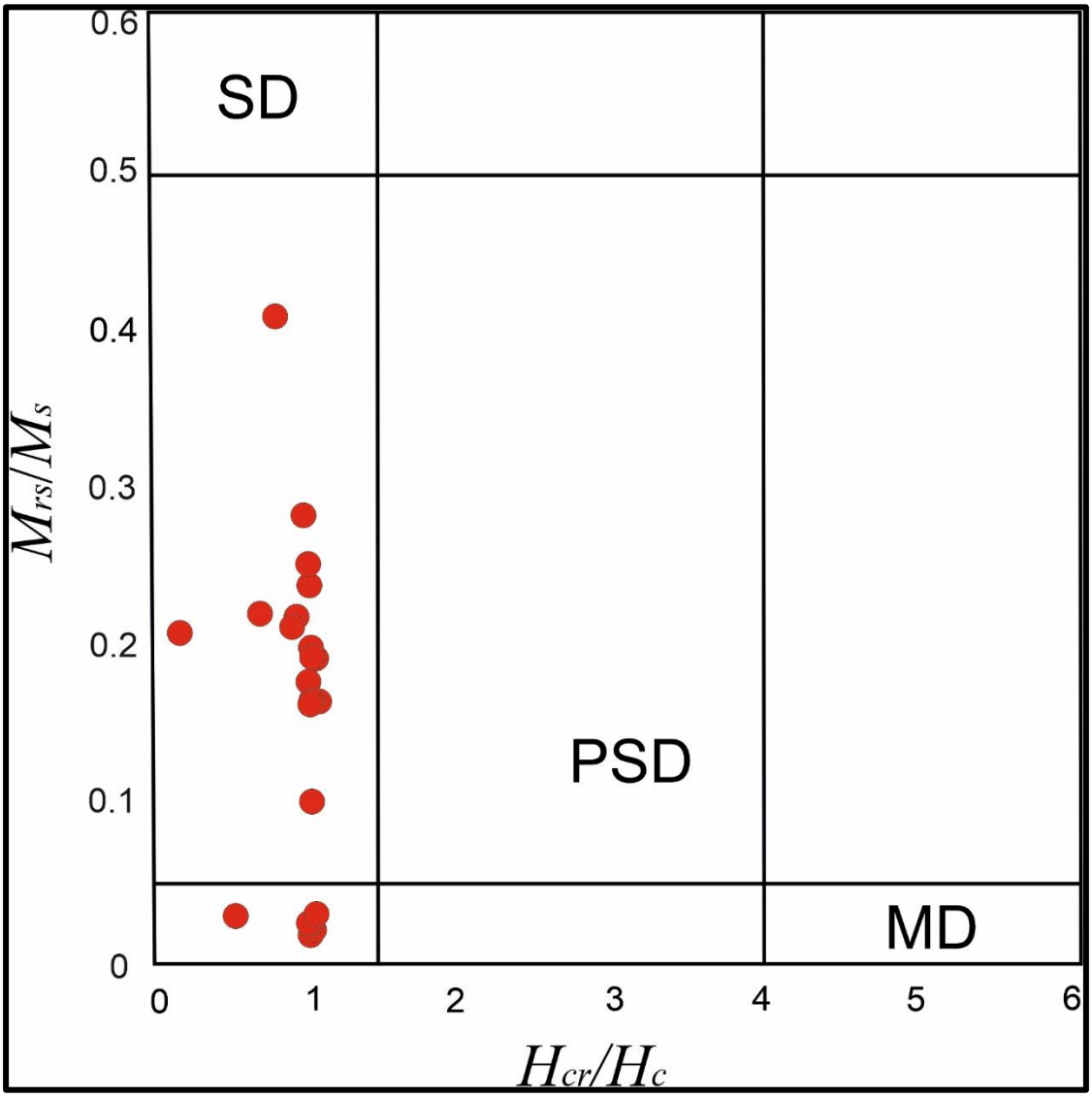

Fig. 6.11: Domain state distribution of the titanomagnetite in different rocks of the studied area (Day et al., 1977).

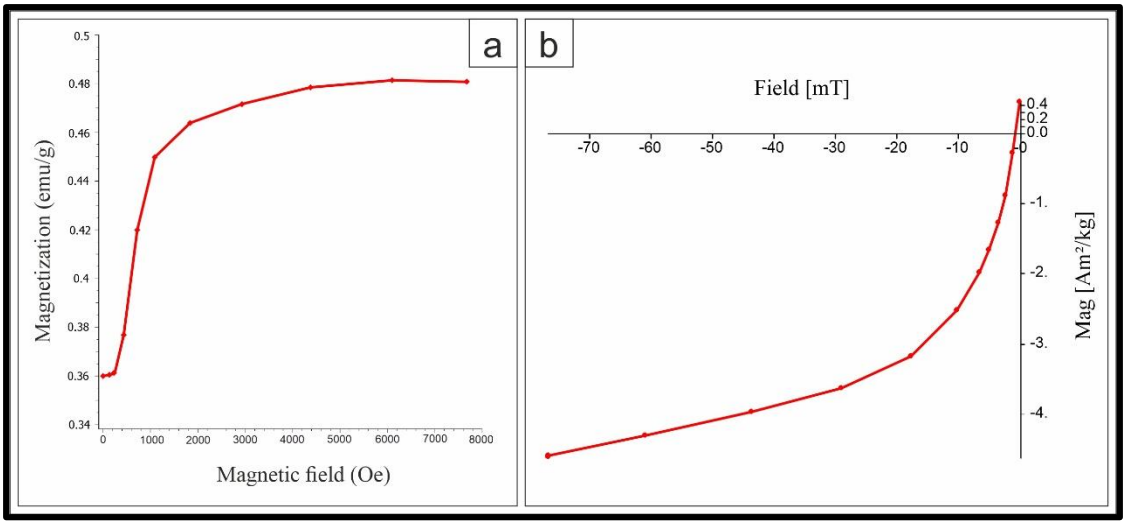

Fig. 6.12.1: Isothermal Remanent Magnetization (IRM) acquisition curve and corresponding coercivity spectra.

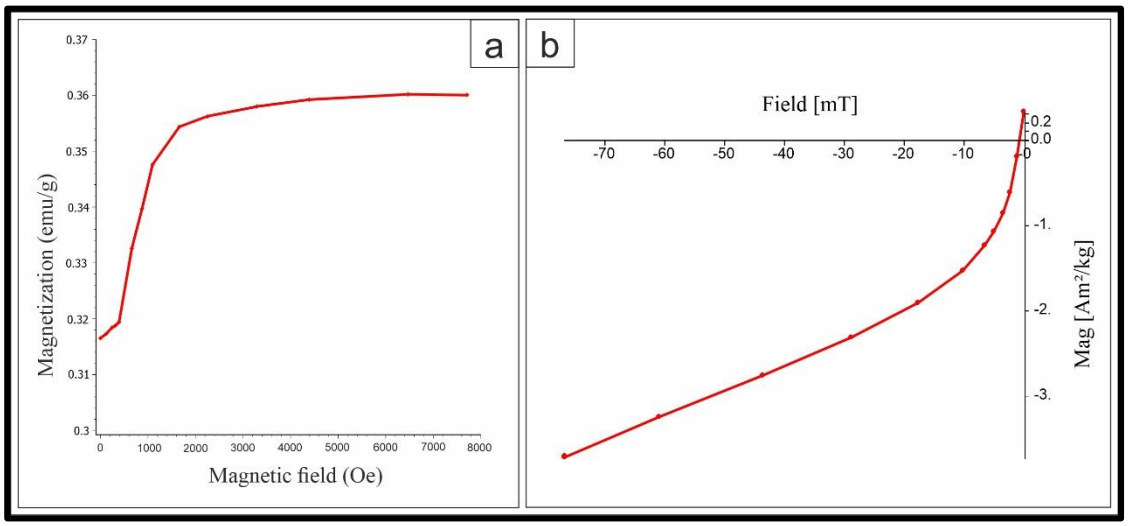

Fig. 6.12.2: Isothermal Remanent Magnetization (IRM) acquisition curve and corresponding coercivity spectra.

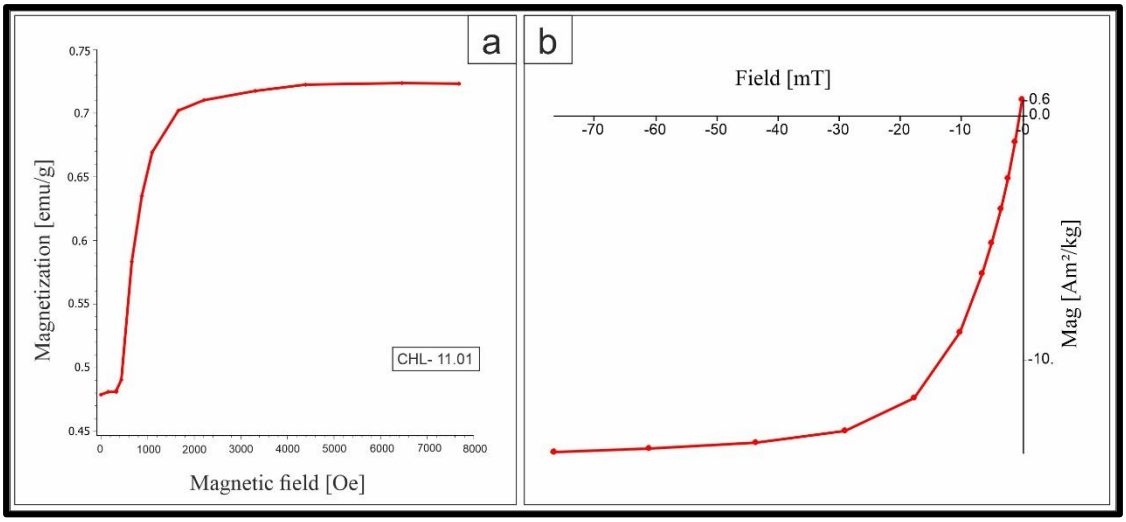

Fig. 6.12.3: Isothermal Remanent Magnetization (IRM) acquisition curve and corresponding coercivity spectra.

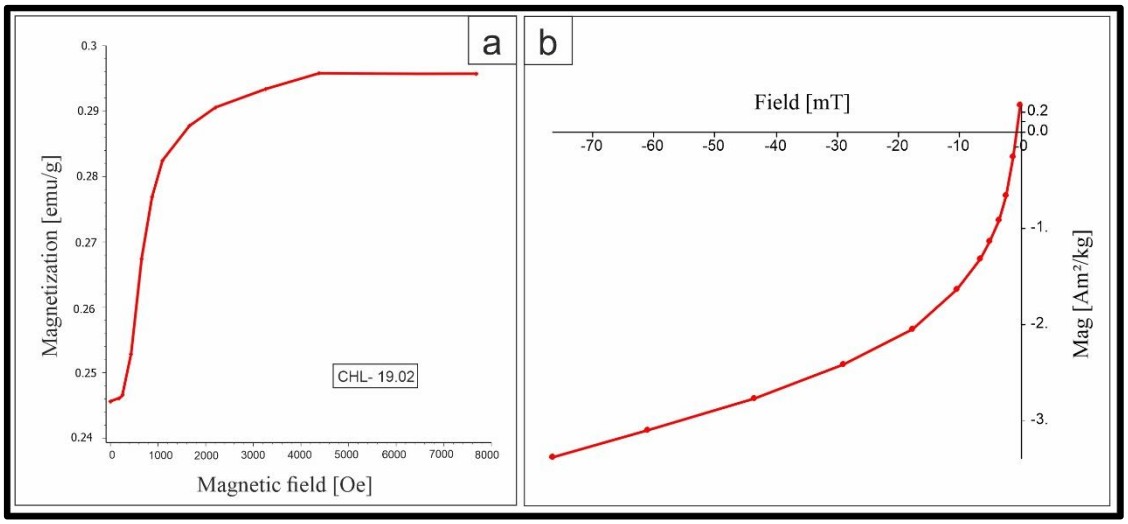

Fig. 6.12.4: Isothermal Remanent Magnetization (IRM) acquisition curve and corresponding coercivity.

Chapter: 7

ANISOTROPY OF MAGNETIC SUSCEPTIBILITY (AMS)

7. Anisotropy of Magnetic Susceptibility (AMS):

Anisotropy of Magnetic Susceptibility (AMS) is a technique which helps to infer the magnetic fabrics present within the rock samples and to correlate it with the deformation of the studied rocks. It is an accurate, fast, non-destructive and inexpensive process. The Anisotropy of Magnetic Susceptibility (AMS) is a technique that actually helps to identify the preferred magnetic orientation of the magnetic minerals within a rock. Within the rocks the magnetic susceptibility is not uniform in all directions; it varies from rock to rock. The anisotropy within the rock samples may develop due to some external stresses like natural tectonic stresses or be intrinsic due to the shape or crystalline anisotropy of magnetic minerals present. Geometrically, the AMS is represented by an ellipsoid, known as magnitude ellipsoid. The semi-axes of the magnitude ellipsoid are proportional to the Eigen values (K_1, K_2, K_3). The directions of the Eigen vectors are the principal susceptibility axes of the ellipsoid and the Eigen values $K_1 \geq K_2 \geq K_3$ are the principal susceptibilities. AMS is the change in magnetic susceptibility with direction (Hrouda, 1982 and Tarling and Hrouda, 1993). These three principal susceptibility axes are maximum susceptibility axis (K_1), intermediate susceptibility axis (K_2) and minimum susceptibility axis (K_3) along which the numeric values are denoted. The value of these three lineation axes when plotted denotes the magnetic fabrics. Voigt and Kinoshita (1907) first introduced this method to study fabrics which Ising (1942) and Graham (1954) later used as petro-fabric indicator.

On the basis of these Eigen values, many parameters are calculated to determine the anisotropy degree and the shape of AMS ellipsoid (Table-7.1).

The shape of the ellipsoid is classified on the basis of the Eigen values:

$k_1 \geq k_2 \geq k_3$..... the AMS ellipsoid is triaxial (Fig. 7.2)

$k_3 << k_2 \approx k_1$..... the AMS ellipsoid is oblate in shape (Fig. 7.2)

$k_1 \approx k_2 \approx k_3$..... the AMS ellipsoid is a sphere, isometric ellipsoid (Fig. 7.2)

$k_1 >> k_2 \approx k_3$.....the AMS ellipsoid is prolate in shape (Fig. 7.2).

Determination of the petro-fabric within a rock is represented by AMS, for which the following parameters are required. The Anisotropy Degree (P) is defined as the ratio of the maximum and minimum susceptibilities. However, the corrected

Parameter Name	Parameter symbol	Parameter formula	Author
Anisotropy degree	P	k_1 / k_3	Nagata (1961)
Corrected anisotropy degree	P'	$\exp\{2[(\boldsymbol{\eta}_1 - \boldsymbol{\eta})^2 + (\boldsymbol{\eta}_2 - \boldsymbol{\eta})^2 + (\boldsymbol{\eta}_3 - \boldsymbol{\eta})^2]\}^{½}$	Jelinek (1981)
Mean susceptibility	k_m	$(k_1 + k_2 + k_3)/3$	Nagata (1961)
Shape parameter	T	$2(\boldsymbol{\eta}_2 - \boldsymbol{\eta}_3)/(\boldsymbol{\eta}_1 - \boldsymbol{\eta}_3) - 1$	Jelinek (1981)
Magnetic lineation	L	k_1 / k_2	Balsley and Buddington (1960)
Magnetic foliation	F	k_2 / k_3	Stacey et al. (1960) Balsley and Buddington (1960)

Table 7.1: Most commonly used AMS parameters.

Anisotropy Degree (P′) is more accurate. The mean susceptibility is defined as the arithmetic mean of the three susceptibility axes. The value of Shape Parameter (T) lies with in -1 and +1, i.e. $-1 < T < +1$. The Magnetic Lineation (L) is the ratio between the maximum and intermediate susceptibilities and the Magnetic Foliation (F) is the ratio between the intermediate and minimum susceptibilities.

The structural evolution and origin of any rock can be interpreted from the magnetic susceptibility sources and their anisotropy data. Different origin of rocks preserves fabrics of different time. The igneous rocks have the capability to preserve the primary fabric during their crystallization from magmatic fluids at higher temperatures. The metamorphic rocks show the fabric which are directly or indirectly involved with the effect of tectonic processes during metamorphism. The results obtained from the AMS data helps in determining the spatial distribution and orientation of the magnetic mineral grain. By the spatial distribution of the grain, the geological processed involved or the tectonic events can also be determined.

A material when exposed to any external magnetic field, it acquires a magnetic moment. Every magnetic material has its own ability of acquiring magnetization which is known as magnetic susceptibility. Magnetic susceptibility can be negative or positive. Negative susceptibility is termed, when the magnetic polarization is in opposite direction to the applied magnetic field. Similarly, positive susceptibility obtained by a material is when the magnetization is parallel to that of the applied

magnetic field. The magnetic susceptibility (K) of a material is defined as the ratio of intensity of magnetization (M) within the material to the applied magnetic field (H).

$$K=M/H$$

Magnetic susceptibility is dimensionless.

The susceptibility of a material does not depend on the total amount of magnetic minerals residing in the sample, but it depends upon how much ferrimagnetic minerals present in the sample, which are mostly magnetite or other magnetic minerals of the titanomagnetite series. The susceptibility of 25 sites from anorthosite and high-grade rocks of Balugaon-Rambha sector nearby Chilka Lake, Eastern Ghats Belt of India was measured. Atleast 6 cores per site are required for this study.

7.1. AMS and Magnetic Fabrics in Rocks:

7.1.1: Introduction:

The importance of AMS study and the magnetic fabrics for the high-grade metamorphic rocks present in the studied area are because they are often correlatable to the deformation history and tectonic events experienced by the studied geological terrain (Tarling and Hrouda, 1993).The AMS study is very important for the study of deformation and tectonic events for the metamorphic rocks (Hrouda and Janak, 1976; Pares and Van der Pluijm, 2002; and Ferre et al., 2004). The AMS can trace the large-scale deformations (Cifelli et al., 2004, 2009; Borradaile and Jackson, 2004 and Agarwal et al.; 2021). In India, the magnetic properties of the high-grade metamorphic terrain are not much studied but they cover a huge area of the continental crust (Raposo and Egydio-Silva, 2001 and Viegas et al., 2013). The Eastern Ghats Belt (EGB) is such a terrain which is remarkable to study the magnetic properties and magnetic fabrics. For understanding the deformation, the magnetic fabrics and AMS are studied in high-grade metamorphic rocks (Fodor et al., 2020; Viegas et al., 2013 and Ferre et al., 2014). Using the magnetic fabric the tectonic events are already unravelled for the Southern Granulite Terrain (Mondal et al., 2009), the Chotonagpur Granite Gneissic Complex (Chatterjee et al., 2018b) and the high-grade rocks of Kondapalle area (Gain et al., 2022). This study deals with the AMS and the study of magnetic fabrics of rocks from the Chilka area of EGB.

7.1.2: Graphical Representation of AMS:

The magnitudes and shape of the magnetic fabrics can be identified using the above-mentioned parameters in Table-1. For determining the shape of the susceptibility ellipsoid, the Jelinek Plot is used.

Jelinek Plot or Shape Plot (Jelinek, 1981 and Hrouda, 1982) is a P_j versus T plot which helps in determination of the shape and magnitude of the magnetic susceptibility ellipsoids (Fig.7.1). The graph represents the prolate ellipsoids with negative T values ($-1 < T < 0$), the plane strain ellipsoids shape has zero value ($T=0$) and oblate ellipsoids with positive values ($0 < T < 1$).

P_j– K_m Plot is plotted by corrected anisotropy (P_j) along the abscissa and mean susceptibility (K_m) along the ordinate, which shows the change in susceptibility with anisotropy within a sample.

For set of samples (at least six per site) the AMS data are plotted and conventionally visualised in equal area projection, lower hemisphere, where k_1 axes is symbolized by square, k_2 axes as triangle and k_3 as circle **(**Ellwood et al., 1988**).**

7.2. Anisotropy of Magnetic Susceptibility studies of EGB:

The AMS is used to determine the grain alignments within the rock with an ambient stress field during its formation and the prolonged journey till date. All the parameters related to AMS depending upon the rock types are stated in Table-2. The mean values of individual AMS parameters are also stated there.

The average magnetic susceptibility (K_m) examining for all CHL sites individually ranges from 2.94 $x10^{-6}$ CGS units to 560.32$x10^{-6}$ CGS units. The susceptibility in the granulites has a wide range, from 560.32 $x10^{-6}$ CGS units to 14.38$x10^{-6}$ CGS units. Overall, the Southern Sector Granulites have the higher values than the Northern Sector Granulites, though CHL 22 has the highest value of susceptibility being in the Northern Sector Granulites. The mean value of the K_m in Northern Sector Granulites is 124.5$x10^{-6}$ CGS units, whereas, in the Southern Sector Granulites it is 273.4$x10^{-6}$ CGS units. The average magnetic susceptibility of anorthosite ranges from 43.39$x10^{-6}$ CGS units to 2.94$x10^{-6}$ CGS units. The mean magnetic susceptibility of all the Anorthosite CHL samples is 16.6$x10^{-6}$ CGS units.

In the Leptynite, the average magnetic susceptibility ranges from 9.75×10^{-6} CGS units to 19.41×10^{-6} CGS units. The mean magnetic

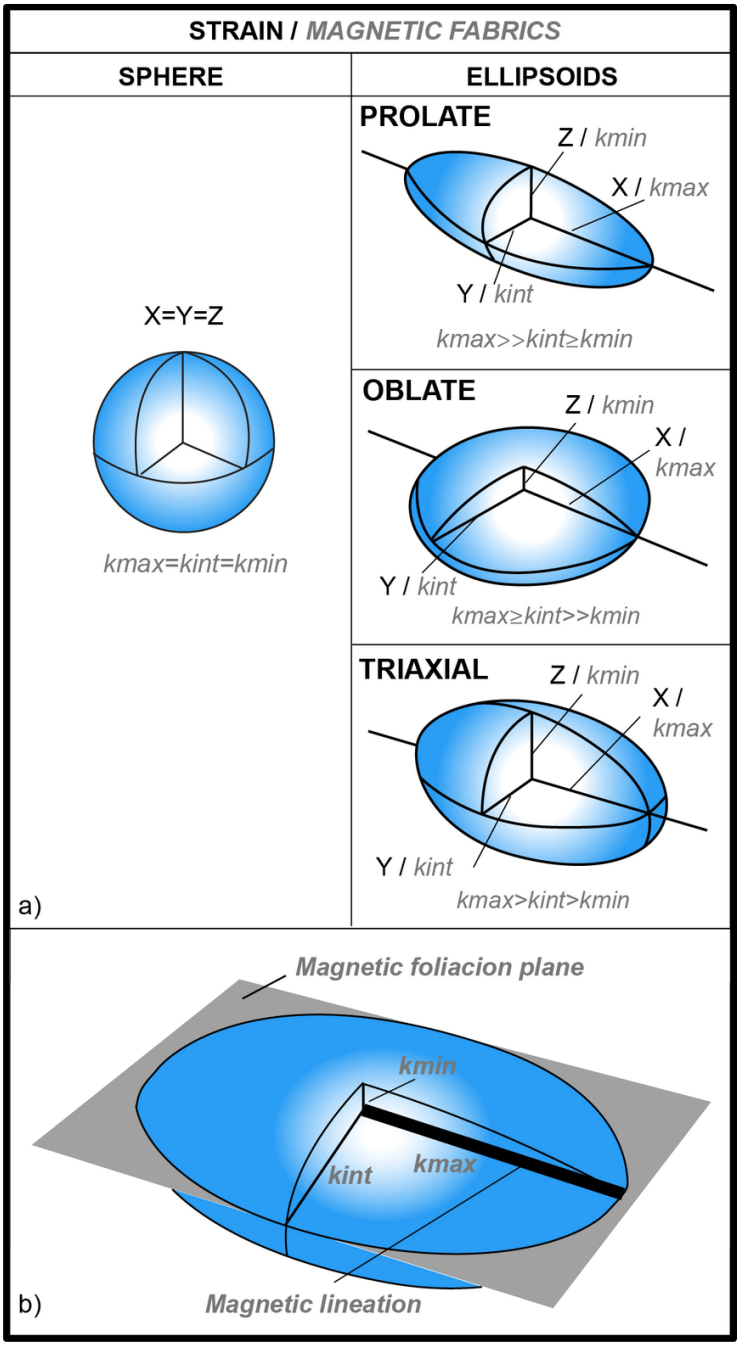

Fig. 7.1: Magnetic Susceptibility Ellipsoids.

susceptibility of the Leptynite is 15.09×10^{-6}CGS units. The mean of K_m is higher for the Granulites than the Anorthosite and Leptynite samples. More specifically the

southern sector granulites have the highest mean K_m value 273.4 $x10^{-6}$ CGS units, whereas, the leptynite shows 15.09 $x10^{-6}$ CGS units, the least among the four sectors.

Site No.	No. of Cores	K_1 (D°/I°)	α_{95} for K_1	K_3 (D°/I°)	α_{95} for K_3	F	L	P_J	T_J	K_m ($x10^{-6}$ CGS)
Northern Sector Granulite										
CHL 1	6	85.9/61.7	11.6	306.3/36.4	27.0	1.3	1.06	1.42	0.15	31.00
CHL 2	6	329.1/60.2	55.7	161.0/40.0	13.9	1.14	1.02	1.18	0.72	48.07
CHL 3	7	120.0/23.2	26	287.6/60.9	18.8	1.20	1.02	1.3	0.78	64.62
CHL 4	6	263.6/79.8	43.5	146.5/35.4	70.2	1.13	1.03	1.18	0.59	24.61
CHL 23	8	322/34.6	16.9	176.0/64.7	14.3	1.10	1.10	1.16	0.31	18.42
CHL 22	7	249.5/26.6	9.2	171.4/56.8	29.3	1.30	1.40	1.78	0.19	560.32
Mean		319.5/86.7		197.8/80.2		1.19	1.11	1.34	0.45	124.5
Southern Sector Granulite										
CHL 5	6	93.1/78.1	73.6	037.1/35.5	34.7	1.5	1.1	1.6	0.76	526.32
CHL 6	6	205.7/50.7	18	077.4/27.5	14.2	1.4	1.1	1.65	0.55	261.52
CHL 10	7	235/23	8.9	355.5/50.3	4.8	1.9	1.06	2.23	0.82	132.07
CHL 11	6	217.3/82.1	55.4	317.9/51.5	45.9	1.5	1.1	1.76	0.59	183.21
CHL 13	6	236.6/63.3	41.8	24.5/21.0	16.5	1.2	1.06	1.31	0.56	14.38
CHL 16	6	100/42.3	18.9	227.9/33.3	18.9	1.3	1.1	1.38	0.37	306.69
Mean		200.1/60.9		022.6/54.0		1.47	1.09	1.66	0.61	273.4
Anorthosite										
CHL 8	10	25.7/46.5	31.4	237.7/38.7	3.9	1.2	1.01	1.25	0.82	35.82
CHL 9	6	166.7/56.9	35.9	022.1/52.7	15.8	1.1	0.9	1.25	0.02	43.39
CHL17	7	323.7/62.6	39.4	103.2/39.7	43.3	1.3	1.3	1.89	0.02	3.37
CHL 17	7	219.7/79.1	38	333.6/40.7	46.6	1.3	1.2	2.59	0.16	14.43
CHL 19	11	100.3/43.3	35.2	218.6/23.9	11.5	1.2	1.1	1.27	0.44	18.47
CHL 20	13	142.1/49.	27.1	264.0/71.4	26.4	1.4	1.3	2.42	0.17	2.94
CHL 21	9	284.4/58.1	22.9	179.0/44.1	30.9	1.2	1.2	1.49	0.06	17.82
CHL 24	6	228.0/50.6	46.1	331.2/30.1	39	1.2	1.1	1.33	0.22	8.17
CHL 25	7	065.3/47.8	35	273.9/49.6	19.7	1.2	1.1	1.43	0.29	5.38
Mean		086.7/77.6		246.5/63.6		1.23	1.13	1.66	0.24	16.6
Leptynite										
CHL 7	6	359.2/7.21	50.2	250.6/31.4	22.3	1.2	1.1	1.39	0.26	12.49
CHL 12	7	152.6/64.6	60.6	129/33.2	29	1.2	1.1	1.3	0.35	18.71
CHL 14	7	257.2/56.9	27.8	118.6/55.8	21.7	1.3	1.2	1.54	0.38	9.75
CHL 15	7	308.3/63.7	46.4	101.0/19.2	37.7	1.1	1.02	1.2	0.69	19.41
Mean		249.7/78.1		150.3/40.6		1.2	1.11	1.36	0.42	15.09

Table 7.2. AMS parameters from samples from different sectors of different rock types.

The values of Magnetic Lineation (L) ranges for all the CHL samples from 0.9 to 1.4 and the Magnetic Foliation (F) ranges from 1.1 to 1.9. In the Northern Sector Granulites the L ranges from 1.02 to 1.4 while in the Southern Sector Granulites L ranges from 1.06 to 1.1. The F ranges from 1.1 to 1.3 in case of Northern Sector Granulites and 1.2 to 1.9 for the Southern Sector Granulites. In anorthosite L ranges from 0.9 to 1.3 and F ranges from 1.1 to 1.4. In leptynite L ranges from 1.02 to 1.1 and F ranges from 1.1 to 1.3. The Degree of Anisotropy (P_j) is almost uniform in all the samples; values fall in between 1.1 and 2.6 and the Shape Parameter (T_j) shows positive values except some of the samples. All the P_j values range within a certain limit, still there are values >1.05 or every mean value of the four divided sections are >1.05 (Table 1), which is the verge value for magnetic fabric which is tectonically controlled (Mondal et al., 2022; Chatterjee et al., 2018a; Tarling and Hrouda, 1993 and Dvorak and Hrouda, 1975).

For the shape analysis the AMS data are represented using the different parameters, P_j, T_j and K_m. The average degree of anisotropy all over the studied area are plotted with shape parameter called as the Jelinek plot (Jelinek, 1981). However, the P_j-T_j plots) ranges from oblate to prolate (Fig. 7.3). The most dominant shape of the magnetic susceptibility ellipsoid is oblate. The P_j-K_m plot (Fig. 7.4) is plotted to see the susceptibility change related with the corrected anisotropy.

7.3. Magnetic Fabrics:

The lower hemisphere equal area plots of all principal susceptibility axes of the different sectors of rock types are more of dispersed all throughout than clustered (Fig. 7.4). Theα_{95} value for both K_1 and K_3 also range widely (Table-2). The trend of magnetic lineation and pole to magnetic foliation varies lithologically (Figs. 7.5 and 7.6). The magnetic lineation has high plunge and variable trend. The mean of magnetic lineation of different rocks are NW-SE for Northern Sector Granulites, almost E-W for Anorthosite, NE-SW in Leptynite and NE-SW in Southern Sector Granulites. The magnetic lineation map (Fig. 7.7) and magnetic foliation map (Fig. 7.8), which represent the magnetic fabrics of the studied area are provided.

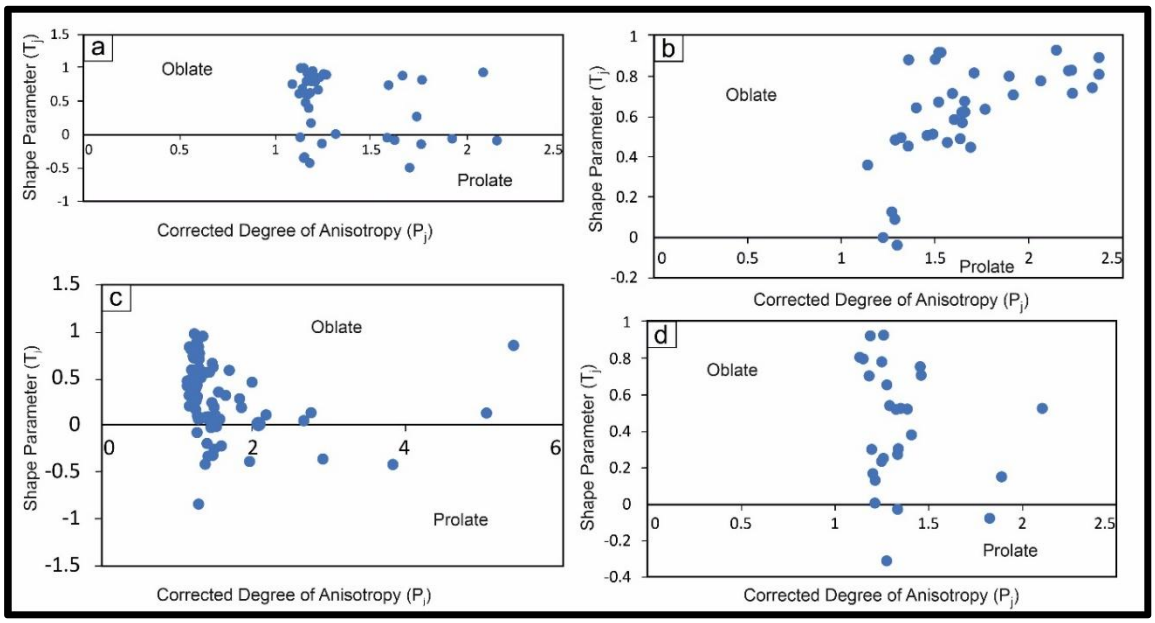

Fig. 7.2: P_j vs T_j Plots for (a) Northern Sector Granulite; (b) Southern Sector Granulite; (c) Anorthosite and (d) Leptynite.

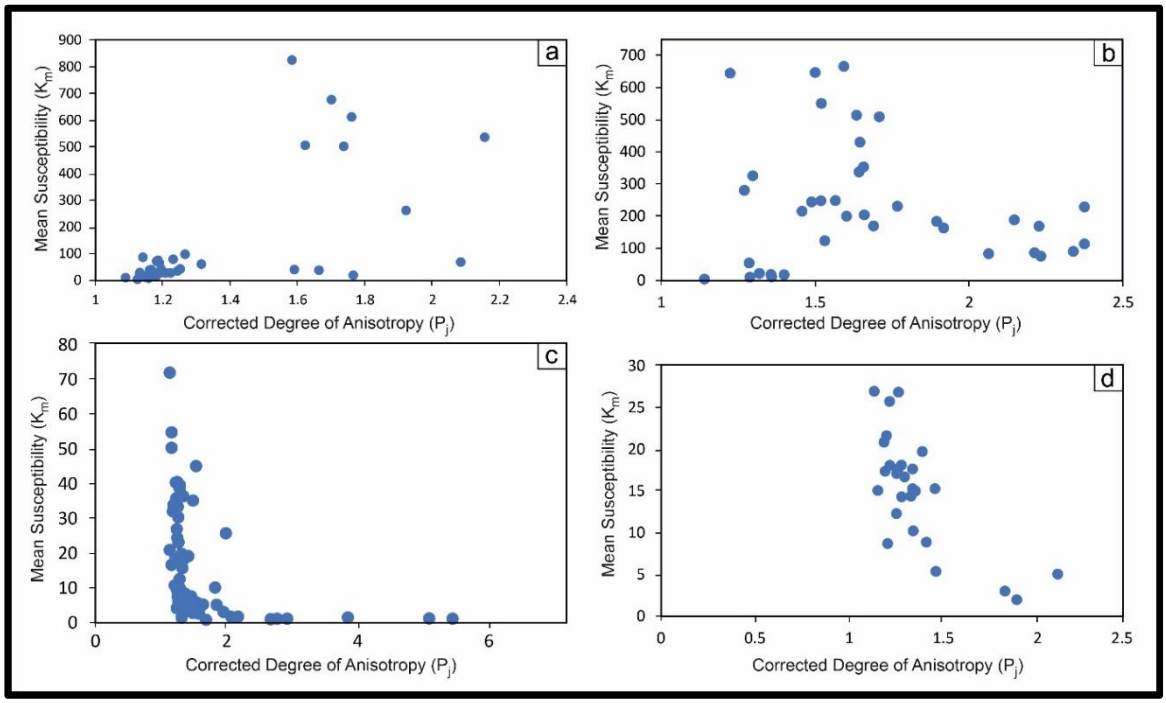

Fig. 7.3: P_j vs K_m Plots for (a) Northern Sector Granulite; (b) Southern Sector Granulite; (c) Anorthosite and (d) Leptynite.

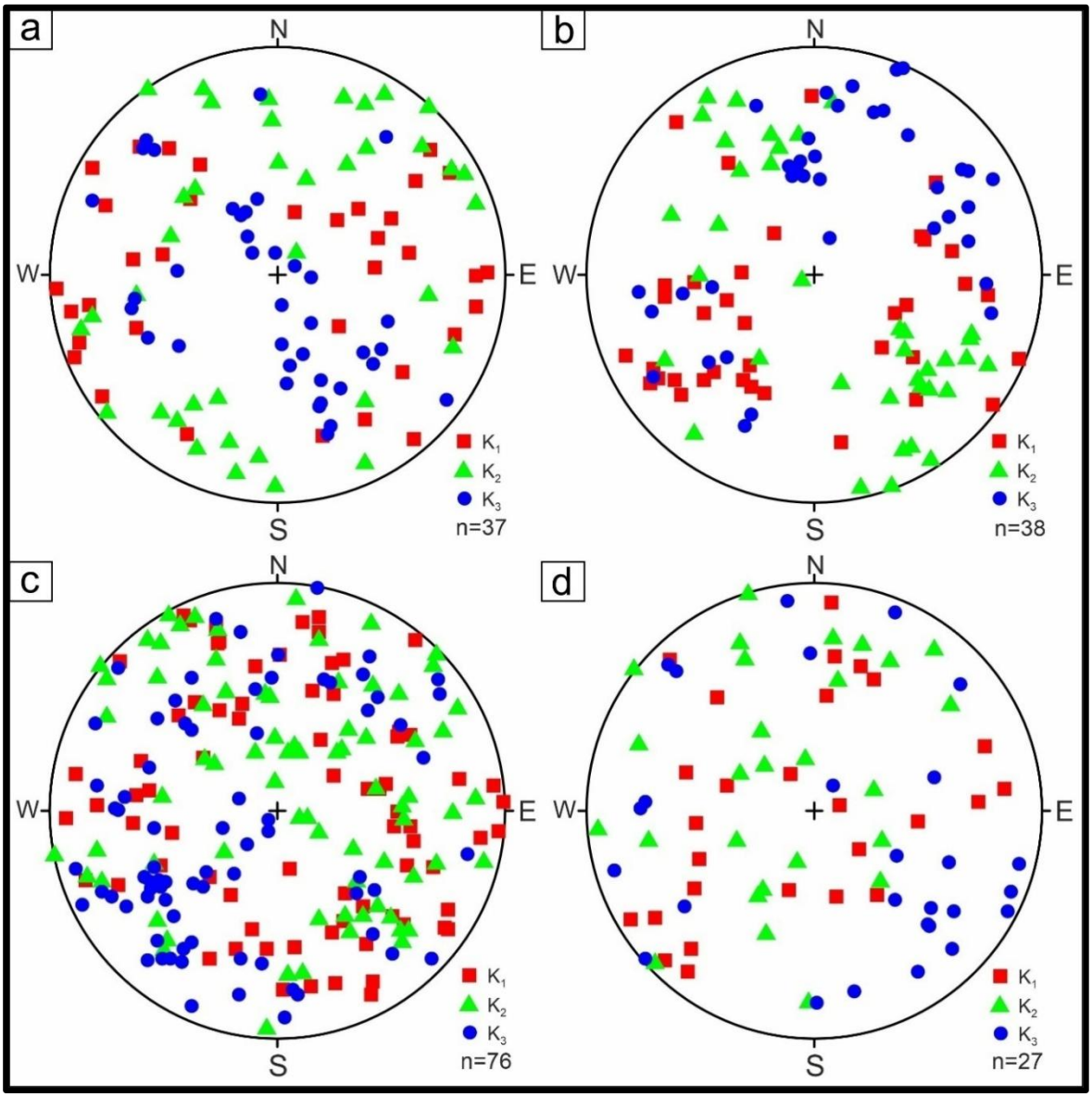

Fig. 7.4: Lower Hemisphere Equal Area Plots for all the Principal Susceptibility Axes for (a) Northern Sector Granulite; (b) Southern Sector Granulite; (c) Anorthosite and (d) Leptynite.

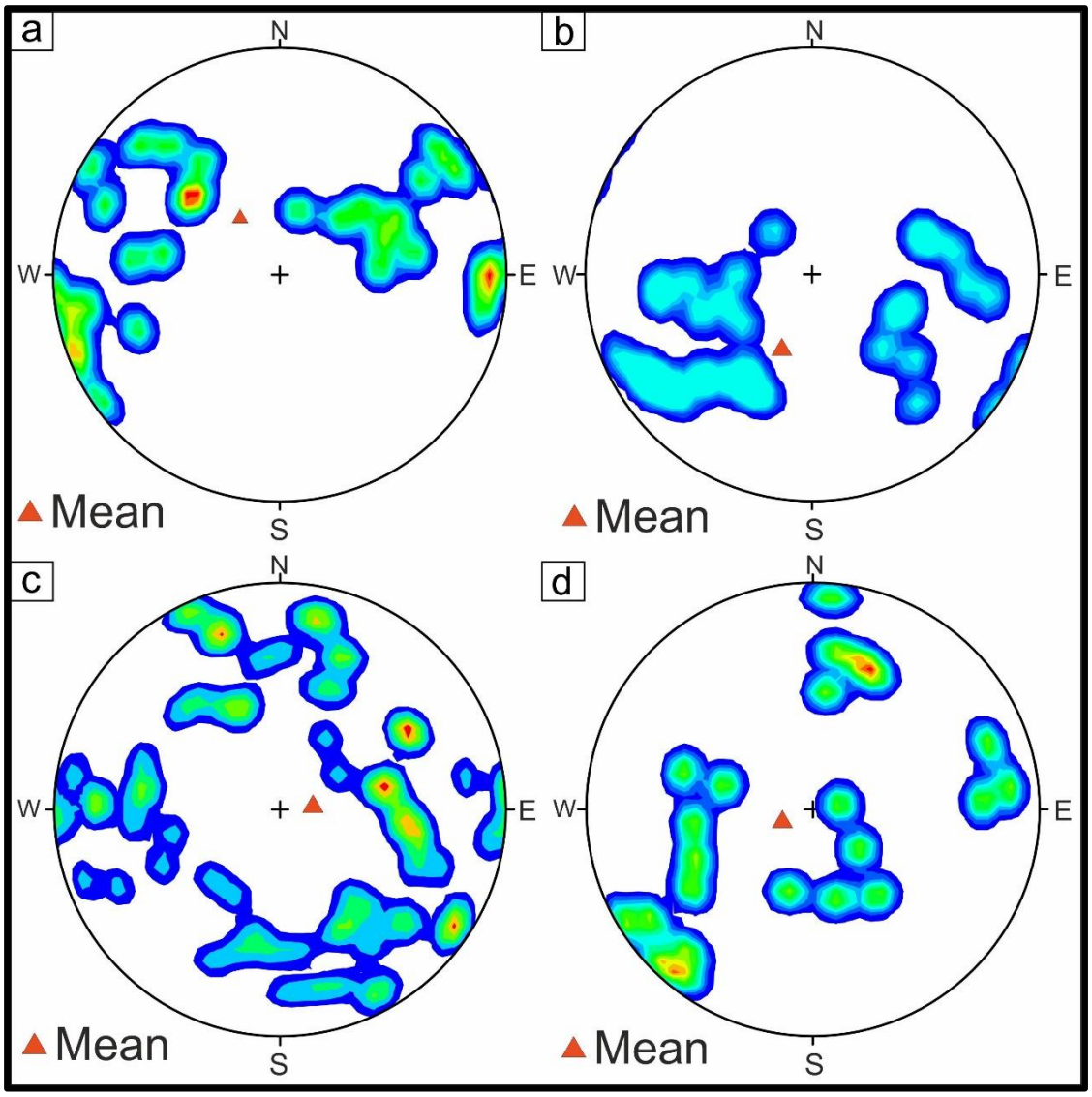

Fig.7.5: Lower Hemisphere Equal Area Plots for the Magnetic Lineation for (a) Northern Sector Granulite; (b) Southern Sector Granulite; (c) Anorthosite and (d) Leptynite.

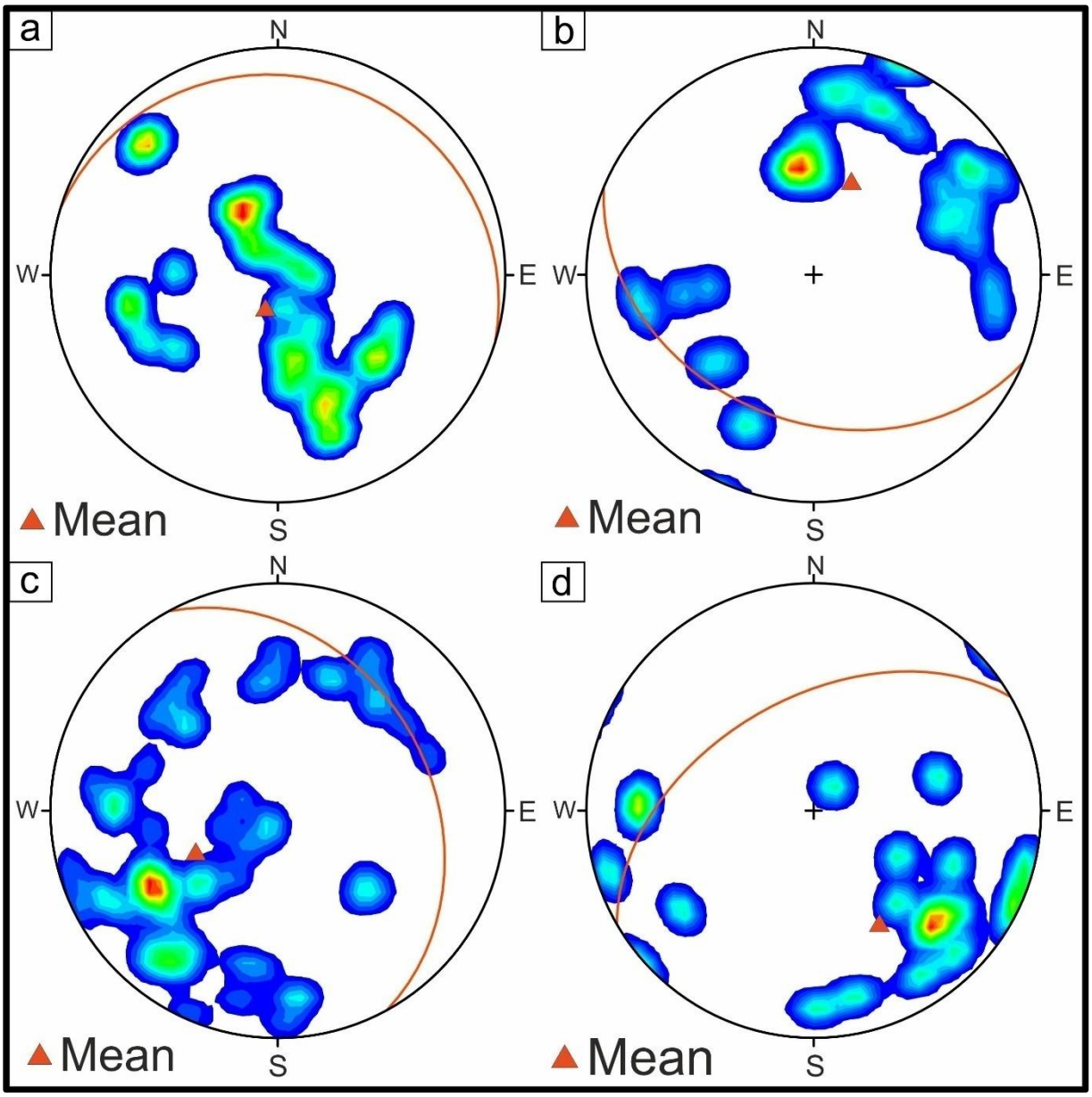

Fig. 7.6: Lower Hemisphere Equal Area Plots showing the Magnetic Foliation for (a) Northern Sector Granulite; (b) Southern Sector Granulite; (c) Anorthosite and (d) Leptynite.

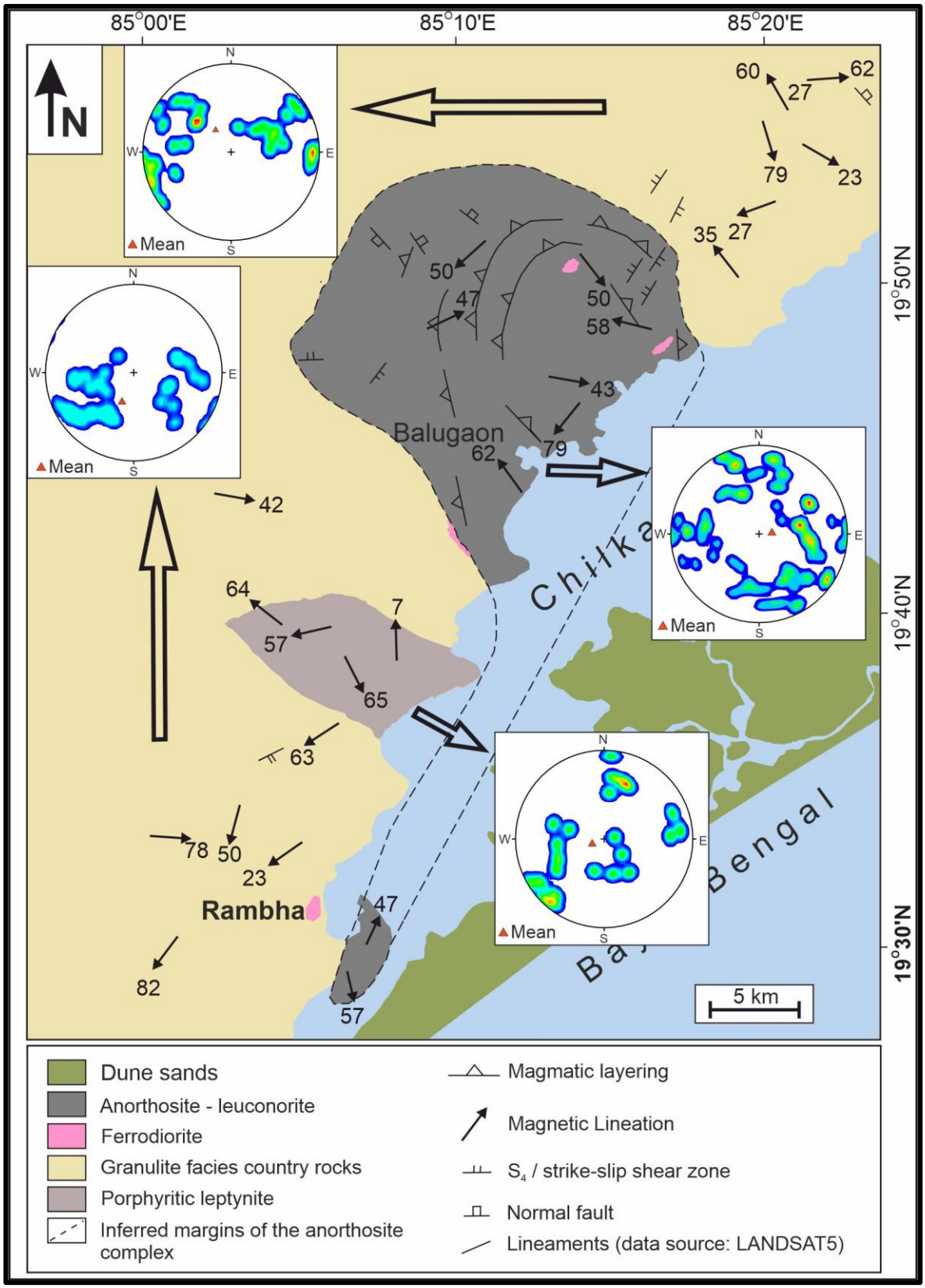

Fig.7.7: Magnetic Lineation distribution of the study area. Different sector plots are shown in individual equal area diagram.

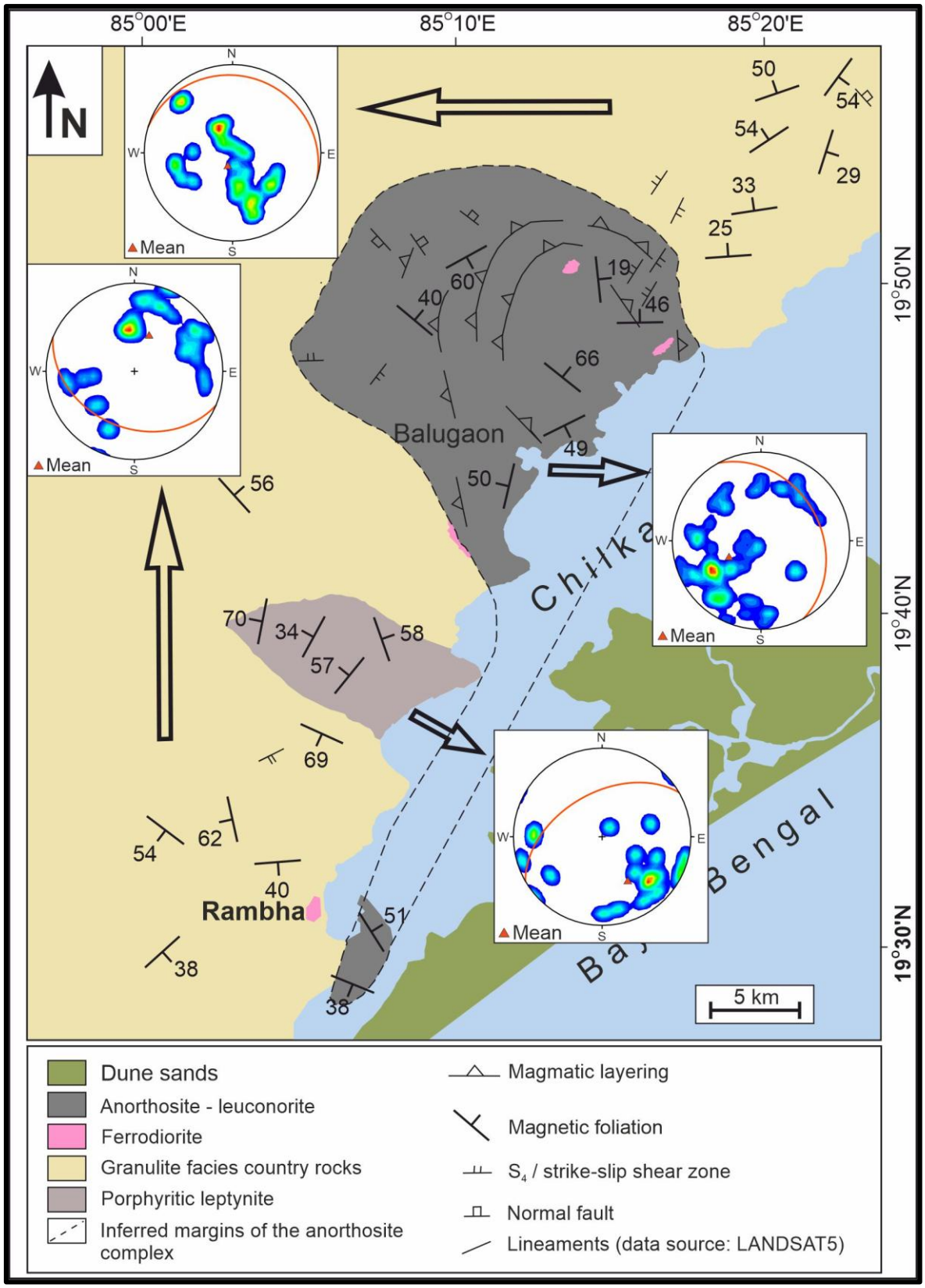

Fig.7.8: Magnetic Foliation distribution of the study area. Different sector plots are shown in individual equal are diagram.

Chapter: 8

PALAEOMAGNETIC STUDY

8. Palaeomagnetic Study:

8.1. The Principle and Objectives:

The main objectives of the palaeomagnetic study are to recognize and separate the Natural Remanent Magnetization (NRM) components which the rocks of different geological times have acquired within itself. At the time of formation, the rock acquires a magnetization termed as primary magnetization and the magnetization acquired during the later phase after formation is termed as secondary magnetization. Demagnetization process is a very unique process which helps to unravel the magnetization history of the rock over a prolonged period of geologic time. This demagnetization process is also known as ′cleaning process′, which helps in distinguishing the different components of magnetization due to different blocking temperature and coercivity spectra. There are two types of "cleaning process" which are widely used:

1. Alternating Field (AF) Demagnetization, and
2. Thermal Demagnetization.

In the AF Demagnetization, the rock specimens are exposed to an Alternating Magnetic Field in a space with no external field. Thermal Demagnetization can be either continuous or progressive, but having same motive of unblocking the magnetization of the residing magnetic minerals by the heating process from room or ambient temperature to respective Curie Temperature (T_c).

In case of Thermal Demagnetization, the samples are heated to such a temperature, where the blocking temperature (T_b) ≤ thermal demagnetization temperature (T_{mag}), where the remanent magnetization, H=0, hence clearing all NRM also within the grain. Hence, the samples are heated until the sample demagnetize completely, removing the NRM (Natural Remanent Magnetization) carried by the grains. All magnetic minerals have a specific relaxation time, specific time constant for different magnetic particles. The relaxation time (τ), is the time at which the particle requires to come in equilibrium with the surrounding.

$$\tau = \frac{1}{c} exp \frac{\text{vBc Js}}{2kT}$$

c= frequency factor (~ $10^{10}S^{-1}$)

v= volume of particle

B_c= coercivity of the particle

J_s= spontaneous magnetization of the particle

k= Boltzman's constant

T= absolute temperature

Both T and B_c plays an important role on 'τ'.

The NRM within the sample gets lost when the sample is heated to the relaxation time for some time. After this if the sample is cooled in presence of an ambient magnetic field, then the rock will acquire a pTRM but if the rock is cooled at zero ambient field, then there will be no contribution of NRM in the rock because the particle will be oriented randomly. The rock exposed to heating process for thermal cleaning, the NRM is measured at the raised temperature. Hence, the lower blocking temperature components are removed leaving behind the magnetic particles of higher Curie temperature.

8.2. Natural Remanent Magnetization (NRM):

NRM is permanent magnetization which records the electromagneticfield all throughout the geologic time scale after formation. Before any demagnetization process the bulk magnetization is termed as NRM (J) and is the summation of all the vectors of multiple remanent components, NRM has both directions (declination and inclination, D_m/I_m) and magnitude (intensity of magnetization). It is expressed as:

$$J = J_i + J_r \qquad \text{(Butler, 1992)}$$

where,

J_i=Induced Magnetization (acquired parallel to direction to EMF)

J_r= Remanent Magnetization.

But J_i doesnot affect the magnetization which the rock has captured during its formation, which is very important for the study of palaeomagnetism (Butler, 1992 and Tarling, 2007). There are two kinds of NRMs, primary and secondary NRMs. Primary NRM is captured during the formation of the rock which is parallel to the ambient Earth's magnetic field and the secondary NRM is acquired during the geological processes which the rock suffered after formation (Butler, 1992).

8.3. Palaeomagnetic Experiment and Data Analysis:

In present study, the high-grade metamorphic rocks and Anorthosite samples were heated in progressive steps during the thermal demagnetization experiment. The process of this demagnetization contains few steps. Initially, before start of heating process, the NRM of the samples were measured and then after every heating step of a batch of samples and cooling them at a field free environment to room temperature, the magnetization was again measured. Initially, a trial run was conducted using samples from each site by progressive thermal treatment at intervals of 50˚C-100˚C upto a temperature where the magnetic intensity of the specimens were completely diminished in order to comprehend the demagnetization behaviour of these rocks and to recognize the demagnetization history. By this trial study, the importance of this investigation to know the blocking temperature range till the Curie temperature by the thermal heating, of the magnetic minerals within the sample. After this trial run, analyze the demagnetization result of each sample, the ideal site for this experiment were identified. This is also indicated the demagnetization levels and accordingly all six core samples from each of the site progressively demagnetized step by step, 50˚C interval till 500˚C and then 20˚C up to a temperature ~580˚C the Curie temperature of magnetic mineral. Each of the samples was kept for 30 minutes at that particular temperature, so that the entire sample till the core reach the specific desired demagnetization temperature. Batch wise samples were heated till each of the core demagnetized below 0.5×10^{-5} $Am^2 kg^{-1}$, rewarded in portable Spinner Magnetometer. The magnetization intensity value is considered to be very low, but not zero because every sample started the demagnetization process with magnetization intensity about 1000×10^{-5} Am^2kg^{-1}. In between each heating step, the cores were kept in a cylindrical container which shielded the samples from exterior magnetic fields.

The demagnetization data were analyzed by a Statistical Process, which is known as Principal Component Analysis (PCA) Process for the high-grade metamorphic rocks as well as the Anorthosites of the Chilka Lake area, Odisha, EGB have been plotted and helped in illustrating the magnetization history by the help of the three following plots: 1) Stereo Plot, 2) Intensity Plot and 3) Orthogonal Plot. In Stereo plot, we plot the Declination Vs Inclination in a stereonet and observe the nos. of clusters present in the studied samples. In Intensity plot, we plot the Intensity of Magnetization Vs Heating temperature and observe the nos. of steady vectors present

in the studied samples. The orthogonal plot is a construction technique that projects the magnitude and direction of magnetization vectors (declination and inclination) onto the horizontal and vertical planes (Zijderveld, 1976). Hence, this plot is also named as Zijderveld Plot. While demagnetizing when after one step one component is subtracted then that step is marked by a straight line segment and after the later steps of demagnetization then the last one component is remaining in specific samples, the line will meet towards the origin. PCA is a technique that may be used to calculate the magnetic component direction that make up the NRM, by separating them on the orthogonal plot. On the basis of the nature of the trajectories, the magnetic vectors present within the demagnetized samples can be identified. The stereo plot is a method that helps in identifying the movement of the vectors by plotting the magnetization direction vectors of each step of demagnetization. Whereas, the intensity plot helps in identifying the blocking temperature range by plotting the intensity of magnetization after each demagnetization step.

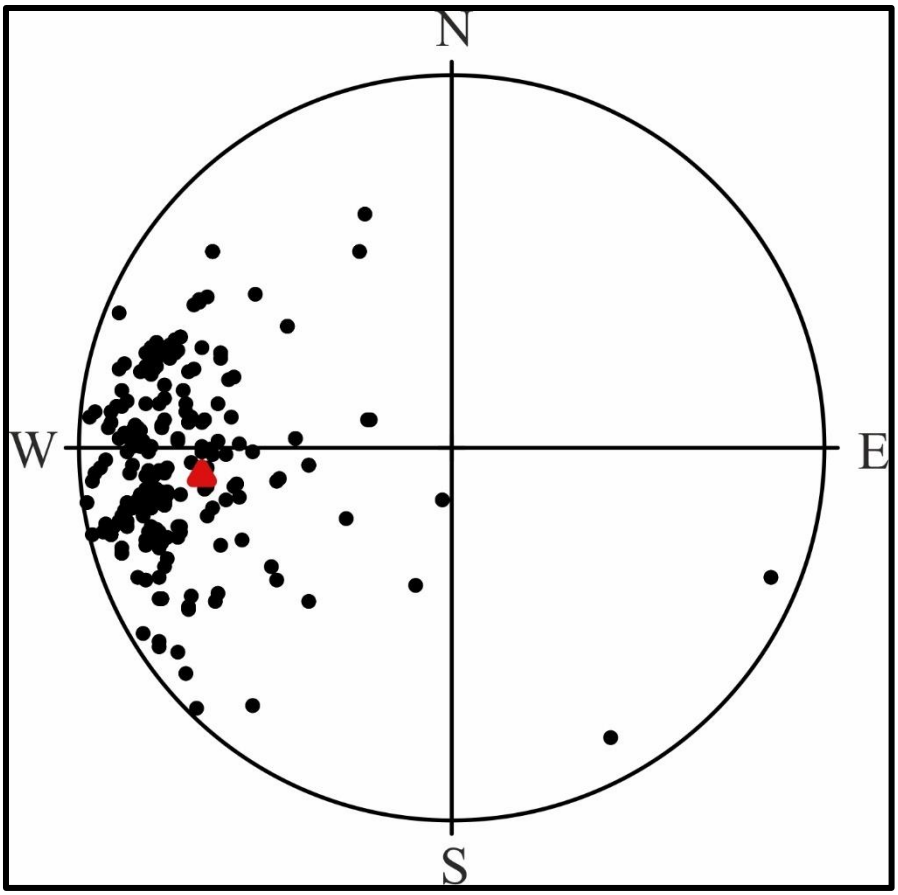

Fig. 8.1: Stereoplot showing palaeomagnetic directions for Anorthosite samples from Balugaon and Rambha Area.

The high-grade metamorphic granulite rocks along with the anorthosite from Balugaon Area possesses different magnetization vectors. In case of the Anorthosite rock samples, all the magnetic declination and magnetic inclination vectors i.e. D/I of all the Anorthosite samples are plotted and indicate a mean D/I from the stereo plot (Fig. 8.1). From the stereo plot, the D/I are plotted towards the West, ranging from 238˚/41˚ ⟶ 292˚/ 34˚. From the stereo plot, considering all the D/I in the stable cluster, the mean D/I value (red mark) was selected from the plot (Fig. 8.1). On heating the sample upto about 600˚C, the demagnetization vector shows a blocking temperature of a specific magnetic component (Fig. 8.2). From the Zijderveld plot, almost a straight segment is observed from different locations of the Anorthosite rock type (Fig. 8.3). This indicates a single component stable magnetization. The nature of the Zijderveld plot indicates the presence of one stable vector is present in Anorthosite samples of Balugaon Area. The Granulites from Balugaon Area, Odisha show a haphazard orientation, when all the D/I were plotted on the stereo plot, the data were not showing any suitable and stable cluster, the D/I were not forming any prominent cluster (Fig. 8.4). Hence, for the further steps for the pole finding a specific mean D/I cannot be selected from the haphazard orientation of all the D/I. Thermal demagnetization curves for Chilka Lake specimens indicate multicomponent magnetism which varies from rock types. The studied area consisting of high-grade metamorphic which exhibit multi phase deformation in local scale, this deformation episode occurred after the acquisition of magnetization. For this reason, the studied high-grade metamorphic does not exhibit any suitable clusters in stereoplots. For the Anorthosite samples the magnetization vector falls on the southwest (SW) quadrant mostly (Fig.8.1). The blocking temperature of this D/I cluster, is at a high temperature, ~580˚C (Fig. 8.2) for Anorthosite samples. Hence, the mean declination and mean inclination for all the Anorthosite samples associated with this study is D_m=262˚ and I_m= 35˚ (Fig. 8.1).

A positive direction has been identified from Balugaon Anorthosite Massif from Chilka Area. No signature of reversals is observed, though the magnetization process was long. It may be possible that the massif got magnetized for a long time under constant polarity when the terrain uplifted.

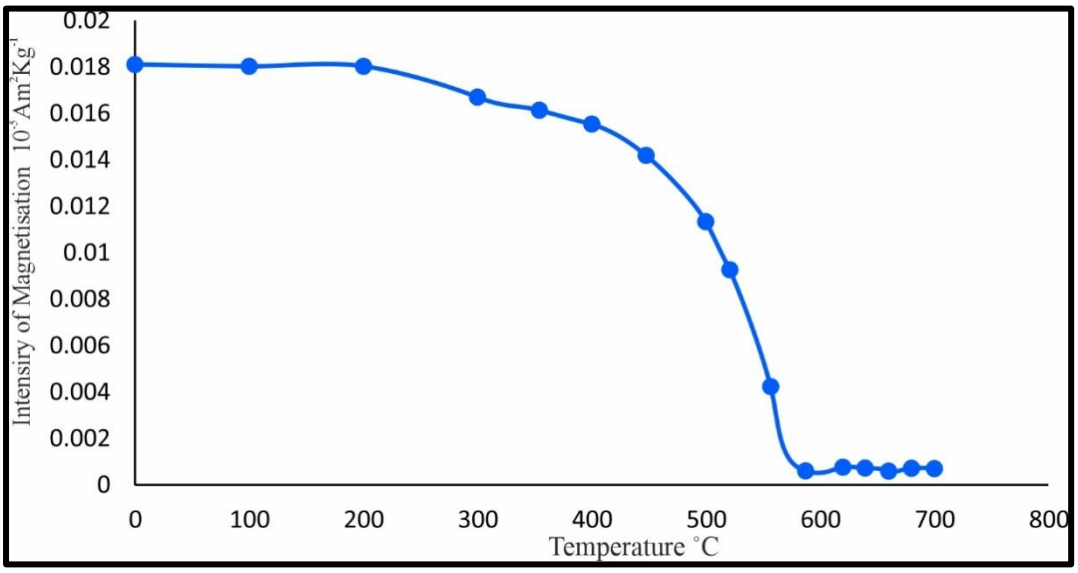

Fig. 8.2a: The intensity plot showing the thermal demagnetization behaviour of Anorthosite.

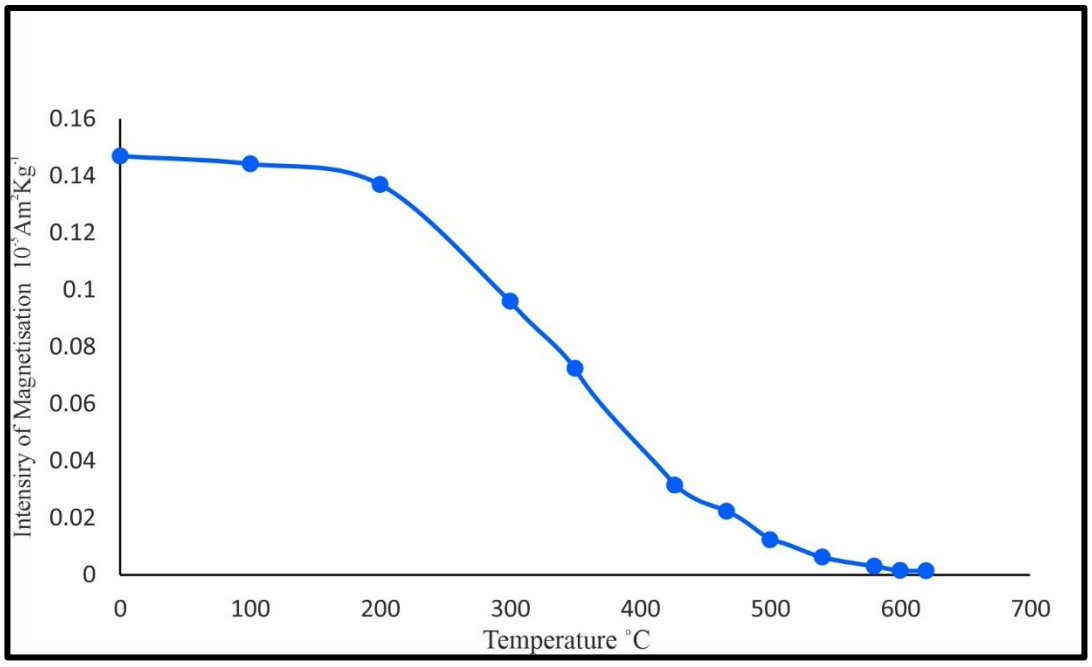

Fig. 8.2b: The intensity plot showing the thermal demagnetization behaviour of Anorthosite.

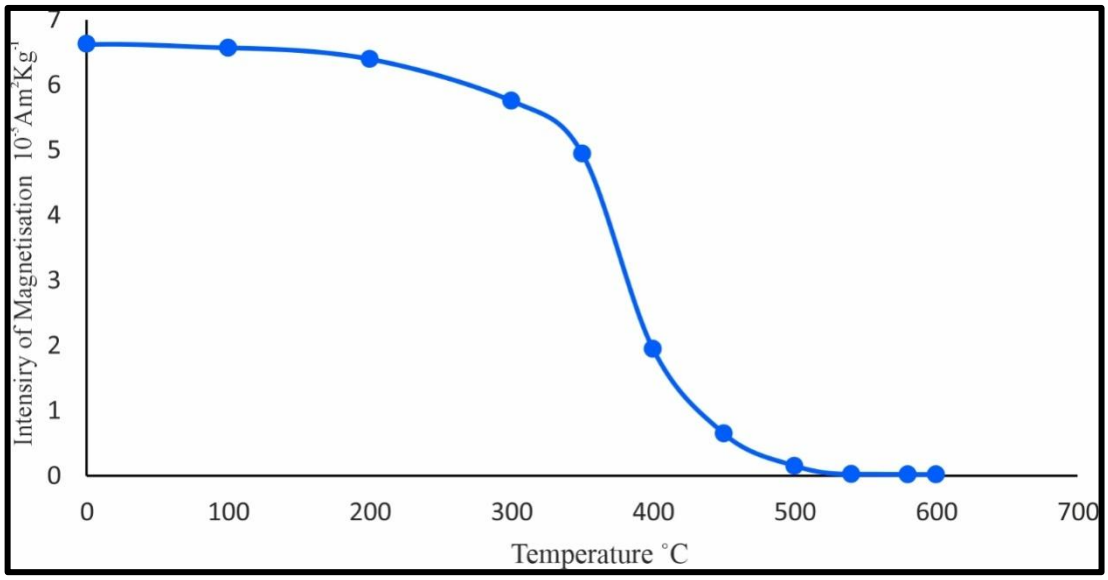

Fig. 8.2c: The intensity plot showing the thermal demagnetization behaviour of Anorthosite.

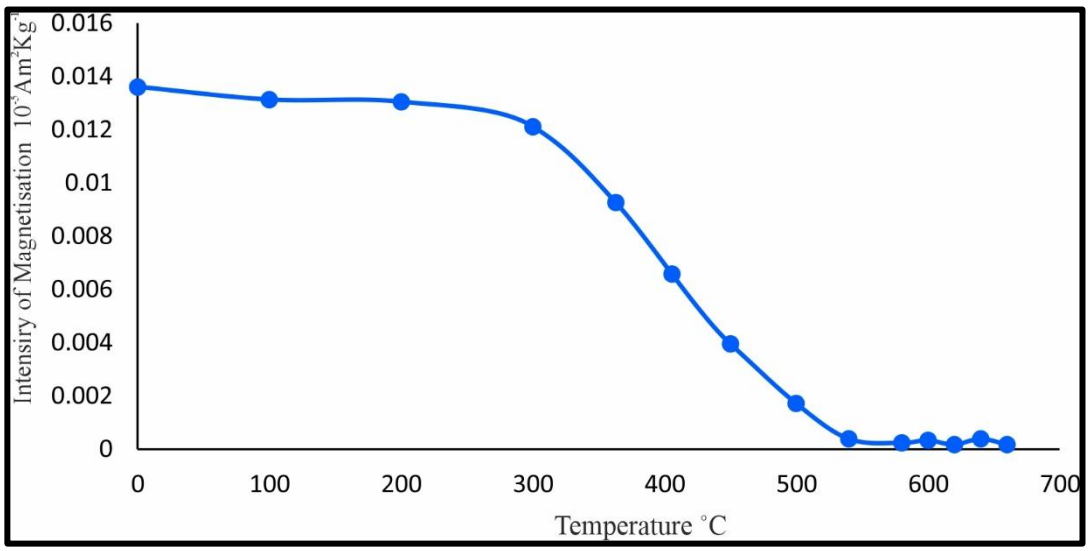

Fig. 8.2d: The intensity plot showing the thermal demagnetization behaviour of Anorthosite.

8.4. Statistical Analysis and Pole Position:

8.4.1: Statistical Analysis for Directional Stability of Magnetization:

Statistical analysis of palaeomagnetic data is crucial for determining a mean direction and evaluating the importance of the field tests of palaeomagnetic stability. Resolving the orientations of two or more magnetization is a common difficulty that

is typically faced in varying degrees of complexity, particularly with high-grade metamorphic rocks. All the samples from both sampling locations of Balugaon and Rambha and associated areas, underwent progressive thermal field cleaning to resolve the magnetic components that make up the total NRM.

In evaluating the accuracy of population grouping for palaeomagnetic directions, Sir R.A. Fishers' probability density function was used which was developed in 1953. Fisher statistics used a circular-symmetrical density function, plotting directions as points on a sphere, similar to the two-dimensional Gaussian distribution. The directions plotted are distributed according to the probability density function P(Ψ), given by:

$$P(\Psi) = \frac{\mathrm{k}}{4\pi \sinh k} \exp(kcos\ \Psi),$$

where, Ψ is the angle from true direction, and k is the precision parameter.

The features of this distribution are widely used to determine the quality is grouping in a population:

i. Alpha (α95): the radius in degrees of the 95 percent cone of confidence about the mean direction.
ii. K, the precision parameter, the best estimate of which is calculated by:

$$k = \frac{\mathrm{N} - 1}{N - R}$$

where, N is the number of samples, R is the resultant vector.

Value of k can have many variations, but must be observed carefully. A number larger than ~10 indicates that the computed mean direction is near to the true mean. While k grows quickly for low values upto ~8, higher values do not significantly enhance the estimate of the mean direction.

From the thermal demagnetization results of the Anorthosite from both Balugaon and Rambha Massifs, a characterized single component magnetization is observed. The data show a moderate inclination at a high blocking temperature. Whereas, the granulite facies rock does not show any stable magnetization vector, hence a precise declination and inclination cannot be marked; even the blocking temperature is not prominent.

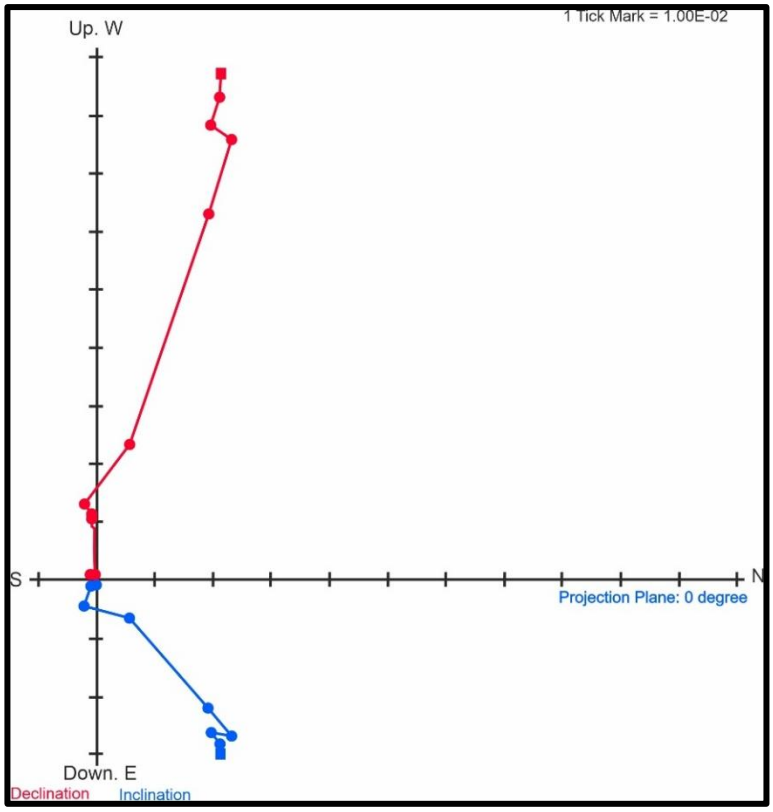

Fig. 8.3a: The orthogonal plot showing the thermal demagnetization behaviour of representative Anorthosite sample.

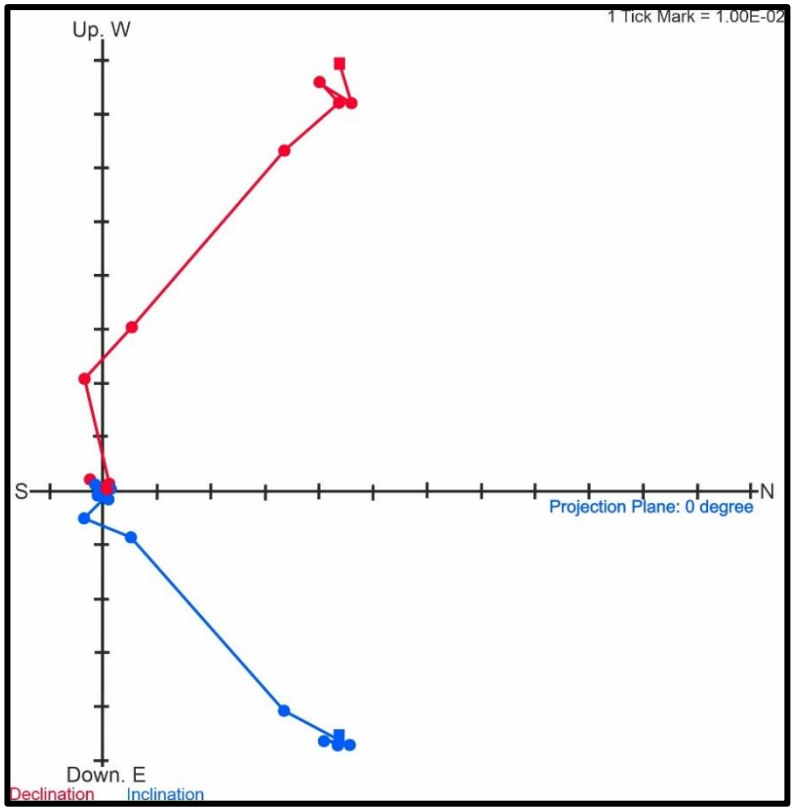

Fig. 8.3b: The orthogonal plot showing the thermal demagnetization behavior of representative Anorthosite sample.

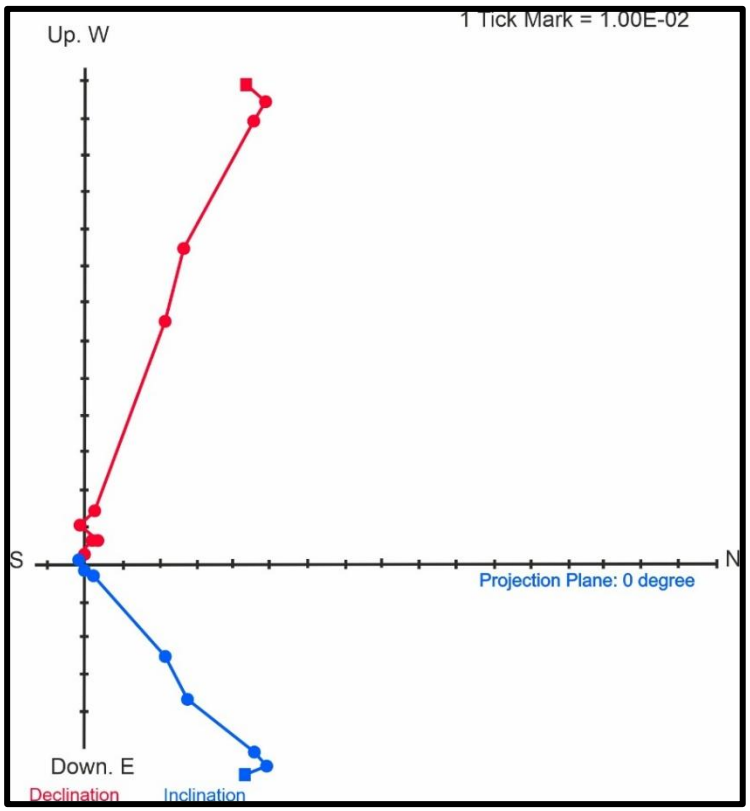

Fig. 8.3c: The orthogonal plot showing the thermal demagnetization behavior of representative Anorthosite sample.

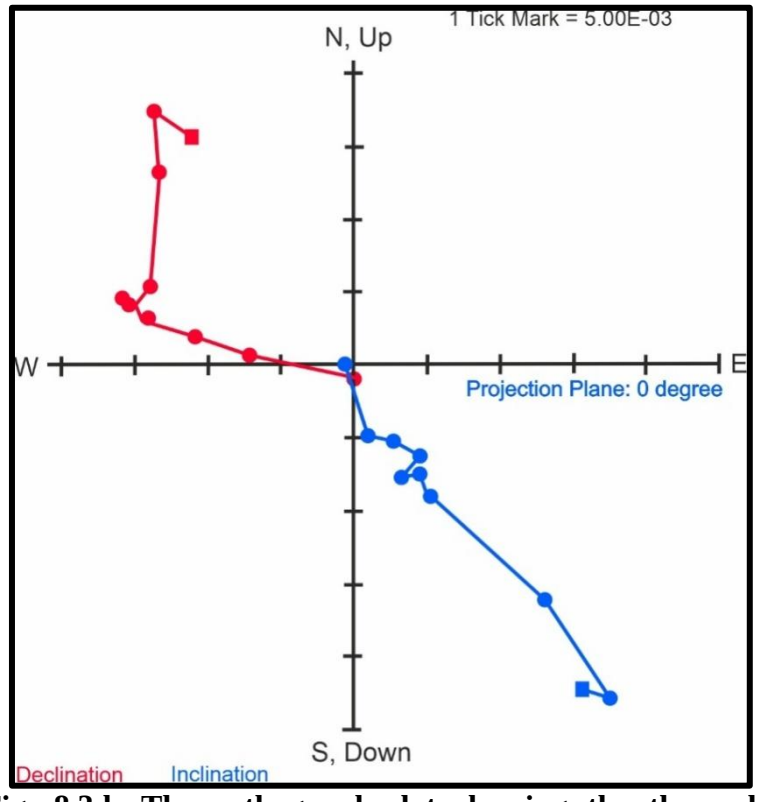

Fig. 8.3d: The orthogonal plot showing the thermal demagnetization behavior of representative Anorthosite sample.

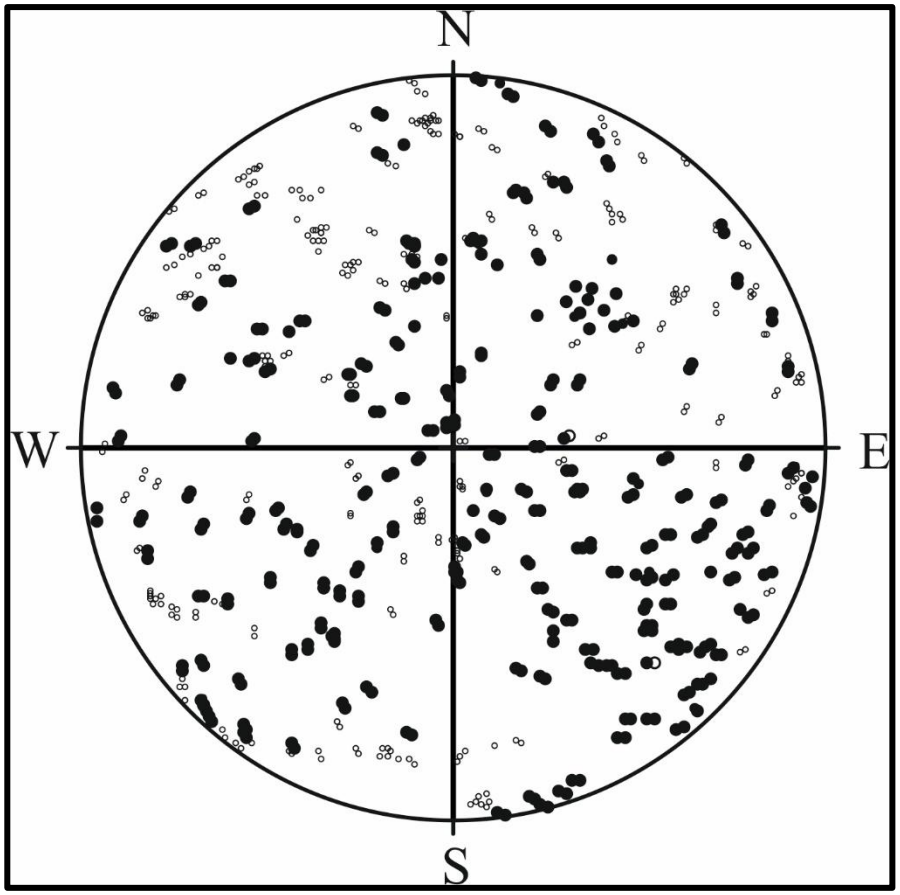

Fig. 8.4: Stereo plot showing palaeomagnetic directions for the high-grade granulite samples.

8.4.2: Palaeomagnetic Pole Positions:

The palaeopole and the palaeo-latitudes are obtained from the mean D/I vectors acquired by plotting all D/I vectors of the thermal demagnetization. Then the pole is plotted on the stereonet. The magnetic pole moves due to secular variation, but its position is affected by Earth's rotation. The pole's instantaneous position is a virtual geomagnetic pole, but when arranged over 10^3-10^4 years, its mean approaches the geomagnetic pole.

The metamorphic rocks exhibit a diverse magnetization orientation. The samples under investigation of this study are multiphase deformed, hence they have uplifted and cooled over millions of years while metamorphism, then the TRM's will average out secular variations by calculating component directions from individual samples, defining palaeomagnetic poles and ancient geographic poles. So, stereoplots were plotted separately for Anorthosite and the high-grade granulite rocks. In the

stereoplots of the Anorthosite, a moderately dipping westerly cluster was observed (Fig. 8.1), where as in case of the granulites, no specific cluster was observed (Fig.8.4). The mean D/I was obtained from the cluster on the stereo plot noted as D.

Mean Vector	**Number of Samples (N)**	**Mean Declination (D_m)˚**	**Mean Inclination (I_m)˚**	**α95**	**k**
D	56	262	35	13.9	11.75

Referring the palaeomagnetic pole locations, can help locating the current latitude, longitudes and palaeo-lattitude. Let, the present latitude and longitude of the site are λ_s and φ_s and the mean declination be D_m and mean inclination be I_m of the site, then the latitude (λ_p) and longitude (φ_p) of the ancient pole can be expressed as:

$$\lambda_p = \sin^{-1}(\sin\lambda_s . \cos p + \cos\lambda_s . \sin p . \cos D_m)$$

There are two possibilities for pole longitudes,

If, $\cos p \geq (\sin\lambda_s . \sin\lambda_p)$, then $\varphi_p = (\varphi_s + ß)$,

Or, $\cos p < (\sin\lambda_s . \sin\lambda_p)$, then $\varphi_p = \varphi_s + (180^\circ - ß)$,

Where, $ß = \sin^{-1}(\sin p . \sin D_m / \cos\lambda_p)$.

Here, ß is longitudinal difference between pole and site,

p is apparent or ancient magnetic colatitude of the site, given by

$$p = tan^{-1}\left(\frac{2}{\tan Im}\right)$$

The oval of 95% confidence about the pole location is the name given to the polar error, which is determined by d_p and d_m. The respective d_p and d_m are given by

$$d_p = \frac{1}{2}\alpha 95(1+3\cos^2 p),$$

$$\text{and } d_m = \alpha 95(\sin p / \cos I_m)$$

The plot of the stable component of the Balugaon and Rambha Massif Anorthosite clearly show one distinct cluster of remanent magnetizations (Fig. 8.1). This pole is represented by **C**, showing a positive direction with negative inclination. Since, the samples have experienced high temperature about ~600˚C, it is suspected that they experience a high temperature deformational event. The pole obtained from this study is **C**, with $\boldsymbol{\lambda_p = 1.15^\circ}$ **S** and $\boldsymbol{\varphi_p = 16.15^\circ}$ **E** and the palaeo-latitude was 19.3˚N. This pole correlates to the historical event experienced by Indian subcontinent.

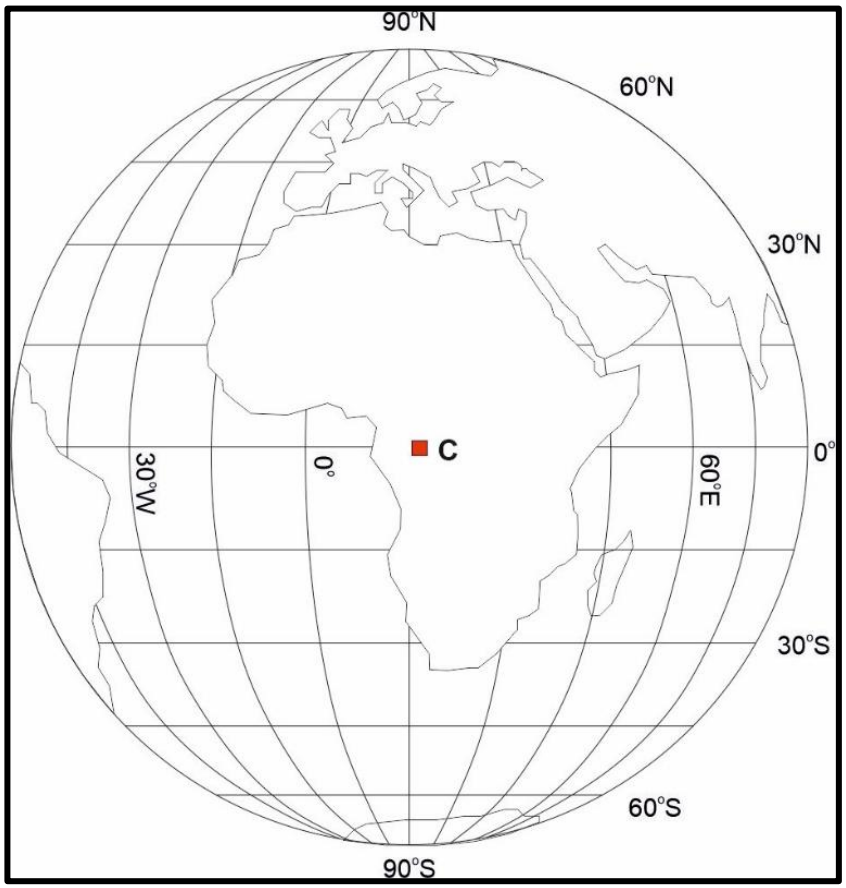

Fig. 8.5: Pole position obtained from the studied Anorthosite samples.

Chapter: 9

RESULTS AND DISCUSSIONS

9. Results and Discussions:

The current study combines petrological and magnetic studies to determine the geological and geophysical properties of the rock samples from Balugaon and Rambha Anorthosite Massifs along with the surrounding high grade granulite rocks. The initial important work is to characterize the rocks petrologically both in the mesoscopic and microscopic scales, since the magnetic parameters vary depending on the rock types and mineral assemblages (Tarling and Hrouda, 1993; Butler, 1992 and Tauxe, 2010). Hence, after the petrological study of all the collected rock samples, five major rock types were identified. Anorthosite mainly belongs to Balugaon and Rambha areas, surrounded by high-grade poly-deformed granulite facies rocks. These high-grade granulite facies rocks are Orthopyroxene granulite, Mafic granulite, Leptynite and Khondalite. In all the rock types, the porphyroblasts are refined or broken down in finer portions when they experienced the deformational and metamorphic events. The breakdown of the garnet by multiple fractures, undulose extinction in quartz and discontinuous tapered lamellae in plagioclase feldspar indicates that the granulite rocks have experienced poly-deformation. Due to high temperature metamorphism, quartz and feldspar went under recrystallization. The undulose extinction within the quartz is as result of high temperature metamorphism. These above-mentioned features indicate that during the post peak deformational event (D_3), the peak assemblage underwent crystal plastic deformation (Das et al., 2012). Some of the textures indicate isothermal decompression (Hollister, 1977 and Harley, 1989). The coronal garnet around the Fe-Ti oxides and the reaction textures indicate that a pressure drop took place at the thermal peak condition of metamorphism (Thompson, 1976; Schenk, 1984 and Tracy et al., 1976). Myrmekite is a significant signature of metamorphism, gives evidence of rapid decompression. Hence, presence of both myrmekite and coronal garnet indicates that the granulites from the Chilka Lake area, Odisha have a history of experiencing an isothermal decompression. This indicates that the granulites were highly affected during post peak metamorphic episode.

The studied samples have Fe-Ti oxides, which exhibit different generations and stages of oxidation. Both low temperature (<350˚C) and high temperature (>600˚C) oxidations of primary oxides are observed. In Anorthosite, signatures of only high temperature oxidations are observed. It is evident by the homogeneous

oxide grain of C-1 Stage. The grain with hair-like ilmenite lath signifies C-2 Stage. In C-3 Stage, presence of broad exsolved ilmenite lamellae within the inhomogeneous titanomagnetite indicate increased oxidation. These high temperature oxides within the anorthosite were formed during the massif anorthosite emplacement, which was a plutonism event. Hence, the high temperature Fe-Ti oxides are syn-tectonic with the magmatism event.

Within the granulite rocks, both high temperature and low temperature oxides are observed. The high temperature oxides observed within the granulite rocks formed during this area's peak metamorphic as well as deformational event, M_2-D_2 (Das et al., 2012). These low temperature oxides formed during the retrograde process, which suffered low temperature upliftment related oxidation (Akimoto et al., 1984). Different stages of low temperature oxidation are also observed, Stage-1, Stage-2, Stage-3, Stage-4 and Stage-5. The inclusions of oxides within garnet are primary oxides. During the retrograde path the high temperature oxides suffered i.e., the low temperature oxidation, made the grain boundary of high temperature oxides corrugated. Small secondary oxide grains along the fractures in silicates, along the cleavage planes of silicate and also along the grain boundaries of silicates are observed. Under the microscope, magnetite and Fe-Ti oxides are identified. The high temperature oxides observed within the anorthosite and granulite rocks of the Chilka Lake area are result of different geological events.

The rockmagnetic measurements identify the presence of ferromagnetic magnetite and paramagnetic haematite within the studied anorthosite and granulite. Magnetite is identified by a drop in the heating curve at the Curie temperature T_c~580˚C. These magnetites give a steady and stable magnetization. The thermomagnetic curves also give the indication of the presence of paramagnetic haematite with T_c~680˚C. The hysteresis curves, indicating saturation and remanence, typically for ferromagnetic magnetite. Few of the hysteresis curves also exhibits minimal remanence, and their unsaturated nature state suggest that both paramagnetic and ferromagnetic minerals are residing within the same sample. IRM curves also indicate the presence of magnetite. So, from the rockmagnetic study, it is evident that the most significant magnetic mineral present within the studied samples is ferromagnetic magnetite along with paramagnetic haematite. Presence of adequate amount of iron oxides made the way for the further investigation for the

palaeomagnetic study. The Day plot shows that fine grained SD Ti-magnetites are the primary source of magnetic remanence.

The magnetic fabric has an important role in giving the tectonic implications. The orientation of K_1 in the Balugaon-Rambha sector in and around Chilka Lake region could potentially reveal the direction of stress field during orogenic events of the EGMB. This is because the maximum susceptibility axes (K_1) are aligning itself along the direction of maximum elongation or the maximum extensional stress and evidently stays perpendicular to the direction of shortening or the maximum compressive stress (Gain et al., 2022 and Mondal et al., 2009). Based on this, the evolution of the magnetic fabrics in the Chilka Lake area may be categorized as two stages, each associated with specific tectonic event in this terrain (Das et al., 2024).

Stage 1 (Metamorphism):

The earliest stage of magnetic fabric emergence is recorded in the granulitic rocks of the studied samples. Dasgupta et al., (2013) concluded that the Eastern Ghats Belt's oldest rocks (~2.0Ga) show signs of retreating orogeny and subduction between 2 Ga and 1.7 Ga. The direction of the magnetic fabric in granulite indicates that K_1 mostly trends NE-SW with minor variations seen in the southern granulite (Figs. 7.6a and 7.6b), aligning with the regional F_1 fold axis resulting from D_1 deformation. This demonstrates that at this point, the distribution of the highest compressional stress (σ_1) was oriented NW-SE. However, the magnetic foliation plane formed at this period is not aligned with the regional schistosity. The deviation in the magnetic fabric from the mesoscopic scale may be attributed to the increased susceptibility of the magnetite grains, which form exclusively during this phase due to Ultra High Temperature (UHT) metamorphism (Dasgupta et al., 2013 and Sengupta et al., 1999). High susceptibility magnetite grains can rotate the magnetic foliation plane in the direction of mineral development, diverting it from the mesoscopic schistosity. A significant association between P_j and K_m in both northern and southern sector granulite confirms the same (Figs. 7.4a ad 7.4b).

Stage 2 (Magmatism):

An analogy with the maximum susceptibility axes as a proxy from this σ_1 orientation, both in Anorthosite and Leptynite which are products of post subduction magmatism, it is observed that the orientation of stress field was not constant.

The magnetic lineation of Leptynite, which eventually grades to an E-W orientation and becomes entirely random in the Anorthosite, still retains part of the σ_1 orientation, which was initially NW-SE during the metamorphism stage. Hence, the Leptynite marks the transitional zone between the metamorphism, and the final magmatism stage. According to the magnetic fabrics, Leptynite is therefore prior to Anorthosite. Signatures of D_1 and D_2microscopically are absent within anorthosite and the E-W orientation of the K_1 fabric within the Leptynite has accordance with the D_3 deformation. During the felsic magmatism, the anorthosite mostly feature unoriented magnetic fabrics that do not preserve regional tectonics because these rocks were deposited after the termination of the D_3 phase of the deformation, after the emplacement of the Leptynite. So, it concludes that the anorthosite originated last and experienced the least amount of deformation (Das et al., 2024).

From this study the existence of low temperature oxidized Ti-magnetite and ultrafine secondary magnetite grains, within the metasedimentary granulite in and around Balugaon Massif and Rambha Massif Anorthosites, suggests upliftment accompanied by gradual cooling. During the upliftment or exhumation, the release of pressure occurred resulting in the formation of fractures within the oxide minerals, which were subsequently filled with silicates. Therefore, these characteristics can be linked to slow cooling and upliftment of the deposited sediments. Whereas the high temperature oxides within some of the granulite rocks indicate that they have also experienced the peak metamorphic as well as deformational event, M_2-D_2. The oldest supracrustal rocks of the Chilka Lake area experienced the deformation (D_1), prior the peak deformation of this area 964-924 Ma (Dobmeier and Simmat, 2002). The Grenvillean metamorphic event (950-1100 Ma), which defined the fabric in most areas, is in good agreement with the ages of the Eastern Ghat Belts. The characteristics, however are not observed within the Balugaon and Rambha Anorthosites. Within the Anorthosite the Ti-magnetite grains are high temperature fresh grains. During the felsic magmatism, the Anorthosites occurred forming the high temperature oxidation of Fe-Ti oxides. The occurrences of this resultant characterised by magmatism, was localised.

Following D_2, the rocks of the Chilka Lake area underwent a number of deformational events. The deformational process after D_2 significantly impacted the granulite, which in turn affected the previously conserved fabrics within the magnetic

minerals. But these deformational imprints are not observed within the Anorthosite. The magnetization acquired by the granulite rocks during formation was significantly influenced by subsequent deformations. Consequently, an appropriate D/I cluster was not achieved while visualizing the demagnetization vector. Conversely, the anorthosites formed a cluster subsequent to the plotting of the demagnetization D/I vectors. A suitable mean $\mathbf{D_m / I_m}$**, 262˚/35˚** was acquired for pole computation about the Anorthosites.

The pole position depicted on an equal area projection to correlate with previously established and dated pole positions and to estimate the age of pole established from the current investigations. The pole (C) obtained from the study area has an average age 850-900 Ma (Radhakrishna et al., 1996). The **Pole 'C′;** λ_p**= 1.15˚S;** φ_p**= 16.15˚E** for the Anorthosite of Balugaon and Rambha Massifs falls on the Apparent Polar Wandering Path (APWP) of India during Proterozoic time (Radhakrishna et al., 1996 and reference therein). During this time the anorthosite magmatism took place (Kaurse et al., 2001; Dobmeier and Raith 2002 and Chatterjee et al., 2008). The AMS study (Das et al., 2024) indicated that this period was characterised by felsic magmatism. This magmatism formed a high temperature regime, during cooling around 580º C, the high temperature primary magnetite was formed. These magnetites recorded the magnetic vector for the pole 'C′.

On the basis of magneto-mineralogical and micro textural analysis study under reflected light setup, it is evident that at least three generations of Fe-Ti oxides are present in the studied samples. In anorthosite, the first generation of titanomagnetite was evident. But in case of high-grade granulite rocks all three generations of titanomagnetite were observed. On the basis of statistical analysis of demagnetization data only one stable vector from the massif Anorthosite Complexes of Balugaon and Rambha was evident. This vector is co-relatable with the magnetic remanence carrier, the primary titanomagnetite rescinding in the Anorthosite. In case of high-grade granulite rocks, three different generations of magnetic minerals were evident but there were no suitable clusters visible in the stereo plot. The reason behind this is because, part of the studied area which exhibits the presence of high-grade granulitic rocks were highly deformed.

Chapter: 10

CONCLUSIONS

10. Conclusions:

This research work represents the first attempt to ascertain the palaeomagnetic characteristics, Anisotropy of Magnetic Susceptibility (AMS) and Rockmagnetic properties of the Anorthosite and high-grade granulite rocks from Chilka Lake Area, Odisha, Eastern Ghats Belt of India in connection with petrological and tectonic evolution. The following key conclusions can be made based on field and experimental observations:

1) Based on the petrological and magneto-mineralogical features, the identification of specific magnetic minerals present in the rocks is very important for interpreting the characteristics magnetic remanence of the studied rocks. The major rock types identified by petrological studies are Anorthosite, Orthopyroxene granulite, Mafic granulite, Leptynite and Khondalite.

2) Under reflected light microscopic study, at least three generations of Fe-Ti oxides are observed. Their textural relationship indicates the rocks suffered an extensive metamorphism. Only high temperature oxides are present within the Anorthosite, which indicate their formation during the formation of the Anorthosite itself. Within the Granulite, few high temperature oxides, mostly low temperature oxides and secondary oxides are present. During prograde metamorphism, the high temperature oxides were generated. The low temperature oxides were formed during the retrograde phase, experiencing low temperature upliftment associated with oxidation.

3) According to rockmagnetic data, it is evident that, the titanomagnetite is primarily responsible for ferromagnetic properties and remanence recording potential of rocks. The grain size of the remanence carrier magnetic mineral is SD category. The rocks from the Chilka Lake area, appears to be appropriate for recording magnetic remanence based on its magnetic characteristics.

4) The magnetizations are all carried by magnetite and haematite. They are identified by different rockmagnetic measurements through the thermomagnetic, hysteresis and IRM curves of the studied rocks.

5) The magnetic fabrics of the high-grade granulite rocks of the study area are controlled tectonically, mostly by the paramagnetic minerals. The AMS study mostly revealed that the stress pattern and orientation varied throughout the Chilka Lake area rocks evolution history. Principal compressional stress orientation changes with the different geological events. Based on magnetic fabrics, the magnetic lineation trends NE-SW in the granulites with some exceptions in the southern granulites. Following this, Leptynite experiences magmatic episodes, whose K_1 trends from NE-SW to S-E. The Anorthosite follows which lacks this magnetic fabric orientation.

6) Palaeomagnetic investigations identified a distinct mean magnetization component (D) in Anorthosite of the Balugaon, Chilka Lake area, Odisha, which reflects the Neoproterozoic magnetic field.

$$\mathbf{D_m / I_m = 262^{\circ}/35^{\circ}}$$

7) The **Palaeopole (C)** position derived from the Anorthosites Massifs of the Balugaon and Rambha, Chilka Lake area, Odisha, (CHL):

$$\mathbf{C \text{ at } \lambda_p = 1.15^{\circ}S;\ \varphi_p = 16.15^{\circ}E,}$$

and

dp/dm= 9.21/16.0.

The above mentioned pole is the first documented palaeopole position for the Balugaon-Rambha Massif type Anorthosites of Chilka Lake area in Eastern Ghats Belt of India. The pole falls on the APWP of the Indian subcontinent during the Proterozoic time. There is also a further scope of working with the Bengal Anorthosite, to determine the palaeopole position and develop the correlation with the Chilka Lake Anorthosite Massifs in India.

APPENDIX

THERMAL DEMAGNETIZATION DATA FOR ANORTHOSITE				
Sample No.	**Demagnetizing Temperature (°C)**	**Declination (Deg.)**	**Inclination (Deg.)**	**Intensity (x 10^{-5} Am^2/Kg)**
CHL 8.01	NRM	272.65	17.38	0.0986426
	100	272.9	17.61	0.0940789
	200	272.78	17.02	0.0915871
	300	273.42	17.39	0.0913529
	350	271.31	17.02	0.0824961
	400	273.71	16.47	0.0514795
	450	269.94	15.61	0.0228728
	500	274.14	9.68	0.0110291
	540	275.58	4.59	0.00980242
	580	334.98	41.6	0.00113067
	600	235.55	62.03	0.000979472
	620	106.47	-39.53	0.0015239
CHL 8.02	NRM	289.56	23.68	0.146888
	100	292.25	23.18	0.144168
	200	292.17	22.79	0.136895
	300	288.76	23.38	0.0959598
	350	289.98	20.89	0.0724223
	400	278.11	13.1	0.0144922
	450	277.04	10.46	0.0138831
	500	272.21	13.39	0.0123057
	540	284.12	10.9	0.00619967
	580	301.42	24.29	0.0030057
	600	310.31	-3.98	0.00155237
	620	260.35	41.62	0.00138355
CHL 8.03A	NRM	271.61	16.38	0.0986426
	100	271.85	16.61	0.0940789
	200	271.76	16.02	0.0915871
	300	272.39	16.39	0.0913529
	350	270.27	16	0.0824961
	400	272.69	15.44	0.0514795
	450	268.94	14.61	0.0228728
	500	273.14	8.68	0.0110291
	540	274.56	3.59	0.00980242
	580	332.98	40.6	0.00113067
	600	234.52	61.03	0.000979472
	620	105.47	-38.53	0.0015239
CHL 8.03B	NRM	288.56	22.66	0.146888
	100	291.22	22.18	0.144168

	200	291.12	21.77	0.136895
	300	287.76	22.38	0.0959598
	350	288.98	19.89	0.0724223
	400	277.07	12.01	0.0144922
	450	276.04	9.46	0.0138831
	500	271.19	12.34	0.0123057
	540	283.12	9.9	0.00619967
	580	300.42	23.26	0.0030057
	600	309.31	-2.98	0.00155237
	620	259.35	40.62	0.00138355
CHL 8.04	NRM	284.74	19.16	0.0944577
	100	285.24	19.12	0.0900726
	200	285.1	18.94	0.0847855
	300	288.07	19.78	0.0837651
	350	287.86	19.38	0.0694222
	400	284.62	16.35	0.0248766
	450	261.88	18.24	0.0139741
	500	265.57	5.29	0.0118102
	540	267.69	7.94	0.0111654
	580	64.17	63.63	0.000808212
	600	223.99	2.49	0.00101371
	620	227.51	7.73	0.000146727
CHL 8.07A	NRM	283.74	18.16	0.0944577
	100	284.24	18.12	0.0900726
	200	284.07	17.94	0.0847855
	300	287.07	18.77	0.0837651
	350	286.86	18.38	0.0694222
	400	283.58	15.35	0.0248766
	450	260.88	17.24	0.0139741
	500	264.55	4.29	0.0118102
	540	266.69	6.91	0.0111654
	580	63.17	61.63	0.000808212
	600	222.99	3.49	0.00101371
	620	228.51	8.73	0.000146727
CHL 9.01	NRM	264.72	-26.94	0.184249
	100	264.83	-26.85	0.179657
	200	265.73	-26.67	0.174043
	300	265.69	-27.23	0.144601
	350	266.68	-27.99	0.107934
	400	263.31	-27.51	0.100372
	450	266.16	-27.94	0.0889007
	500	262.83	-26.97	0.0513512
	540	261.41	-26.08	0.0438174

	580	260.91	-20.06	0.00288024
	600	281.89	-4.29	0.0017411
	620	250.87	-8.31	0.00142199
	640	339.78	34.1	0.000279147
	660	89.11	62.39	0.00114926
	680	193.99	58.56	0.001673
CHL 9.02	NRM	252.99	15.88	0.0558359
	100	255.06	17.95	0.0515208
	200	258.37	17.73	0.0499341
	300	253.84	19.82	0.0402518
	350	254.33	19.37	0.0320345
	400	24.96	22.29	0.0248391
	450	253.43	24.76	0.022656
	500	248.26	19.18	0.0134928
	540	251.86	19.37	0.0118666
	580	253.36	25.71	0.0106631
	600	236.36	6.54	0.00199027
	620	259.38	51.73	0.00314046
	640	260.9	34.34	0.000947768
	680	288.64	71.82	0.00104757
CHL 9.03	NRM	263.72	-25.94	0.184249
	100	263.83	-25.85	0.179657
	200	264.73	-25.67	0.174043
	300	264.69	-26.23	0.144601
	350	265.68	-26.99	0.107934
	400	262.31	-26.51	0.100372
	450	265.16	-26.93	0.0889007
	500	261.82	-25.97	0.0513512
	540	260.41	-25.08	0.0438174
	580	259.91	-19.06	0.00288024
	600	280.89	-3.27	0.0017411
	620	249.87	-7.28	0.00142199
	640	338.76	33.08	0.000279147
	660	88.11	61.39	0.00114926
	680	192.99	57.56	0.001673
CHL 9.04	NRM	251.99	14.88	0.0558359
	100	254.01	16.92	0.0515208
	200	257.37	16.71	0.0499341
	300	252.82	18.82	0.0402518
	350	253.33	18.37	0.0320345
	400	251.96	21.29	0.0248391
	450	251.41	23.76	0.022656
	500	247.26	18.16	0.0134928

	540	250.86	18.37	0.0118666
	580	252.35	24.69	0.0106631
	600	235.36	5.54	0.00199027
	620	258.38	50.73	0.00314046
	640	259.9	33.34	0.000947768
	680	287.62	70.82	0.00104757
CHL 9.05	NRM	235.86	-20.05	0.111848
	100	236.41	-19.53	0.10485
	200	236.51	-19.36	0.0996703
	300	235.64	-19.68	0.074927
	350	236.42	-18.64	0.0701896
	400	237.64	-19.19	0.0692539
	450	234.33	-17.94	0.0565005
	500	233.86	-17.6	0.0408694
	540	235.84	-17.96	0.0325622
	580	233.89	-20.57	0.0142149
	600	240.74	-15.12	0.0106877
	620	229.31	-12.16	0.00362467
	640	150.95	11.76	0.00108754
	680	237.63	26.83	0.000830487
	700	190.37	79.46	0.00150887
CHL 9.06	NRM	234.86	-19.05	0.111848
	100	235.38	-18.53	0.10485
	200	235.51	-18.31	0.0996703
	300	234.63	-18.68	0.074927
	350	235.37	-17.63	0.0701896
	400	236.64	-18.15	0.0692539
	450	233.32	-16.91	0.0565005
	500	232.86	-16.6	0.0408694
	540	234.84	-16.96	0.0325622
	580	232.89	-19.57	0.0142149
	600	239.71	-14.12	0.0106877
	620	228.31	-11.16	0.00362467
	640	149.95	10.76	0.00108754
	680	236.63	25.81	0.000830487
	700	189.37	78.46	0.00150887
CHL 18.01	NRM	203.67	20.48	0.0319154
	100	202.92	21.37	0.0312809
	200	203.74	21.47	0.0306093
	300	203.04	20.24	0.0287191
	350	202.43	20.31	0.024112

	400	202.21	15.66	0.0194668
	500	238.47	18.35	0.00301114
	540	222.82	12.98	0.00291125
	580	229.51	17.28	0.00308852
	600	272.09	27.21	0.000846668
	620	4.84	-11.01	0.00109349
	640	39.57	38.99	0.000652286
	680	234.78	77.19	0.000572338
	700	299.06	22.27	0.000559077
CHL 18.02	NRM	202.16	25.95	0.265967
	100	204.26	25.92	0.262571
	200	202.65	24.82	0.251774
	300	204.38	24.29	0.22673
	350	203.13	23.1	0.150784
	400	196.64	23.68	0.0455718
	450	190.81	-34.55	0.00313179
	500	229.16	19.46	0.0035099
	540	235.82	41.71	0.00397939
	580	216.31	45.82	0.00395977
	600	239.76	20.92	0.00340939
	620	193.68	-34.3	0.00183567
CHL 18.03	NRM	165.33	29.57	6.49498
	100	161.18	29.51	6.56964
	200	165.61	29.17	6.39703
	300	165.34	28.13	5.75614
	350	164.28	27.65	4.94749
	400	164.93	26.25	1.95118
	450	176.3	24.79	0.651889
	500	161.32	41.48	0.0180937
	540	177.8	30.65	0.0280484
	580	212.03	50.12	0.0244988
	600	192.35	24.85	0.0230732
CHL 18.04	NRM	166.33	30.57	6.49498
	100	162.08	30.51	6.56964
	200	166.61	30.17	6.39703
	300	166.34	29.13	5.75614
	350	165.28	28.65	4.94749
	400	165.93	27.25	1.95118
	450	177.29	25.79	0.651889
	500	162.32	42.48	0.0180937
	540	178.8	31.65	0.0280484
	580	213.03	51.12	0.0244988
	600	193.25	25.85	0.0230732

CHL 18.05	NRM	204.57	21.48	0.0319154
	100	203.91	22.37	0.0312809
	200	204.72	22.47	0.0306093
	300	202.74	21.24	0.0287191
	350	201.83	21.01	0.024112
	400	203.21	16.66	0.0194668
	500	238.78	18.75	0.00301114
	540	223.82	13.98	0.00291125
	580	230.51	18.28	0.00308852
	600	271.09	28.01	0.000846668
	620	5.76	-12.01	0.00109349
	640	40.57	39.99	0.000652286
	680	235.58	78.19	0.000572338
	700	300.06	23.17	0.000559077
CHL 18.06	NRM	203.06	26.85	0.265967
	100	205.26	26.91	0.262571
	200	203.65	25.82	0.251774
	300	205.38	25.29	0.22673
	350	204.13	24.06	0.150784
	400	197.64	24.68	0.0455718
	450	191.81	-35.45	0.00313179
	500	230.16	20.46	0.0035099
	540	236.82	42.71	0.00397939
	580	217.31	46.82	0.00395977
	600	240.76	21.92	0.00340939
	620	194.68	-35.3	0.00183567
CHL 20.01	NRM	261.36	1.43	0.000475444
	100	252.87	8.6	0.000469101
	200	269.47	34.69	0.000357791
	300	258.27	10.55	0.000452361
	350	246.19	8.97	0.000680373
	400	239.59	4.79	0.000339078
	450	69.84	-52.47	0.000364977
	500	310.1	17.95	7.18E-05
	540	243.12	13.64	0.00060435
	580	307.98	34.39	0.000192441
	600	290.95	34.63	7.27E-05
	620	286.46	-9.76	0.000176666
	640	276.28	31.04	0.000154073
	680	165.98	64.03	0.000904283
	700	295.95	64.22	0.000404375
CHL 20.02 B	NRM	260.36	0.43	0.000475444

	100	251.87	7.6	0.000469101
	200	268.67	33.69	0.000357791
	300	257.27	9.55	0.000452361
	350	228.16	6.29	0.000759215
	400	238.59	3.89	0.000339078
	450	68.84	-51.47	0.000364977
	500	309.1	18.64	7.18E-05
	540	311.3	-21.05	0.000466967
	580	308.8	33.39	0.000192441
	600	291.95	33.93	7.27E-05
	620	285.46	-8.76	0.000176666
	640	275.28	30.04	0.000154073
	680	164.98	63.03	0.000904283
	700	294.95	63.22	0.000404375
CHL 20.03	NRM	226.28	-3.78	0.000813854
	100	232.96	1.13	0.000776406
	200	233.12	9.38	0.000831375
	300	233.19	-12.51	0.000633736
	350	211.31	19.81	0.000705444
	400	245.56	15.66	0.000731161
	450	225.04	-19.63	0.000468773
	500	139.65	71.34	0.000162673
	540	222.28	52.67	0.000448181
	580	242.22	54.57	0.000406116
	600	246.4	11.72	7.63E-05
	620	306.44	44.57	0.000174257
	640	157.27	37.16	0.00018664
	680	135.97	45.02	0.000375976
	700	345.94	53.86	0.000649367
CHL 20.04	NRM	259.18	21.81	0.0292232
	100	261.63	21.05	0.029395
	200	261.15	23.97	0.0275172
	300	260.34	24.03	0.0277361
	350	261.06	22.79	0.0236209
	400	262.35	19.89	0.0131322
	450	223.95	-2.12	0.00183949
	500	289.26	17.29	0.000578326
	540	259.25	20.27	0.00115562
	580	261.07	17.06	0.000604463
	600	214.51	21.85	0.00117749
	620	62.2	54.03	0.000868765
CHL20.06 A	NRM	258.18	22.41	0.0292232
	100	260.63	22.05	0.029395

	200	260.15	22.97	0.0275172
	300	259.34	23.03	0.0277361
	350	260.06	21.99	0.0236209
	400	261.35	18.89	0.0131322
	450	223.82	-1.12	0.00183949
	500	288.26	16.29	0.000578326
	540	258.25	19.27	0.00115562
	580	260.07	16.16	0.000604463
	600	213.51	20.85	0.00117749
	620	61.2	53.03	0.000868765
CHL 20.06 B	NRM	260.36	0.43	0.000475444
	100	251.87	7.6	0.000469101
	200	268.67	33.69	0.000357791
	300	257.27	9.55	0.000452361
	350	228.16	6.29	0.000759215
	400	238.59	3.89	0.000339078
	450	68.84	-51.47	0.000364977
	500	309.1	18.64	7.18E-05
	540	242.12	13.27	0.00060435
	580	308.8	33.39	0.000192441
	600	291.95	33.93	7.27E-05
	620	285.46	-8.76	0.000176666
	640	275.28	30.04	0.000154073
	680	164.98	63.03	0.000904283
	700	294.95	63.22	0.000404375
CHL 22.01	NRM	259.74	-12.82	0.0181135
	100	258.97	-13.12	0.0180384
	200	258.74	-14.48	0.0180403
	300	254.6	-12.3	0.0167047
	350	248.04	-7.6	0.0151617
	400	248.36	-5.97	0.0153844
	450	246.75	-8.31	0.0156874
	500	239.81	-11.22	0.0113386
	540	244.25	-3.8	0.01248
	580	296.36	51.61	0.00432969
	600	138.07	-17.49	0.00134958
	620	241.68	11.77	0.000773543
	640	261.84	-1.16	0.00148247
	660	119.81	-29.23	0.000605932
	680	236.43	-36.09	0.000725381
	700	92.87	70.72	0.000714208
CHL 22.02	NRM	260.64	-13.82	0.0181135
	100	259.77	-14.12	0.0180384

	200	259.54	-15.48	0.0180403
	300	255.6	-13.3	0.0167047
	350	249.04	-8.6	0.0151617
	400	249.36	-6.67	0.0153844
	450	247.75	-9.31	0.0156874
	500	240.81	-12.11	0.0113386
	540	245.25	-4.8	0.01248
	580	297.36	52.31	0.00432969
	600	139.07	-18.49	0.00134958
	620	242.68	12.77	0.000773543
	640	262.64	-2.16	0.00148247
	660	120.71	-30.23	0.000605932
	680	237.33	-37.09	0.000725381
	700	93.67	71.62	0.000714208
CHL 22.03	NRM	264.2	21.43	0.0025734
	100	265.41	14.53	0.00243846
	200	264.54	19.13	0.00220747
	300	256.16	11.28	0.00252048
	350	257.66	11.65	0.00244509
	400	258.88	14.25	0.00249692
	450	215.28	37.71	0.00540784
	500	202.18	-21.4	0.00299234
	540	235.08	23.4	0.0031986
	580	254	0.65	0.00229315
	600	160.16	72.72	0.000983268
	620	204.65	53.03	0.000448791
	640	286.69	38.55	0.000935506
	660	145.96	-6.44	0.000481478
	680	232.71	40.72	0.000496658
	700	225.35	27.32	0.000250466
CHL 22.04	NRM	265.2	22.43	0.0025734
	100	266.41	15.43	0.00243846
	200	265.34	20.13	0.00220747
	300	257.16	12.28	0.00252048
	350	258.66	12.65	0.00244509
	400	259.88	15.25	0.00249692
	450	216.28	38.71	0.00540784
	500	203.18	-22.4	0.00299234
	540	236.08	24.4	0.0031986
	580	255.98	1.45	0.00229315
	600	161.16	73.72	0.000983268
	620	205.65	54.03	0.000448791
	640	287.69	39.55	0.000935506
	660	146.76	-7.44	0.000481478

	680	233.71	41.72	0.000496658
	700	226.35	28.32	0.000250466
CHL 22.05	NRM	318.76	-26.95	0.00235622
	100	320.92	-33.73	0.00248736
	200	307.88	-50.55	0.00234585
	300	317.24	-54.48	0.00230261
	350	316.28	-52.81	0.00196835
	400	314.79	-46.87	0.00165215
	450	321.5	-72.64	0.00171186
	500	214.98	-60.41	0.00276473
	540	324.48	-88.79	0.00427114
	580	213.62	15.81	0.00366401
	600	342.69	56.65	0.00508576
	620	220.06	-57.44	0.00672093
	640	245.89	36.83	0.00139156
	660	243.7	66.21	0.00136874
	680	192.15	45.48	0.00203051
	700	218.59	2.5	0.000903973
CHL 22.06	NRM	317.76	-25.95	0.00235622
	100	319.92	-32.73	0.00248736
	200	306.88	-49.55	0.00234585
	300	316.24	-53.48	0.00230261
	350	315.28	-51.81	0.00196835
	400	313.79	-45.87	0.00165215
	450	320.5	-71.64	0.00171186
	500	213.98	-59.41	0.00276473
	540	323.48	-87.79	0.00427114
	580	212.62	14.81	0.00366401
	600	341.69	55.65	0.00508576
	620	219.06	-56.44	0.00672093
	640	244.89	35.83	0.00139156
	660	242.7	65.21	0.00136874
	680	191.15	44.48	0.00203051
	700	217.59	1.5	0.000903973
CHL 23.01	NRM	298.7	33.9	0.0333938
	100	301.69	33.74	0.0275069
	200	308.03	35.52	0.0239179
	300	280.95	21.92	0.0263755
	350	278	28.23	0.0222343
	400	279.42	35.62	0.0236491
	450	283.68	17.85	0.0230518
	500	271.67	14.73	0.0229342
	540	291.1	19.13	0.0203431

	580	300.74	13.58	0.0149409
	600	278.84	10.43	0.0123909
	620	265.27	-11.65	0.00822821
	640	304.29	31.16	0.0028338
	660	336.66	-22.16	0.00421372
	680	255.24	-46.29	0.00646759
	700	250.45	-48.16	0.00307494
CHL 23.02	NRM	299.7	34.9	0.0333938
	100	302.69	34.74	0.0275069
	200	309.03	36.52	0.0239179
	300	281.95	22.92	0.0263755
	350	279.01	29.23	0.0222343
	400	280.42	36.62	0.0236491
	450	284.68	18.85	0.0230518
	500	272.67	15.73	0.0229342
	540	292.1	20.13	0.0203431
	580	301.74	14.58	0.0149409
	600	279.84	11.43	0.0123909
	620	266.27	-12.65	0.00822821
	640	305.29	32.16	0.0028338
	660	337.66	-23.16	0.00421372
	680	256.24	-47.29	0.00646759
	700	251.45	-49.16	0.00307494
CHL 23.03	NRM	324.85	49.21	0.0293117
	100	321.95	45.9	0.0318163
	200	314.43	40.64	0.0246756
	300	290.86	31.07	0.0174212
	350	285.56	23.67	0.0168073
	400	281.92	27.25	0.0166352
	450	285.71	24.42	0.0181212
	500	281.87	22.51	0.0143633
	540	292.59	27.72	0.0133646
	580	274.34	23.28	0.0123087
	600	275.37	33.29	0.00843846
	620	177.34	-11.33	0.000785374
	640	184.34	24.01	0.00214898
	660	120.48	-68.47	0.00190669
	680	37.99	71.41	0.00269593
CHL 23.04	NRM	325.85	50.21	0.0293117
	100	322.95	46.9	0.0318163
	200	315.43	41.64	0.0246756
	300	291.86	32.07	0.0174212
	350	286.56	24.67	0.0168073

	400	282.92	28.25	0.0166352
	450	286.71	25.42	0.0181212
	500	282.87	23.51	0.0143633
	540	293.59	28.72	0.0133646
	580	275.34	24.28	0.0123087
	600	276.37	34.29	0.00843846
	620	178.34	-12.33	0.000785374
	640	185.33	25.01	0.00214898
	660	121.48	-69.47	0.00190669
	680	38.99	72.41	0.00269593
CHL 23.05	NRM	287.69	38.95	0.0430848
	100	295.49	40.38	0.0394962
	200	293.29	27.36	0.0372127
	300	286.98	29.11	0.0268603
	350	270.82	18.62	0.0292884
	400	270.19	20.94	0.0268591
	450	257.15	5.82	0.0209851
	500	260.01	12.78	0.0199066
	540	265.66	24.83	0.0208716
	580	139.98	58.75	0.00278813
	600	253.24	38.89	0.00584049
	620	239.21	-22.89	0.00545793
	640	232.29	-62.46	0.00991381
	660	201.09	26.84	0.003566
	680	280.18	-10.56	0.00353443
	700	196.34	-22.28	0.00539133
CHL 23.06	NRM	286.69	37.95	0.0430848
	100	294.49	39.48	0.0394962
	200	292.29	26.36	0.0372127
	300	285.98	28.11	0.0268603
	350	269.82	17.62	0.0292884
	400	269.19	19.94	0.0268591
	450	256.15	4.82	0.0209851
	500	259.01	11.78	0.0199066
	540	264.66	23.83	0.0208716
	580	139	57.75	0.00278813
	600	252.24	37.89	0.00584049
	620	238.21	-21.89	0.00545793
	640	231.29	-61.46	0.00991381
	660	200.09	25.84	0.003566
	680	279.18	-9.56	0.00353443
	700	195.34	-21.28	0.00539133
CHL 24.01	NRM	53.39	-59.29	0.0648376

	100	48.1	-61.01	0.0607589
	200	56.39	-57.56	0.0624738
	300	57.64	-53.7	0.0604118
	350	60.94	-51.94	0.0456643
	400	93.4	-69.69	0.0140351
	450	64.01	14.8	0.00134028
	500	52.38	-0.6	0.000843473
	540	99.17	46.12	0.000959926
	580	62.07	-59.37	0.00118242
	600	297.93	-36.75	0.000385872
CHL 24.02	NRM	278.33	21.98	0.00135065
	100	290.85	3.9	0.0014325
	200	274.19	-14.89	0.00157954
	300	265.04	5.32	0.00132428
	350	287.3	15.6	0.00122843
	400	245.24	3.38	0.0012708
	450	227.3	10.89	0.000664398
	500	323.34	7.48	0.000214664
	540	118.23	54.27	0.000258995
	580	253.42	17.38	0.000212262
	600	247.36	35.76	0.000298806
	620	95.68	45.65	0.000849956
	640	269.35	61.47	0.000172384
	660	140.97	66.41	0.000283223
	680	127.03	59.94	0.000193551
	700	34.13	56.42	0.000108491
CHL 24.03	NRM	54.39	-60.29	0.0648376
	100	49.1	-62.01	0.0607589
	200	57.39	-58.56	0.0624738
	300	57.64	-54.7	0.0604118
	350	61.94	52.94	0.0456643
	400	94.4	-70.69	0.0140351
	450	65.01	15.8	0.00134028
	500	53.38	-1.6	0.000843473
	540	100.17	47.12	0.000959926
	580	63.07	-60.37	0.00118242
	600	298.93	-37.75	0.000385872
CHL 24.04	NRM	279.33	22.98	0.00135065
	100	291.85	4.9	0.0014325
	200	275.19	-15.89	0.00157954
	300	266.04	6.32	0.00132428
	350	288.3	16.6	0.00122843
	400	246.24	4.38	0.0012708

	450	228.3	11.89	0.000664398
	500	324.34	8.48	0.000214664
	540	119.23	55.27	0.000258995
	580	254.42	18.38	0.000212262
	600	248.36	36.76	0.000298806
	620	96.68	46.65	0.000849956
	640	270.35	62.47	0.000172384
	660	141.97	67.41	0.000283223
	680	128.03	60.94	0.000193551
	700	35.13	57.42	0.000108491
CHL 24.05	NRM	88.36	51.05	0.0136045
	100	88.71	51.02	0.0131281
	200	89	49.5	0.013046
	300	88.76	52.39	0.0121156
	350	87.76	61.87	0.00849523
	400	281.62	70.13	0.00338934
	450	271.68	27.73	0.00395967
	500	86.13	30.21	0.00172214
	540	15.34	-10.1	0.000388723
	580	87.67	53.37	0.000240949
	600	270.71	-1.71	0.000331682
	620	342.44	51.07	0.000176413
	640	291.78	29.24	0.000388039
	660	325.91	67.39	0.000177963
CHL 24.06	NRM	89.36	52.05	0.0136045
	100	89.71	52.02	0.0131281
	200	90.01	50.5	0.013046
	300	89.76	53.39	0.0121156
	350	88.76	62.87	0.00849523
	400	282.62	71.13	0.00338934
	450	272.68	28.73	0.00395967
	500	87.13	31.21	0.00172214
	540	16.34	-11.1	0.000388723
	580	88.67	54.37	0.000240949
	600	271.71	-2.71	0.000331682
	620	343.44	52.07	0.000176413
	640	292.78	30.24	0.000388039
	660	326.91	68.39	0.000177963
CHL 25.01	NRM	319.15	16.36	0.0383865
	100	319.88	15.99	0.0375716
	200	320.83	14.71	0.038037
	300	318.87	13.2	0.0357272
	350	319.09	12.11	0.0322561

	400	321.68	16.64	0.0181412
	450	331.52	-18.23	0.0016315
	500	350.32	19.04	0.000830564
	540	212.87	-68.3	0.00144578
	580	178.07	42.67	0.00102977
	600	21.53	-23.53	0.000460218
CHL 25.02	NRM	307.61	20.83	0.0189791
	100	307.94	19.49	0.0193227
	200	308.36	18.17	0.0193294
	300	309.47	17.16	0.0183746
	350	308.87	14.19	0.0115886
	400	313.27	14.19	0.00991901
	450	92.41	6.46	0.000960364
	500	129.74	-31.35	0.00144953
	540	215.11	18.24	0.00102125
	580	288.1	43.72	0.0001134
	600	248.34	-10.25	0.000440832
CHL 25.03	NRM	306.61	19.83	0.0189791
	100	306.94	18.49	0.0193227
	200	307.36	17.17	0.0193294
	300	308.47	16.16	0.0183746
	350	307.87	13.19	0.0115886
	400	312.27	13.19	0.00991901
	450	91.41	5.46	0.000960364
	500	128.74	-30.35	0.00144953
	540	214.11	17.24	0.00102125
	580	287.1	42.72	0.0001134
	600	247.34	-9.25	0.000440832
CHL 25.04	NRM	318.15	15.36	0.0383865
	100	318.88	14.99	0.0375716
	200	319.83	13.71	0.038037
	300	317.87	12.2	0.0357272
	350	318.09	11.11	0.0322561
	400	320.68	15.64	0.0181412
	450	330.52	-17.23	0.0016315
	500	349.32	18.04	0.000830564
	540	211.87	-67.3	0.00144578
	580	177.07	41.67	0.00102977
	600	20.53	-22.53	0.000460218
CHL 25.05	NRM	294.83	30.52	0.0217058
	100	292.12	30.74	0.0210629
	200	294.68	29.1	0.0204679

	300	295.42	27.3	0.020589
	350	291.49	27.15	0.0176422
	400	281.72	36.75	0.00892659
	450	262.93	-38.82	0.000974848
	500	192.69	5.72	0.000444245
	540	296.81	12.38	0.00134609
	580	92.41	33.59	0.00355261
	600	129.74	36.72	8.62E-05
CHL 25.06	NRM	293.83	29.52	0.0217058
	100	291.12	29.74	0.0210629
	200	293.68	28.1	0.0204679
	300	294.42	26.3	0.020589
	350	290.49	26.15	0.0176422
	400	280.72	35.75	0.00892659
	450	261.93	-37.82	0.000974848
	500	191.69	4.72	0.000444245
	540	295.81	11.38	0.00134609
	580	91.41	32.59	0.00355261
	600	128.74	35.72	8.62E-05
CHL 16.01	NRM	311.52	-5.4	0.0440578
	100	310.13	-9.65	0.0450613
	200	305.47	-37.28	0.0424636
	300	299.75	-23.78	0.0417781
	350	291.36	-21.77	0.0270762
	400	294.74	-14.57	0.0260408
	450	282.24	-11.9	0.0303943
	500	262.88	-1.35	0.0131845
	540	271.39	15.4	0.0126125
	580	259.5	18.94	0.0118267
	600	23.43	27.87	0.00648934
	620	231.34	-13.65	0.00512521
	640	137.83	5.62	0.0120717
	660	191.24	-10.82	0.00297877
	680	74.89	14.41	0.00240672
	700	204.54	-30.29	0.00311206
CHL 16.02	NRM	311.52	-5.4	0.0440578
	100	310.13	-9.65	0.0450613
	200	305.47	-37.28	0.0424636
	300	299.75	-23.78	0.0417781
	350	291.36	-21.77	0.0270762
	400	294.74	-14.57	0.0260408
	450	282.24	-11.9	0.0303943
	500	262.88	-1.35	0.0131845

	540	271.39	15.4	0.0126125
	580	259.5	18.94	0.0118267
	600	23.43	27.87	0.00648934
	620	231.34	-13.65	0.00512521
	640	137.83	5.62	0.0120717
	660	191.24	-10.82	0.00297877
	680	74.89	14.41	0.00240672
	700	204.54	-30.29	0.00311206
CHL 16.03	NRM	323.12	4.89	0.0290886
	100	322.91	3.55	0.0282083
	200	318.07	1.9	0.0235503
	300	318.19	-5.04	0.0186973
	350	309.47	-9.79	0.0140399
	400	315.24	-0.64	0.0124892
	450	255.38	6.38	0.00716994
	500	217.29	13.84	0.00460695
	540	213.3	5.7	0.00763901
	580	184.72	-16.12	0.0109393
	600	261.87	-63.25	0.00220869
	620	227.81	-15.34	0.00257376
	640	112.3	7.39	0.00408598
	660	137.6	54.42	0.00313885
	680	66.29	8.68	0.00251426
	700	135.36	-22.32	0.00199884
CHL 16.04	NRM	242.15	-28.6	0.0713697
	100	241.96	-32.33	0.0675291
	200	232.83	-39.2	0.0612171
	300	226.92	-49.38	0.0553264
	350	224.79	-51.11	0.0487215
	400	209.54	-8.75	0.0321714
	450	203.87	-8.71	0.0271233
	500	236.11	-43.39	0.018106
	540	161.96	-17.1	0.00611068
	580	262.17	58.56	0.0105021
	580	272.79	56.02	0.0084452
	600	174	76.78	0.00566086
	620	307.24	2.41	0.00509479
	640	258.98	22.92	0.00545753
	680	319.47	36.05	0.00146441
	700	182.14	-1.48	0.00205092
CHL 16.05	NRM	323.12	4.89	0.0290886
	100	322.91	3.55	0.0282083
	200	318.07	1.9	0.0235503

	300	318.19	-5.04	0.0186973
	350	309.47	-9.79	0.0140399
	400	315.24	-0.64	0.0124892
	450	255.38	6.38	0.00716994
	500	217.29	13.84	0.00460695
	540	213.3	5.7	0.00763901
	580	184.72	-16.12	0.0109393
	600	261.87	-63.25	0.00220869
	620	227.81	-15.34	0.00257376
	640	112.3	7.39	0.00408598
	660	137.6	54.42	0.00313885
	680	66.29	8.68	0.00251426
	700	135.36	-22.32	0.00199884
CHL 16.06	NRM	243.15	-29.6	0.0713697
	100	242.91	-33.36	0.0675291
	200	233.83	-40.2	0.0612171
	300	227.92	-50.38	0.0553264
	350	225.79	-52.11	0.0487215
	400	210.54	-9.75	0.0321714
	450	204.87	-9.71	0.0271233
	500	236.11	-44.39	0.018106
	540	161.96	-17.1	0.00611068
	580	272.79	56.02	0.0084452
	600	174	76.78	0.00566086
	620	307.24	2.41	0.00509479
	640	258.98	22.92	0.00545753
	680	319.47	36.05	0.00146441
	700	182.14	-1.48	0.00205092
THERMAL DEMAGNETIZATION DATA FOR GRANULITES				
Sample No.	**Demagnetizing Temperature (°C)**	**Declination (Deg.)**	**Inclination (Deg.)**	**Intensity (x 10^{-5} Am^2/Kg)**
CHL 1.01	NRM	150.71	-43.7	0.00772428
	100	152.01	-43.36	0.00763475
	200	149.43	-42.62	0.00747844
	300	153.08	-43.97	0.00673464
	350	148.58	-45.13	0.00565939
	400	150.61	-44.54	0.00534761
	450	145.49	-36.75	0.00357927
	500	145.48	-31.71	0.0030462
	540	153.02	-23.46	0.00262525
	580	145.65	-27.29	0.00144691
	600	94.56	10.21	0.000107607
	620	7.79	85.12	4.75E-05

CHL 1.02	NRM	149.71	-42.7	0.00772428
	100	151	-42.36	0.00763475
	200	148.43	-41.62	0.00747844
	300	152.08	-42.97	0.00673464
	350	147.58	-44.13	0.00565939
	400	149.61	-43.54	0.00534761
	450	144.49	-35.75	0.00357927
	500	144.48	-30.71	0.0030462
	540	152.02	-22.46	0.00262525
	580	144.65	-26.29	0.00144691
	600	93.56	9.21	0.000107607
	620	7.1	84.12	4.75E-05
CHL 1.03	NRM	234.23	-41.8	0.00433507
	100	242.5	-42.89	0.00406353
	200	278.29	-66.15	0.00343697
	300	347.51	-81.35	0.0036803
	350	31.54	-76.51	0.00345562
	400	26.3	-72.9	0.00355275
	450	24.87	-74.36	0.00356915
	500	23.73	-63.82	0.00292722
	540	20.23	-51.29	0.00279473
	580	165.97	1.14	0.0021912
	600	163.71	-11.85	0.00125201
	620	216.11	34.62	0.000520787
	640	308.45	13.4	0.000257779
	680	346.6	21.01	0.00022692
	700	245.02	49.15	0.000167887
CHL 1.04	NRM	215.52	-26.52	0.00718046
	100	213.64	-24.74	0.00710844
	200	201.36	-38.59	0.00598506
	300	183.45	-43.3	0.00596593
	350	169.44	-47.07	0.00553427
	400	166.99	-47.08	0.00506981
	450	164.45	-53.63	0.00480865
	500	157.57	-51.06	0.00397385
	540	123.01	-65.03	0.00212292
	580	80.38	-67.61	0.00249446
	580	72.93	-68.61	0.00246552
	600	38.36	-62.88	0.0020571
	620	172.89	1.46	0.00363867
	620	174.21	-2.3	0.00355023
	640	257.36	16.04	0.000420574
	680	235.95	28.03	0.00052545

	700	229.68	12.84	0.00048873
CHL 1.05	NRM	233.23	-40.8	0.00433507
	100	241.5	-41.89	0.00406353
	200	277.29	-65.15	0.00343697
	300	346.51	-80.35	0.0036803
	350	30.54	-75.51	0.00345562
	400	25.3	-71.9	0.00355275
	450	23.87	-73.36	0.00356915
	500	22.73	-62.82	0.00292722
	540	19.23	-50.29	0.00279473
	580	164.97	0.14	0.0021912
	600	162.71	-10.85	0.00125201
	620	215.11	33.62	0.000520787
	640	307.45	12.4	0.000257779
	680	345.6	20.01	0.00022692
	700	244.02	48.15	0.000167887
CHL 1.06	NRM	214.52	-25.52	0.00718046
	100	212.64	-23.74	0.00710844
	200	200.36	-37.59	0.00598506
	300	182.45	-42.3	0.00596593
	350	168.44	-46.07	0.00553427
	400	165.99	-46.08	0.00506981
	450	163.45	-52.63	0.00480865
	500	156.57	-50.06	0.00397385
	540	122.01	-64.03	0.00212292
	580	71.93	-67.61	0.00246552
	600	37.36	-61.88	0.0020571
	620	171.89	0.46	0.00363867
	620	173.21	-1.3	0.00355023
	640	256.36	15.04	0.000420574
	680	234.95	27.03	0.00052545
	700	228.68	11.84	0.00048873
CHL 4.01	NRM	150.1	-32.9	0.0148065
	100	148.48	-33.02	0.0148106
	200	148.38	-32.86	0.0141524
	300	147.09	-34.69	0.0137225
	350	148.01	-35.19	0.0121087
	400	129.38	-21.32	0.00658441
	450	127.03	-21.79	0.00642121
	500	119.77	-18.84	0.00540434
	540	120.09	-19.69	0.00400856
	580	113.67	-13.59	0.0037046
	600	114.3	-11.37	0.00295544

	620	100.04	4.7	0.0022421
	640	112.45	9.9	0.000804498
	680	218.36	30.97	0.000438647
	700	199.46	32.44	0.000298202
CHL 4.02	NRM	149.1	-31.9	0.0148065
	100	147.48	-32.02	0.0148106
	200	147.37	-31.86	0.0141524
	300	146.03	-33.69	0.0137225
	350	147	-34.19	0.0121087
	400	128.38	-20.32	0.00658441
	450	122.99	-17.75	0.00702269
	500	118.77	-17.81	0.00540434
	540	119.09	-18.69	0.00400856
	580	112.67	-12.59	0.0037046
	600	113.3	-10.37	0.00295544
	620	99.04	3.7	0.0022421
	640	111.45	8.7	0.000804498
	680	217.33	29.97	0.000438647
	700	198.42	31.44	0.000298202
CHL 4.03	NRM	274.32	-6.28	0.027539
	100	274.52	-6.29	0.0272397
	200	278.21	-5.8	0.0255245
	300	273.14	-8.26	0.0256477
	350	275.62	-8.84	0.0243951
	400	275.19	-7.92	0.0218828
	450	250.27	-11.14	0.0110256
	500	242.32	-8.89	0.00837268
	540	242.42	-10.51	0.00714727
	580	229.83	-8.13	0.00652775
	600	213.02	-7.51	0.00253644
	620	207.51	-6.38	0.00212094
	640	204.48	-3.83	0.00252672
	680	304.72	61.81	0.000564516
	700	216.53	62.02	0.00034427
CHL 4.04	NRM	275.32	-7.28	0.027539
	100	275.52	-7.29	0.0272397
	200	279.21	-6.8	0.0255245
	300	274.18	-9.29	0.0256477
	350	276.62	-9.84	0.0243951
	400	276.19	-8.92	0.0218828
	450	250.27	-12.14	0.0110256
	500	243.32	-9.9	0.00837268
	540	243.42	-11.51	0.00714727

	580	230.86	-9.13	0.00652775
	600	214.08	-8.56	0.00253644
	620	208.53	-7.38	0.00212094
	640	205.48	-4.85	0.00252672
	680	305.74	62.82	0.000564516
	700	217.56	63.04	0.00034427
CHL 4.05	NRM	64.61	-11.53	0.0210781
	100	64.08	-11.29	0.0203337
	200	62.92	-11.32	0.020094
	300	59.45	-15.01	0.0183816
	350	60.13	-14.29	0.0182941
	400	62.63	-13.39	0.0170576
	450	49.25	-4.95	0.00876548
	500	44.82	-5.77	0.005686
	540	48.52	-2.42	0.00524938
	580	39.11	-2.12	0.00327984
	600	25.54	9.98	0.00178079
	620	261.55	-37.12	0.000194955
	640	128.42	54.36	0.000442872
CHL 4.06	NRM	63.61	-10.53	0.0210781
	100	63.08	-10.29	0.0203337
	200	61.92	-10.32	0.020094
	300	58.45	-14.01	0.0183816
	350	59.13	-13.29	0.0182941
	400	61.63	-12.39	0.0170576
	450	48.25	-3.95	0.00876548
	500	43.82	-4.77	0.005686
	540	46.52	-1.42	0.00524938
	580	38.11	-1.12	0.00327984
	600	24.54	8.98	0.00178079
	620	260.55	-36.12	0.000194955
	640	127.42	53.36	0.000442872
CHL 6.01	NRM	349.33	44.59	0.104019
	100	349.68	44.79	0.101754
	200	349.86	44.15	0.0991914
	300	347.78	42.96	0.0878184
	350	348.46	40.92	0.0860068
	400	347.72	43.5	0.0863371
	450	348.55	47.9	0.0834795
	500	347.31	53.2	0.0563469
	540	350.85	52.06	0.0511202
	580	355.91	52.45	0.0494368
	600	355.4	51.26	0.0464

	620	347.7	47.34	0.0269582
	640	305.1	45.63	0.00227034
	660	99.8	49.3	0.00215532
CHL 6.02	NRM	348.33	43.59	0.104019
	100	348.68	43.79	0.101754
	200	348.83	43.11	0.0991914
	300	346.75	40.96	0.0878184
	350	347.45	39.91	0.0860068
	400	347.72	42.5	0.0863371
	450	348.55	46.89	0.0834795
	500	347.31	52.19	0.0563469
	540	349.85	51.06	0.0511202
	580	354.91	50.41	0.0494368
	600	354.39	49.26	0.0464
	620	346.69	45.3	0.0269582
	640	304.1	43.61	0.00227034
	660	98.79	47.27	0.00215532
CHL 6.03	NRM	56.12	41.23	0.137349
	100	55.34	43.82	0.131951
	200	53.07	44.87	0.128696
	300	47.93	44.37	0.131236
	350	44.86	45.98	0.121734
	400	43.3	44.68	0.125374
	400	42.58	45.26	0.123901
	450	47.76	46.45	0.124552
	500	44.98	50.1	0.0825492
	540	41.18	48.64	0.0745879
	580	43.68	49.17	0.0505614
	600	53.08	39.48	0.00501108
	620	353.96	44.6	0.0058617
	640	177.44	62.53	0.00531181
CHL 6.04	NRM	7.01	43.69	0.145876
	100	7.94	43.47	0.142807
	200	5.8	42.99	0.140122
	300	4.94	44.16	0.133272
	350	3.45	42.88	0.128845
	400	7.34	44.23	0.120942
	450	6.56	43.59	0.11405
	500	1.99	40.59	0.0806259
	540	7.26	43.42	0.0734609
	580	8.75	46.67	0.0133962
	600	356.47	48.62	0.0166731
	620	14.24	48.65	0.0112936

	640	272.66	46.15	0.00468011
	660	147.78	72.32	0.00219138
	680	134.28	9.18	0.0022551
CHL 6.05	NRM	55.12	40.23	0.137349
	100	54.34	42.82	0.131951
	200	52.07	43.87	0.128696
	300	47.13	43.21	0.130695
	350	43.86	44.98	0.121734
	400	41.58	44.26	0.123901
	450	46.76	45.45	0.124552
	500	43.99	49.09	0.0825492
	540	40.16	47.62	0.0745879
	580	42.66	48.15	0.0505614
	600	52.03	38.46	0.00501108
	620	352.94	43.58	0.0058617
	640	176.43	61.51	0.00531181
CHL 6.06	NRM	6.01	42.69	0.145876
	100	6.93	42.45	0.142807
	200	4.79	41.99	0.140122
	300	3.94	43.16	0.133272
	350	2.45	41.88	0.128845
	400	6.34	43.13	0.120942
	450	5.52	42.58	0.11405
	500	0.99	39.59	0.0806259
	540	6.26	42.42	0.0734609
	580	7.75	45.67	0.0133962
	600	355.47	47.62	0.0166731
	620	13.24	47.65	0.0112936
	640	271.66	45.15	0.00468011
	660	146.78	71.32	0.00219138
	680	133.28	8.18	0.0022551
CHL 10.01	NRM	150.09	-24.23	0.0198381
	100	149.15	-21.26	0.0195111
	200	143.37	-16.85	0.0179788
	300	143.22	-12.69	0.0125766
	350	145.59	-9.98	0.0136631
	350	144.8	-10.07	0.013643
	400	141.49	3.57	0.0115809
	450	136.94	9.65	0.00758487
	500	107.69	28.92	0.00520914
	540	102.02	27.97	0.00516082
	580	167.58	4.35	0.00145974
	600	223.94	4.09	0.0016571

	620	143.84	25.39	0.000433186
	640	333.57	56.37	0.00101937
	660	255.9	-7.94	0.000599626
	680	141.67	77.69	0.000837596
	700	208.45	10.4	0.00160305
CHL 10.02	NRM	149.09	-23.22	0.0198381
	100	148.15	-20.26	0.0195111
	200	142.3	-15.85	0.0179788
	300	142.22	-11.69	0.0125766
	350	143.8	-9.01	0.013643
	400	140.49	2.55	0.0115809
	450	135.94	8.65	0.00758487
	500	106.69	27.92	0.00520914
	540	101.02	26.97	0.00516082
	580	166.58	3.35	0.00145974
	600	222.91	3.09	0.0016571
	620	142.83	24.36	0.000433186
	640	332.57	55.37	0.00101937
	660	254.9	-6.92	0.000599626
	680	142.07	78	0.000837596
	700	207.45	9.4	0.00160305
CHL 10.03	NRM	147.73	14.38	0.00821188
	100	150.31	10.73	0.0077267
	200	144.44	10.73	0.0070602
	300	131.54	19.35	0.00599077
	350	132.27	21.42	0.00507462
	400	126.52	29.66	0.00488182
	450	132.85	29.75	0.00430155
	500	93.69	42.63	0.00309872
	540	117.53	40.79	0.00242139
	580	102.65	37.01	0.00211827
	600	297.22	65.98	0.000613254
	620	149.66	47.67	0.00102014
	640	17.57	69.41	0.00115136
	660	218.38	56.45	0.000775773
	680	63.89	59.29	0.000636128
	700	160.21	-38.89	0.000700149
CHL 10.04	NRM	130.68	-2.44	0.00750137
	100	135.58	-5.57	0.00754066
	200	137.21	4.63	0.00562612
	300	133.08	8.49	0.00457003
	350	136.78	7.37	0.00421656
	400	120.66	12.96	0.00440782

	450	121.88	32.7	0.00396293
	500	159.19	34.63	0.00132942
	580	112.57	37.7	0.00296688
	600	124.17	36.67	0.00198195
	620	307.64	84.69	0.00423307
	640	188.87	-20.76	0.00139797
	660	241.92	68.81	0.00175181
	680	100.94	81.48	0.000510329
	700	246.72	75.84	0.000947946
CHL 10.05A	NRM	146.73	13.38	0.00821188
	100	149.31	9.73	0.0077267
	200	143.44	9.73	0.0070602
	300	130.53	18.35	0.00599077
	350	131.27	20.42	0.00507462
	400	125.52	28.6	0.00488182
	450	131.85	28.75	0.00430155
	500	92.69	41.63	0.00309872
	540	116.51	39.79	0.00242139
	580	101.65	36.01	0.00211827
	600	296.22	64.98	0.000613254
	620	148.66	46.67	0.00102014
	640	16.57	68.41	0.00115136
	660	217.38	55.45	0.000775773
	680	62.86	58.29	0.000636128
	700	159.18	-37.89	0.000700149
CHL 10.05B	NRM	129.68	-1.44	0.00750137
	100	134.58	-4.57	0.00754066
	200	137.18	3.63	0.00562612
	300	132.01	7.49	0.00457003
	350	135.78	6.37	0.00421656
	400	119.66	11.96	0.00440782
	450	119.88	31.7	0.00396293
	500	158.19	33.61	0.00132942
	540	107.89	60	0.00362018
	580	111.57	36.7	0.00296688
	600	123.1	35.67	0.00198195
	620	306.61	83.69	0.00423307
	640	187.82	-19.76	0.00139797
	660	240.92	67.81	0.00175181
	680	99.94	80.48	0.000510329
	700	245.7	74.84	0.000947946
CHL 11.01	NRM	115.15	-42.86	0.0283675
	100	114.3	-44.2	0.025302

	200	112.96	-44.86	0.0223663
	300	118.71	-47.58	0.016244
	350	180.65	-16.94	0.489993
	400	176.69	-12.33	0.259408
	450	173	-12.64	0.129229
	500	174.28	-13.51	0.0418463
	540	175.26	-12.53	0.0339486
	580	176.17	-12.35	0.0300548
	600	174.74	-13.22	0.0234204
	620	176.35	-16.09	0.00376254
	640	206.17	-36.52	0.00143272
	660	174.53	-4.86	0.00177944
CHL 11.02	NRM	116.15	-43.86	0.0283675
	100	115.3	-45.2	0.025302
	200	113.96	-45.86	0.0223663
	300	119.74	-48.61	0.016244
	350	181.67	-17.94	0.489993
	400	177.69	-13.36	0.259408
	450	174.01	-13.64	0.129229
	500	175.28	-14.53	0.0418463
	540	176.26	-13.53	0.0339486
	580	177.22	-13.35	0.0300548
	600	175.72	-14.21	0.0234204
	620	177.35	-17.09	0.00376254
	640	207.17	-37.52	0.00143272
	660	175.55	-5.86	0.00177944
CHL 11.03	NRM	12.17	-17.96	0.150084
	100	13.09	-17.93	0.149906
	200	11.45	-17.99	0.143463
	300	9.57	-18.52	0.127696
	350	7.99	-16.84	0.114916
	400	11.73	-17.95	0.0969845
	450	12.85	-17.32	0.0702094
	500	14.09	-17.11	0.0200798
	540	10.89	-17.32	0.0186902
	580	358.67	-17.5	0.0149067
	600	22.65	-21.38	0.00355713
	620	23.75	-11.33	0.00350662
	640	50.78	6.79	0.00398067
	660	40.3	34.16	0.0029839
CHL 11.04	NRM	11.13	-16.96	0.150084
	100	12.09	-16.91	0.149906
	200	10.45	-16.99	0.143463

	300	8.54	-17.52	0.127696
	350	8.99	-17.84	0.114916
	400	10.71	-16.95	0.0969845
	450	11.85	-16.32	0.0702094
	500	13.09	-16.08	0.0200798
	540	9.89	-16.32	0.0186902
	580	359.03	-16.5	0.0149067
	600	21.65	-20.38	0.00355713
	620	22.73	-10.33	0.00350662
	640	51.75	7.55	0.00398067
	660	39.3	33.16	0.0029839
CHL 11.05	NRM	354.63	-3.53	0.0727446
	100	355.18	-4.34	0.0691105
	200	357.21	-4.56	0.0696016
	300	354.16	-6.97	0.0592959
	350	354.18	-5.06	0.0495161
	400	356.27	-5.28	0.0481707
	450	355.62	-6.5	0.0454846
	500	9.15	4.3	0.0164693
	540	6.77	0.71	0.0150184
	580	3.62	0.81	0.0150136
	600	279.9	8.25	0.00287156
	620	258.02	2.47	0.00307979
	640	141.37	-8.66	0.00224066
	660	273.36	-29.71	0.00176446
	680	263.74	-27.89	0.000654745
CHL 11.06	NRM	353.68	-2.55	0.0727446
	100	356.18	-5.32	0.0691105
	200	358.21	-5.56	0.0696016
	300	355.16	-7.92	0.0592959
	350	355.19	-6.1	0.0495161
	400	357.31	-6.29	0.0481707
	450	356.62	-7.5	0.0454846
	500	10.18	5.3	0.0164693
	540	7.72	1.69	0.0150184
	580	4.62	1.79	0.0150136
	600	278.9	9.25	0.00287156
	620	260.1	3.47	0.00307979
	640	142.37	-9.67	0.00224066
	660	274.37	-29.69	0.00176446
	680	264.76	-28.79	0.000654745
CHL 12.01	NRM	215.13	4.87	0.000842452
	100	215.82	6.94	0.000800696

	200	249.97	13.7	0.000733445
	300	223.61	4.1	0.000748142
	350	265.76	-56.39	0.000454871
	400	258.52	-4.3	0.00087732
	450	292.61	35.25	0.00043024
	500	211.25	38.51	0.000542723
	540	45.43	47	0.000228791
	580	214.51	67.11	0.00021553
	600	346.11	84.9	0.000173613
	620	146.41	58.88	0.000121764
	640	250.57	41.37	0.000145852
	680	188.12	22.62	0.000342066
	700	67.93	69.06	0.0003783
CHL 12.02	NRM	359.32	-69.43	0.00134155
	100	8.2	-69	0.00124305
	200	356.57	-67.13	0.00118336
	300	356.54	-65.33	0.00134628
	350	56.54	-63.44	0.000883927
	400	89.28	-6.63	0.000424479
	450	113.15	-13.06	0.000790384
	500	122.38	37.28	0.00145667
	540	137.09	21.59	0.00118481
	580	100.16	46.34	0.00061501
	600	120.87	71.08	0.000716026
	620	313.82	74.51	0.000251058
	640	304.53	-4.71	0.000233494
	680	3.21E+02	56.75	5.08E-05
	700	294.73	71.62	0.000550282
CHL 12.03	NRM	216.13	5.87	0.000842452
	100	216.82	7.91	0.000800696
	200	250.97	14.7	0.000733445
	300	224.61	5.1	0.000748142
	350	266.76	-57.39	0.000454871
	400	259.52	-5.3	0.00087732
	450	291.68	36.25	0.00043024
	500	216.86	40.75	0.000493347
	540	46.63	48.01	0.000228791
	580	215.51	68.11	0.00021553
	600	347.11	85.6	0.000173613
	620	147.41	59.85	0.000121764
	640	260.28	29.41	0.000168224
	680	189.12	23.62	0.000342066
	700	68.83	70.06	0.0003783

CHL 12.04	NRM	358.68	-70.43	0.00134155
	100	9.2	-70.01	0.00124305
	200	357.52	-68.13	0.00118336
	300	357.54	-66.36	0.00134628
	350	55.84	-62.89	0.000883927
	400	90.28	-7.63	0.000424479
	450	114.05	-14.06	0.000790384
	500	125.46	40.56	0.00142311
	540	138.09	22.59	0.00118481
	580	101.16	47.34	0.00061501
	600	121.87	72.08	0.000716026
	620	314.82	75.51	0.000251058
	640	305.53	-5.71	0.000233494
	680	3.21E+02	55.75	5.08E-05
	700	295.73	72.62	0.000550282
CHL 12.05	NRM	68.49	8.29	0.000903897
	100	81.7	-12.38	0.000796804
	200	71.68	-11.67	0.000829059
	300	56.62	-24.96	0.000837838
	350	83.51	-21.78	0.000884757
	400	130.15	32.89	0.000905415
	450	133.78	28.82	0.000912288
	500	147.27	31.24	0.000424243
	540	146.4	35.03	0.000422267
	580	151.34	42.81	0.000610612
	600	127.14	67.21	0.000399855
	620	246.43	-87.82	0.000121054
	640	306.88	26.36	0.000217895
	660	144.89	29.02	0.000331849
	680	222.68	16.52	0.000165984
	700	190.12	-38.21	0.00026754
CHL 12.06	NRM	67.47	7.29	0.000903897
	100	80.7	-11.38	0.000796804
	200	72.22	-12.6	0.000829059
	300	55.62	-25.96	0.000837838
	350	82.51	-20.78	0.000884757
	400	129.15	33.01	0.000905415
	450	132.78	27.9	0.000912288
	500	146.27	30.24	0.000424243
	540	145.4	34.03	0.000422267
	580	152.34	40.81	0.000610612
	600	126.14	66.17	0.000399855
	620	245.43	-86.86	0.000121054
	640	305.88	25.36	0.000217895

	660	143.89	28.02	0.000331849
	680	221.68	15.51	0.000165984
	700	189.01	-37.13	0.00026754
CHL 13.01	NRM	7.96	-16.38	0.000290147
	100	357.69	-19.11	0.000259512
	200	293.77	41.57	0.000433517
	300	17.81	-16.27	0.000370176
	350	27.78	-7.85	9.48E-05
	400	160.07	5.48	0.000470204
	450	236.02	-4.65	0.000197576
	500	342.45	62.18	0.000199987
	540	241.75	51.09	0.000380197
	580	93.41	22.24	0.000187677
	600	148.52	53.6	0.000340786
	620	60.32	12.74	6.16E-05
	640	124.91	52.85	0.000121106
	680	179.26	63.6	0.000277037
	700	305.68	7.96	0.000413445
CHL 13.02	NRM	16.65	30.92	0.000431684
	100	25.19	43.77	0.000401093
	200	250.75	49.23	0.000455962
	300	23.86	25.26	0.000523847
	350	36.07	-1.91	0.000995598
	400	347.75	-20.42	0.00175052
	450	198.79	-24.17	0.000618384
	500	320.48	17.92	0.000275523
	540	76.85	-43.42	0.000452563
	580	47.33	-28.62	0.00087951
	600	101.42	15.08	0.000769585
	640	234.67	52.38	0.000235095
	680	299.64	23.45	0.000813974
	700	172.93	69.01	0.000741115
CHL 13.03	NRM	15.65	29.92	0.000431684
	100	24.19	42.77	0.000401093
	200	249.77	48.23	0.000455962
	300	22.86	24.26	0.000523847
	350	35.07	-0.97	0.000995598
	400	346.81	-19.42	0.00175052
	450	199.4	-23.17	0.000618384
	500	319.48	16.92	0.000275523
	540	75.55	-42.42	0.000452563
	580	46.33	-27.62	0.00087951
	600	100.42	14.08	0.000769585

	640	233.7	51.38	0.000235095
	680	298.94	22.93	0.000813974
	700	171.93	68.01	0.000741115
CHL 13.04	NRM	261.26	-13.46	0.00037706
	100	259.66	-6.63	0.000294222
	200	219.86	-1.4	0.000449056
	300	283.57	26.01	0.00038719
	350	270.98	11.69	0.000535136
	400	85.26	-18.72	0.000261062
	450	128.37	14.36	0.000489567
	500	162.02	70.03	0.000796698
	540	177.78	60.78	0.00111391
	580	340.92	-61.36	0.000348477
	600	127.82	44.64	0.00056157
	620	211.93	50.79	0.000472936
	640	238.78	23.12	0.000247446
	680	218.17	49.4	0.000471369
	700	313.37	64.06	0.000936964
CHL 13.05	NRM	6.96	-15.38	0.000290147
	100	358.69	-18.11	0.000259512
	200	292.77	40.57	0.000433517
	300	16.84	-15.27	0.000370176
	350	28.28	-8.15	9.48E-05
	400	161.64	2.17	0.000497728
	450	235.02	-5.31	0.000197576
	500	343.45	61.18	0.000199987
	540	240.75	50.92	0.000380197
	580	92.41	21.24	0.000187677
	600	147.52	52.6	0.000340786
	620	59.32	11.8	6.16E-05
	640	126.01	51.85	0.000121106
	680	178.26	62.6	0.000277037
	700	304.88	7	0.000413445
CHL 13.06	NRM	260.26	-12.46	0.00037706
	100	258.66	-5.63	0.000294222
	200	218.86	-0.4	0.000449056
	300	282.54	25	0.00038719
	350	271.88	12.08	0.000535136
	350	347.2	8.77	0.000641893
	400	84.26	-17.71	0.000261062
	450	127.37	13.36	0.000489567
	500	161.61	75.07	0.000744134
	540	176.78	59.78	0.00111391

	580	339.92	-60.36	0.000348477
	600	126.82	43.64	0.00056157
	620	210.93	49.79	0.000472936
	640	239.29	22.18	0.000247446
	680	217.17	48.4	0.000471369
	700	312.37	63.01	0.000936964
CHL 15.01	NRM	110.29	30.17	0.00199125
	100	115.66	23.96	0.00212762
	200	129.47	14.77	0.00198268
	300	115.73	18.59	0.00165039
	350	105.85	49.3	0.000986909
	400	101.75	63.97	0.00096844
	450	90.74	71.82	0.00186108
	500	242.87	-21.71	0.000649112
	540	231.16	7.34	0.000439968
	580	302.06	39.81	0.000496026
	600	295.14	-7.38	0.000632418
	620	310.46	47.02	0.000613125
	640	13.69	30.91	0.000198527
	660	120.06	8.58	0.000488542
	680	146.25	43.34	0.000100039
	700	184.89	51.09	0.000284325
CHL 15.02	NRM	109.29	29.17	0.00199125
	100	114.66	22.96	0.00212762
	200	128.47	13.77	0.00198268
	300	114.73	17.61	0.00165039
	350	104.85	48.3	0.000986909
	400	100.75	62.97	0.00096844
	450	89.74	70.82	0.00186108
	500	241.87	-20.71	0.000649112
	540	230.16	6.34	0.000439968
	580	301.06	38.81	0.000496026
	600	294.14	-6.38	0.000632418
	620	309.46	46.02	0.000613125
	640	14.31	29.93	0.000198527
	660	119.06	7.88	0.000488542
	680	145.25	42.34	0.000100039
	700	183.89	50.09	0.000284325
CHL 15.03	NRM	125.11	-12.93	0.00499934
	100	128.7	-15.7	0.0047172
	200	234.81	-27.53	0.00860069
	300	126.51	-20.73	0.00402601
	350	122.02	-10.75	0.00265686

	400	108.81	15.87	0.00201824
	450	106.08	18.64	0.00197325
	500	216.04	-23.91	0.000352092
	540	251.98	29.98	0.000809091
	580	184.97	-15.29	0.000242692
	600	232.93	38.83	0.000157805
	620	33	55.78	0.000154087
	640	117.54	-58.18	0.000221341
	660	229.62	-54.99	0.000926776
	680	249.95	81.68	0.000529303
CHL 15.04	NRM	126.11	-13.93	0.00499934
	100	129.7	-16.7	0.0047172
	200	235.81	-28.53	0.00860069
	300	127.51	-21.73	0.00402601
	350	123.02	-11.75	0.00265686
	400	109.71	16.87	0.00201824
	450	107.08	19.64	0.00197325
	500	217.04	-24.91	0.000352092
	540	252.98	30.78	0.000809091
	580	185.77	-16.29	0.000242692
	600	233.93	39.83	0.000157805
	620	34.01	56.78	0.000154087
	640	119.54	-59.18	0.000221341
	660	230.62	-53.99	0.000926776
	680	250.92	82.68	0.000529303
CHL 15.05	NRM	237.02	-26.33	0.00899312
	100	235.79	-27.79	0.0089858
	200	237.06	-28.31	0.00905534
	300	237.21	-29.87	0.00809292
	350	240.71	-35.88	0.00683481
	400	110.28	61.33	0.0053608
	450	128.42	10.76	0.00118844
	500	97.23	6.32	0.000670271
	540	230.33	-43.25	0.000490939
	580	86.35	65.07	0.000454721
	600	168.43	-24.35	0.000890547
	620	178.14	-62.08	0.000482092
	640	332.67	64.97	0.00014527
	660	293.04	46.04	0.000266379
	680	57.19	-19.06	0.000261618
CHL 15.06	NRM	236.02	-25.33	0.00899312
	100	234.99	-26.79	0.0089858
	200	236.06	-27.31	0.00905534

	300	236.21	-28.87	0.00809292
	350	239.71	-34.88	0.00683481
	400	109.28	60.33	0.0053608
	450	127.62	9.76	0.00118844
	500	96.23	5.32	0.000670271
	540	229.33	-42.25	0.000490939
	580	85.35	64.07	0.000454721
	600	167.43	-23.35	0.000890547
	620	177.14	-61.08	0.000482092
	640	331.67	63.97	0.00014527
	660	292.04	45.04	0.000266379
	680	56.19	-18.06	0.000261618

REFERENCES

References:

Agarwal, A., Srivastava, D. C., Shah, J. and Mamtani, M. A., 2021. Magnetic Fabrics in an Apparently Undeformed Granite Body Near Main Boundary Thrust (MBT), Kumaun Lesser Himalaya, India. *Tectonophysics*, 815. https://doi.org/10.1016/j. tecto.2021.228996, 228996.

Akimoto, T., Kinoshita, H. and Furuta, T., 1984. Electron probe microanalysis study on processes of low-temperature oxidation of titanomagnetite. *Earth and Planetary Science Letters*, 71(2), pp. 263-278.

Ashwal, L. D., 1993. Anorthosites. Minerals and Rocks. Springer Verlag, Vol. 21, pp. 1-422.

Balsley, J. R. and Buddington, A. F., 1960. Magnetic susceptibility anisotropy and fabric of some Adirondack granites and orthogenesis. *Am. J. Sci*, 258, pp. 6-20.

Basavaiah, N., 2011. Geomagnetism: Solid Earth and Upper Atmosphere Perspective. Springer, Netherlands, pp. 291–386.

Bhattacharya, A., Raith, M., Hoernes, S., Banerjee, D., 1998. Geochemical evolution of the massif-type anorthosite complex at Bolangir in the Eastern Ghats Belt of India. *J. Petrol.* 39, pp. 1169–1195.

Bhattacharya, S. and Kar, R., 2002. High-temperature dehydration melting and decompressive P–T path in a granulite complex from the Eastern Ghats, India. *Contributions to Mineralogy and Petrology*, 143(2), pp. 175-191.

Bhattacharya, S., Sen, S. K. and Acharyya, A., 1993. Structural evidence supporting a remnant origin of patchy charnockites in the Chilka Lake area, India. *Geological Magazine*, 130(3), pp. 363-368.

Bhattacharya, S., Sen, S. K. and Acharyya, A., 1994. The structural setting of the Chilka Lake granulite-migmatite-anorthosite suite with emphasis on the time relation of charnockites. *Precambrian Research*, 66(1-4), pp. 393-409.

Bhowmik, S. K., Dasgupta, S., Hoernes, S. and Bhattacharya, P. K., 1995. Extremely high-temperature calcareous granulites from the Eastern Ghats, India: evidence for isobaric cooling, fluid buffering, and terminal channelized fluid flow. *Euro. J. Miner.* 7, pp. 689–703.

Biswal, T. K., Seward, D. and Jena, S. K., 2001. Eastern Ghats Mobile Belt is an Epitome of Mesoproterozoic fold-thrust belt: a study from its NW margin. *Gondwana Research.,* 4, pp. 579– 581.

Borradaile, G. J. and Jackson, M., 2004. Anisotropy of magnetic susceptibility (AMS): Magnetic petrofabrics of deformed rocks. In: Martín Hern´ andez, F., Lüneburg, C. M., Aubourg, C. and Jackson, M. (Eds.), Magnetic Fabric: Methods and Applications, *Geological Society, London*, Special Publication, Vol. 238, pp. 299–360.

Buchan, K. L. and Dunlop, D. J., 1976. Paleomagnetism of the Haliburton intrusions: Superimposed magnetizations, metamorphism, and tectonics in the late Precambrian. *Journal of Geophysical Research*, 81(17), pp. 2951-2967.

Buddington, A. F. and Lindsley, D. H., 1964. Iron- titanium oxide minerals and synthetic equivalents. *Jour. Petrol.*, V. 5, pp. 310-357.

Butler, R. F., 1992. Palaeomagnetism: Magnetic Domains to Geologic Terranes, Blackwell Scientific Publications.

Butler, R. F., 1992. *Magnetic Domains to Geologic Terranes*. Blackwell.

Chatterjee, S. C., 1960. The Problem of the Anorthosites with Special Reference to the Anorthosites of Bengal. *Prec. 46th Ind. Sci. Cong.* Pt-II.

Chatterjee, S., Mondal, S., Gain, D., Baidya, T. K. and Mazumdar, D., 2018a. Interpretation of magnetic fabrics in the Dalma volcanic rocks and associated meta-sediments of the Singhbhum Mobile Belt. *Journal of Earth System Science*, 127(6), pp. 89.

Chatterjee, S., Mondal, S., Roy, P., Gain, D. and Bhattacharya, A., 2018b. Magneto-mineralogical characterization and manifestations of magnetic fabrics from the gneissic rocks and associated intrusive bodies in and around Bankura and Purulia districts, West Bengal, India. *Current Science*, pp. 1894-1902.

Cifelli, F., Mattei, M., Chadima, M., Lenser, S. and Hirt, A. M., 2009. The magnetic fabric in "Undeformed Clays": AMS and neutron texture analyses from the Rif Chain (Morocco). *Tectonophysics.* 466, pp. 79–88. https://doi.org/10.1016/j.tecto.2008.08.008.

Cifelli, F., Mattei, M., Hirt, A. M. and Günther, A., 2004. The origin of tectonic fabrics in "undeformed" clays: the early stages of deformation in extensional sedimentary basins. *Geophys. Res. Lett*. https://doi.org/10.1029/2004GL019609.

Das, K., Bose, S., Karmakar, S. and Chakraborti, S., 2012. Petrotectonic framework of granulites from northern part of Chilka Lake area, Eastern Ghats Belt, India: compressional vis-à-vis transpressional tectonics. *Journal of Earth System Science*, 121, pp. 1-17.

Das, S., Venkateshwarlu, M., Mondal, S., Chatterjee, S. and Gain, D., 2024. Anisotropy of magnetic susceptibility and rock magnetism of high-grade rocks from Eastern Ghats Mobile Belt, India: Constraints to tectonics. *Journal of Earth System Science*, 133(3), pp. 175.

Dasgupta, S., Sanyal, S., Sengupta, P. and Fukuoka, M., 1994. Petrology of granulites from Anakapalle—evidence for Proterozoic decompression in the Eastern Ghats, India. *Journal of Petrology*, *35*(2), pp. 433-459.

Dasgupta, S., Sengupta, P., Ehl, J., Raith, M. and Bardhan, S., 1995. Reaction textures in a suite of spinel granulites from the Eastern Ghats Belt, India: evidence for

polymetamorphism, a partial petrogenetic grid in the system KFMASH and the roles of ZnO and Fe_2O_3. *Journal of Petrology*, 36(2), pp. 435-461.

Dasgupta, S., Sengupta, P., Fukuoka, M. and Bhattacharya, P. K., 1991. Mafic Granulites from the Eastern Ghats, India: further evidence for extremely high temperature crustal metamorphism. *J. Geol.* 99, pp. 124–133.

Dasgupta, S., Sengupta, P., Fukuoka, M. and Chakraborti, S., 1992. Dehydration melting, fluid buffering and decompressional *P–T* path in a granulite complex from the Eastern Ghats, India. *J. Meta. Geol.* 10, pp. 777–788.

Dasgupta, S., Sengupta, P., Mondal, A. and Fukuoka, M., 1993. Mineral chemistry and reaction textures in metabasites from the Eastern Ghats Belt, India and their implications. *Miner. Mag.* 57, pp. 113–120.

Dasgupta, S., Sengupta, P., Mukhopadhyay, D. K., Mitra, S., Bardhan, S. and Bhattacharya, S., 1996. Petrological evolution of the Eastern Ghats Granulite Belt, India: Summary and conclusions based on recent work. *Journal of African Earth Sciences*, 22(2), pp. IX-XII.

Day, R., Fuller, M. and Schmidt, V. A., 1977. Hysteresis properties of titanomagnetites: grain-size and compositional dependence. *Physics of the Earth and Planetary Interiors*, 13(4), pp. 260-267.

DeWaard, D., Romey, W. D. and Isachsen, Y. W., 1969. Petrogenetic relationships in the anorthosite-charnockite series of Snowy Mountain dome, south-central Adirondacks. *Origin of anorthosites and related rocks*, *18*, pp. 307-315.

De, A., 1969. Anorthosites of the Eastern Ghats, India. In Origin of Anorthosites and Related Rocks. *Mus. Sci. Serv., Mem.* Vol. 18, pp. 425-434.

Dobmeier, C. and Simmat, R., 2002. Post-Grenvillean transpression in the Chilka Lake area, Eastern Ghats Belt—implications for the geological evolution of peninsular India. *Precambrian Research*, 113(3-4), pp. 243-268.

Dobmeier, C. J. and Raith, M. M., 2003. Crustal architecture and evolution of the Eastern Ghats Belt and adjacent regions of India. *Geological Society, London, Special Publications*, *206*(1), pp.145-168.

Dunlop D. J. and Özdemir Ö., 1997. Rock Magnetism: fundamentals and frontiers. Cambridge University Press, Cambridge.

Dvořák, J. and Hrouda, F., 1975. The reflection of the deeper structure of the Artmanov-Osoblaha Block (Nízký Jeseník Mountains, Czechoslovakia) in the magnetic anisotropy and deformation history of overlying palaeozoic sediments. *Věstník ÚÚG*, 50, pp. 285-296.

Ellwood, B. B., Hrouda, F. and Wagner, J. J., 1988. Symposia on magnetic fabrics: introductory comments. *Physics of the Earth and Planetary Interiors*, 51(4), pp. 249-252.

Ferre, E. C., Gebelin, A., Till, J. L., Sassier, C. and Burmeister, C. K., 2014. Deformation and magnetic fabrics in ductile shear zones: a review. *Tectonophysics.* 629, pp. 179– 188.

Ferré, E. C., Martín-Hernández, F., Teyssier, C. and Jackson, M., 2004. Paramagnetic and ferromagnetic anisotropy of magnetic susceptibility in migmatites: measurements in high and low fields and kinematic implications. *Geophysical Journal International*, 157(3), pp. 1119-1129.

Fodor, L. I., Márton, E., Vrabec, M., Koroknai, B., Trajanova, M. and Vrabec, M., 2020. Relationship between magnetic fabrics and deformation of the Miocene Pohorje intrusions and surrounding sediments (Eastern Alps). *International Journal of Earth Sciences*, *109*(4), pp.1377-1401.

Frost, B. R., 1988. A review of graphite- sulfide- oxide- silicate equilibria in metamorphic rocks. *Rendiconti Societa Italiana Mineral. Petrol.*, V. 43, pp. 25-40.

Gain, D., Chatterjee, S. and Mondal, S., 2022. Rock magnetism and AMS studies in Kondapalle-Pangidi layered complex, Eastern Ghats Belt, India: Remanence carriers and tectonic implications. *Physics of the Earth and Planetary Interiors*, 329-330, pp. 106910.

Graham, J. W., 1954. Magnetic susceptibility, an unexploited element of petrofabric. *Geological Society of American Bulletin*, 65, pp. 1257-1258.

Grant, F. S. and West, G. F., 1965. Interpretation Theory in Applied Geophysics. McGraw-Hill Book Co., New York, pp. 583.

Gupta, S., Dobe, R., Sawant, A. D., Misra, S. and Mohanty, W. K., 2020. The northern margin of the Eastern Ghats Mobile Belt: evidence for strike-slip tectonics along a craton-mobile belt boundary. *Structural Geometry of Mobile Belts of the Indian Subcontinent*, pp. 153-174.

Haggerty, S. E., 1976b. Opaque mineral oxides in terrestrial igneous rocks. In: Rumble, D. (Ed.), Oxide minerals. *Mineral. Soc. Am.*, Short Course Notes 3, Hg101–Hg300.

Harley, S. L., 1989. The origins of Granulites: a metamorphic perspective. *Geological Magazine*, 126 (3), pp. 215-247.

Hollister, L. S., 1977. The reaction forming cordierite from garnet, the Khtada Lake metamorphic complex, British Columbia. *The Canadian Mineralogist*, 15(2), pp. 217-229.

Hrouda, F. and Janák, F., 1976. The changes in shape of the magnetic susceptibility ellipsoid during progressive metamorphism and deformation. *Tectonophysics*, 34 (1-2), pp. 135-148.

Hrouda, F., 1982. Magnetic anisotropy of rocks and its application in geology and geophysics. *Geophysical Surveys*, 5(1), pp. 37-82.

Ising, G., 1942. On the magnetic properties of varved clay. Almqvist & Wiksell.

Jelinek, V., 1981. Characterization of the magnetic fabric of rocks. *Tectonophysics*, 79 (3-4), pp. T63-T67.

Johnson, H.P., Hall, J.M., 1978. A detailed rock magnetic and opaque mineralogy study of the basalts from Nazca Plate. *Geophys. J. R. Astr. Soc.* 52, pp. 45–64.

Keary, P., Klepeis, K. A. and Vine, F. J., 2009. Global Tectonics, Willey-Blackwell, pp. 54-68.

Krause, O., Dobmeier, C., Raith, M.M. and Mezger, K., 2001. Age of emplacement of massif-type anorthosites in the Eastern Ghats Belt, India: constraints from U–Pb zircon dating and structural studies. *Precambrian Research*, *109*(1-2), pp. 25-38.

Lattard, D., Engelmann, R., Kontny, A. and Sauerzapf, U., 2006. Curie temperatures of synthetic titanomagnetites in the Fe-Ti-O system: Effects of composition, crystal chemistry, and thermomagnetic methods. *Journal of Geophysical Research: Solid Earth*, 111(B12).

McElhinny, M. W., 1973. Mantle plumes, Palaeomagnetism and Polar Wandering. *Nature*, 241 (5391), pp. 523-524.

McElhinny, M. W., 1979. *Palaeomagnetism and Plate Tectonics*. CUP Archive.

Mezger, K. and Cosca, M. A., 1999. The thermal history of the Eastern Ghats Belt (India) as revealed by U–Pb and 40Ar/39Ar dating of metamorphic and magmatic minerals: implications for the SWEAT correlation. *Precambrian Research*, 94(3-4), pp. 251-271.

Mondal, S., Piper, J. D. A., Hunt, L., Bandyopadhyay, G. and Basu Mallik, S., 2009. Palaeomagnetic and rock magnetic study of charnockites from Tamil Nadu, India, and the 'Ur'protocontinent in Early Palaeoproterozoic times. *Journal of Asian Earth Sciences*, 34(4), pp. 493-506.

Mondal, T. K., Chowdhury, A., Sain, A. and Chatterjee, S., 2022. Understanding the maturity of columnar joints and its spatial relationship with eruptive centre: A critical appraisal from the Rajmahal Basalt, India. *Physics of the Earth and Planetary Interiors*, 326, pp. 106867.

Nagata, T., 1961. Rock Magnetism, 2nd Edition, Maruzen, Tokyo, 350 pp.

Nesbitt, B. E., 1986a. Oxide-Sulfide-Silicate equilibria associated with metamorphosed ore deposits. Part-I. Theoretical Considerations. *Econ. Geol.*, V. 81, pp. 831-840.

Nesbitt, B. E., 1986b. Oxide-Sulfide-Silicate equilibria associated with metamorphosed ore deposits. Part-II. Pelitic and felsic terrains. *Econ. Geol*., V. 81, pp. 841-856.

O'Reilly W., 1984. Rock and Mineral Magnetism. Blackie, Glasgow.

Oldfield, F., 1994. Toward the discrimination of fine-grained ferrimagnets by magnetic measurements in lake and near-shore marine sediments. *Journal of Geophysical Research: Solid Earth*, 99(B5), pp. 9045-9050.

Parés, J. M. and Van Der Pluijm, B. A., 2002. Evaluating magnetic lineations (AMS) in deformed rocks. *Tectonophysics*, 350 (4), pp. 283-298.

Perraju, P., 1960. Occurrence of Anorthosite in Puri District, Orissa. *Indian Minerals*, 14, pp. 310.

Perraju, P., 1973. Anorthosite of Puri District, Orissa. *Rec. Geol. Surv. India*, 105, pp. 102-116.

Piper, J. D. A., 1987. Palaeomagnetism and the Continental Crust, First Edition, John Wiley and Sons, Halsted Press, New York.

Piper, J. D. A., Briden, J. C. and Lomax, K., 1973. Precambrian Africa and South America as a single continent. *Nature*, 245(5423), pp. 244-248.

Radhakrishna, T. and Joseph, M., 1996. Proterozoic palaeomagnetism of the mafic dyke swarms in the high-grade region of southern India. *Precambrian Research*, 76(1-2), pp. 31-46.

Raith, M. M., Dobmeier, C. and Mouri, H., 2007. Origin and evolution of FeAl-granulite in the thermal aureole of the Chilka Lake Anorthosite, Eastern Ghats Province, India. *Proceedings of the Geologists' Association*, 118(1), pp. 87-100.

Ramakrishnan, M. and Vaidyanadhan, R., 2008. *Geology of India* (Vol. 1, pp. 261-333). Bangalore: *Geological Society of India.*

Ramakrishnan, M., 1988, January. Tectonic evolution of the Archaean high-grade terrain of South India. In *Lunar and Planetary Inst., Workshop on the Deep Continental Crust of South India*.

Ramakrishnan, S., Eppenberger, U., Mueller, H., Shinkai, Y. and Narayanan, R., 1998. Expression profile of the putative catalytic subunit of the telomerase gene. *Cancer Research*, 58(4), pp. 622-625.

Raposo, M. I. B. and Egydio-Silva, M., 2001. Magnetic fabric studies of high-grade metamorphic rocks from the Juiz de For a Complex, Ribeira Belt, Southeastern Brazil. *Int. Geol. Rev*. 43 (5), pp. 441–456.

Ray, C., 1952. Anorthosite in Chilka Lake. *Proc. Ind. Sci. Cong. 39th Sess.* Pt-3, 177.

Rickers, K., Mezger, K. and Raith, M. M., 2001. Evolution of the continental crust in the Proterozoic Eastern Ghats Belt, India and new constraints for Rodinia reconstruction: implications from Sm–Nd, Rb–Sr and Pb–Pb isotopes. *Precambrian Research*, 112(3-4), pp. 183-210.

Roy, J. L. and Park, J. K., 1974. The magnetization process of certain red beds: Vector analysis of chemical and thermal results. *Canadian Journal of Earth Sciences*, 11(3), pp. 437-471.

Sarkar, A., Bhanumathi, L. and Balasubrahmanyan, M. N., 1980. Studies on plagioclase feldspars from the Chilka Lake Igneous Complex, Orissa. In *Proceedings, Third Session, Indian Geological Congress, Poona, 1980* (pp. 195). University of Poona.

Sarkar, A., Bhanumathi, L. and Balasubrahmanyan, M. N., 1981. Petrology, geochemistry and geochronology of the Chilka Lake igneous complex, Orissa State, India. *Lithos*, 14(2), pp. 93-111.

Schenk, V., 1984. Petrology of felsic granulites, metapelites, metabasics, ultramafics, and metacarbonates from Southern Calabria (Italy): prograde metamorphism, uplift and cooling of a former lower crust. *Journal of Petrology*, 25(1), pp. 255-296.

Sen, S. K., 1987. Origin of leptynite, an orthopyroxene-free granite-gneiss, in two granulite terrains of India. *Recent Res. Geol*. 13, pp. 117–124.

Sen, S. K., Bhattacharya, S. and Acharyya, A., 1995. A multi-stage pressure–temperature record in the Chilka Lake granulites: the epitome of the metamorphic evolution of the Eastern Ghats, India, *J. Meta. Geol*. 13, pp. 287–298.

Sengupta, P., Dasgupta, S., Bhattacharya, P. K., Fukuoka, M., Chakraborti, S. and Bhowmick, S., 1990. Petro-tectonic imprints in the sapphirine granulites from Anantagiri, Eastern Ghats mobile belt, India. *Journal of Petrology, 31*(5), pp. 971-996.

Sengupta, P., Dasgupta, S., Dutta, N. R. and Raith, M. M., 2008. Petrology across a calcareous rock–anorthosite interface from the Chilka Lake Complex, Orissa: Implications for Neo-Proterozoic crustal evolution of the northern Eastern Ghats Belt. *Precambrian Research*, 162(1-2), pp. 40-58.

Sengupta, P., Karmakar, S., Dasgupta, S. and Fukuoka, M., 1991. Petrology of spinel granulites from Araku, Eastern Ghats, India, and a petrogenetic grid for sapphirine-free rocks in the system FMAS. *J. Meta. Geol*. 9, pp. 451–459.

Shaw, R. K. and Arima, M., 1996a. Mineral chemistry, reaction textures, thermobarometry and *P–T* path from orthopyroxene granulites of Rayagada, Eastern Ghats, India. *J. Southeast Asian Earth Sci.* 14, pp. 175–184.

Shaw, R.K. and Arima, M., 1996b. High-temperature metamorphic imprint on calc-silicate granulites of Rayagada, Eastern Ghats, India: implication for the isobaric cooling path. *Contrib. Miner. Petrol*. 126, pp. 169–180.

Simmat, R. and Raith, M. M., 2008. U–Th–Pb monazite geochronometry of the Eastern Ghats Belt, India: timing and spatial disposition of poly-metamorphism. *Precambrian Research*, 162(1-2), pp. 16-39.

Spall, H., 1971. Precambrian apparent polar wandering: evidence from North America. *Earth and Planetary Science Letters*, 10(2), pp. 273-280.

Stacey, F. D., Joplin, G. and Lindsay, J., 1960. Magnetic anisotropy and fabric of some foliated rocks from SE Australia. *Geofisica pura e applicata*, *47*, pp. 30-40.

Tarling, D. and Hrouda, F. eds., 1993. Magnetic Anisotropy of Rocks. Springer Science & Business Media.

Tarling, D. H., 2007. Palaeomagnetism: Principles and applications in Geology, Geophysics and Archaeology. Chapman and Hall, New York and London.

Tauxe, L., 2010. Essentials of palaeomagnetism, University of California Press, Berkley-Los Angeles-London. ISBN: 978-0-520-26031-3.

Tauxe, L., Butler, R.F., Van der Voo, R. and Banerjee, S. K., 2010. Essentials of Palaeomagnetism: *University of California*. *Press*, pp. 512.

Thompson, A. B., 1976. Mineral reactions in pelitic rocks; II, Calculation of some PTX (Fe-Mg) phase relations. *American Journal of Science*, 276(4), pp. 425-454.

Thompson, R. and Oldfield, F., 1986. Environmental Magnetism. Allen and Unwin, Winchester, M A. https://doi.org/10.1007/978-94-011-8036-8.

Tracy, R. J., Robinson, P. and Thompson, A. B., 1976. Garnet composition and zoning in the determination of temperature and pressure of metamorphism, central Massachusetts. *American Mineralogist*, 61(7-8), pp. 762-775.

Viegas, G. F., Archanjo, C. J. and Vauchez, A., 2013. Fabrics of migmatites and the relationships between partial melting and deformation in high-grade transpressional shear zones: the Espinho Branco anatexite (Borborema Province, NE Brazil). *J. Struct. Geol.* 48, pp. 45–56.

Voigt, W. and Kinoshita, S., 1907. Bestimmung absoluter Werte von Magnetisierungszahlen, insbesondere für Kristalle. *Annalen der Physik*, 329 (13), pp. 492-514.

Walker, T. L., 1902. Geology of Kalahandi State, Central Provinces. *Mem. Geol. Surv. India* 33, pp. 1–22.

Windley, B. F., 1971. The evolution of Archaean low-and high grade terrains. *Geol. Soc. Aust. Spec. Publ.*, 3, pp. 33.

Zhang, J. and Piper, J. D. A., 1994. Magnetic fabric and post-orogenic uplift and cooling magnetisations in a Precambrian granulite terrain: The Datong-Huai'an region of the North China Shield. Tectonophysics, V. 234, pp. 227-246.

Zijderveld, J. D. A., 1967. AC demagnetization of rocks: Analysis of results. *Methods in Palaeomagnetism*, pp. 256-286.